GEORGIA INSTITUTE OF TECHNOLOGY — OFFICE OF CONTRACT ADMINISTRATION

PROJECT ADMINISTRATION DATA SHEET

[X] ORIGINAL

[ ] REVISION NO. ____

Project No. A-2940 DATE: 5/7/81

Project Director: Mr. D. J. Kozakoff ~~School~~/Lab EML/RSD

Sponsor: U. S. Army Missile Command; Redstone Arsenal, AL 35898

Type Agreement: Delivery Order No. 0016 under Contract No. DAAH01-81-D-A003

Award Period: From 4/23/81 To 9/30/81 (Performance) 11/30/81 (Reports)

Sponsor Amount: $30,000 Contracted through:

Cost Sharing: None GTRI/~~GIT~~

Title: Dynamically Aimed Free Flight Rocket Task

ADMINISTRATIVE DATA OCA CONTACT Duane Hutchison x 4820

1) Sponsor Technical Contact: Dr. M. M. Hallum; Systems Simulation and Development Directorate; U. S. Army Missile Command; Attn: DRSMI-RDF; Redstone Arsenal, AL 35898 205/ 876-4141

2) Sponsor Admin./Contractual Contact: Mr. Thomas A. Bryant; ONR Resident Representative; Georgia Institute of Technology; 206 O'Keefe Building; Atlanta, GA 30332.

Reports: See Deliverable Schedule Security Classification: Unclassified

Defense Priority Rating: DO-A2 under DMS Reg. 1

RESTRICTIONS

See Attached DOD Supplemental Information Sheet for Additional Requireme

Travel: Foreign travel must have prior approval - Contact OCA in each case. Domestic travel requires sponsor approval where total will exceed greater of $500 or 125% of approved proposal budget category.

Equipment: Title vests with Government; except that items costing less than $1,000 vests with GIT if prior approval to purchase is obtained from the Contracting Officer.

COMMENTS:

COPIES TO:

Administrative Coordinator
Research Property Management
Accounting Office
Research Security Services
~~Reports Coordinator~~ (OCA)
Legal Services (OCA)
EES Research Public Relatio
Project File (OCA)
Other: ____

GEORGIA INSTITUTE OF TECHNOLOGY OFFICE OF CONTRACT ADMINISTRATION

SPONSORED PROJECT TERMINATION SHEET

Date 1/5/82

Project Title: Dynamically Aimed Free Flight Rocket Task

Project No: A-2940

Project Director: D. J. Kozakoff

Sponsor: U.S. Army Missile Command; Redstone Arsenal, AL

Effective Termination Date: 9/30/81

Clearance of Accounting Charges: 11/30/81 (Rpts)

Grant/Contract Closeout Actions Remaining:

- [x] Final Invoice ~~and Closing Documents~~
- [ ] Final Fiscal Report
- [ ] Final Report of Inventions
- [ ] Govt. Property Inventory & Related Certificate
- [ ] Classified Material Certificate
- [ ] Other _____

Assigned to: EML/RSD (School/Laboratory)

COPIES TO:

Administrative Coordinator	Research Security Services	EES Public Relations (2)
Research Property Management	Reports Coordinator (OCA) ✓	Computer Input
Accounting	Legal Services (OCA)	Project File
Procurement/EES Supply Services	Library	Other _____

Monthly Technical Report No. 1
and
Monthly Cost and Performance Report No. 1

Report Period
23 April - 31 May 1981

DYNAMICALLY AIMED FREE FLIGHT ROCKET TASK

D. J. Kozakoff

Contract No. DAAH01-81-D-A003
Delivery Order No. 0016
EES Project A-2940

Effective Date: 4/23/81
Expiration Date: 9/30/81

Prepared for

U.S. Army Missile Command
Attn: DRDMI-ICBB/Lukens
Redstone Arsenal, Alabama 35809

Prepared by

Georgia Institute of Technology
Engineering Experiment Station
Atlanta, Georgia 30332

WORK PERFORMED IN THIS REPORTING PERIOD

Contract activity was initiated with a literature search. Several trips were made to Redstone Arsenal in May to meet with the contract technical monitor. A full scale zuni rocket was fabricated at Georgia Tech in anticipation of RCS measurements.

PROBLEMS ENCOUNTERED

None

WORK TO BE PERFORMED IN THE NEXT REPORTING PERIOD

RCS measurements and analyses will be performed. Begin tradeoff studies of various sensor categories. Meet with contract technical monitor to discuss results and receive technical direction.

Cost Information

The following charges have been incurred against the contract during period 1 May through 31 May 1981.

	Expended	Encumbered
Personal Services (PS)	$ 1,125.74	$ -0-
Materials and Supplies	244.92	91.60
Travel	121.77	-0-
Overhead (@ 76% of PS)	821.79	-0-
Retirement (@ 10.51% of PS)	114.77	-0-
TOTAL	$ 2,428.99	$ 91.60

The breakdown of personal services is as follows:

	Dollars	Approximate Man Hours
Principal Research Scientists/Engineers	$ -0-	0
Senior Research Scientists/Engineers	793.13	41
Research Scientists II/Engineers II	-0-	0
Research Scientists I/Engineers I	-0-	0
Technicians/Draftsmen	239.81	30
Students	92.80	17
Secretarial/Clerical/Other	-0-	0
TOTAL	$ 1,125.74	88

The current financial status of the contract is as follows:

	Budget As Proposed	Expended	Free Balance
Personal Services (PS)	$ 14,292.37	$ 1,125.74	$ 13,166.34
Materials and Supplies	2,723.42	336.52	2,386.90
Travel and Shipping	750.00	121.77	628.23
Computer	-0-	-0-	-0-
Overhead	10,646.96	821.79	9,825.17
Retirement	1,587.25	114.77	1,472.48
Encumbered	-0-	-0-	-0-
TOTAL	$ 30,000.00	$ 2,520.59	$ 27,479.12

FUNDING

Based on present full funding, the funding and equivalent man hours are sufficient to complete the task. Approximately 8 % of the proposed task has been completed.

Monthly Technical Report No. 2
and
Monthly Cost and Performance Report No. 2

Report Period
June 1 through June 30, 1981

DYNAMICALLY AIMED FREE FLIGHT ROCKET TASK

D. J. Kozakoff

Contract No. DAAH01-81-D-A003
Delivery Order No. 0016
EES Project A-2940

Effective Date: 4/23/81
Expiration Date: 9/30/81

Prepared for

U.S. Army Missile Command
Attn: DRDMI-ICBB/Lukens
Redstone Aresenal, Alabama 35809

Prepared by

Georgia Institute of Technology
Engineering Experiment Station
Atlanta, Georgia 30332

WORK PERFORMED IN THIS REPORT PERIOD

Performance tradeoffs of various types of sensors are underway. A trip was made to MICOM to discuss the results with the contract technical monitor.

Full scale X-band RCS measurements were performed. For horizontal polarization, Figures 1 through 3 are tail aspect RCS for missile roll angles of 0 through 75 degrees (in 15 degree increments). Figure 4 illustrates full 360 degree azimuth RCS for the zero degree roll condition. Figures 5 through 8 plot similar data for the vertical polarization.

PROBLEMS ENCOUNTERED

No problems were encountered during this period.

WORK TO BE PERFORMED IN THE NEXT REPORTING PERIOD

RCS characterization of the full scale Zuni rocket model at the Ka-band (16 GHz) will be obtained, and the sensor tradeoff analyses will continue. Another meeting is planned with the contract technical monitor to discuss study results.

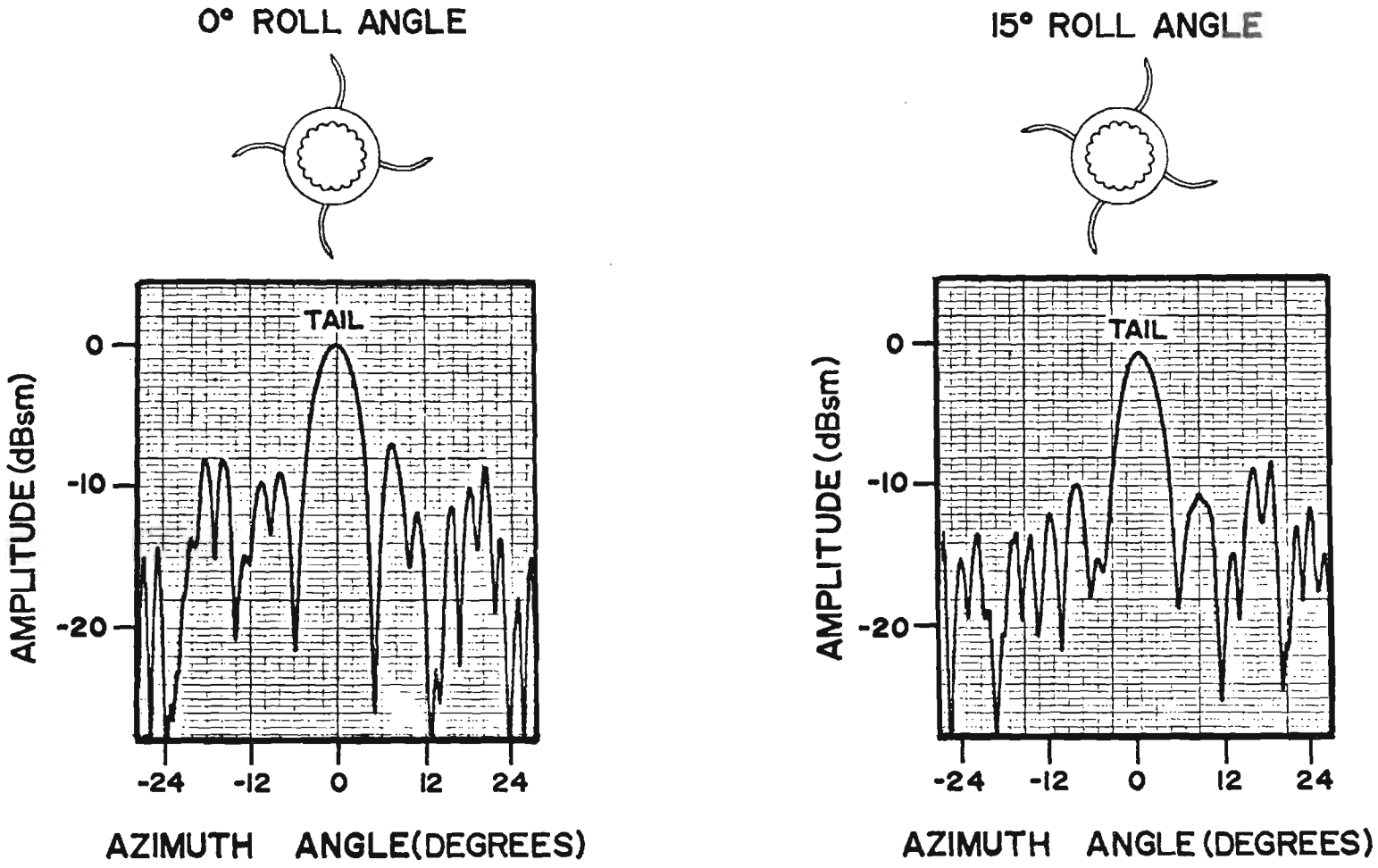

Figure 1. Compact Range RCS Measurements of The Zuni Rocket Tail Section (Rear View) at 0° Roll Angle (Left) and 15° Roll Angle (Right), 10.0 GHz, and Horizontal Polarization.

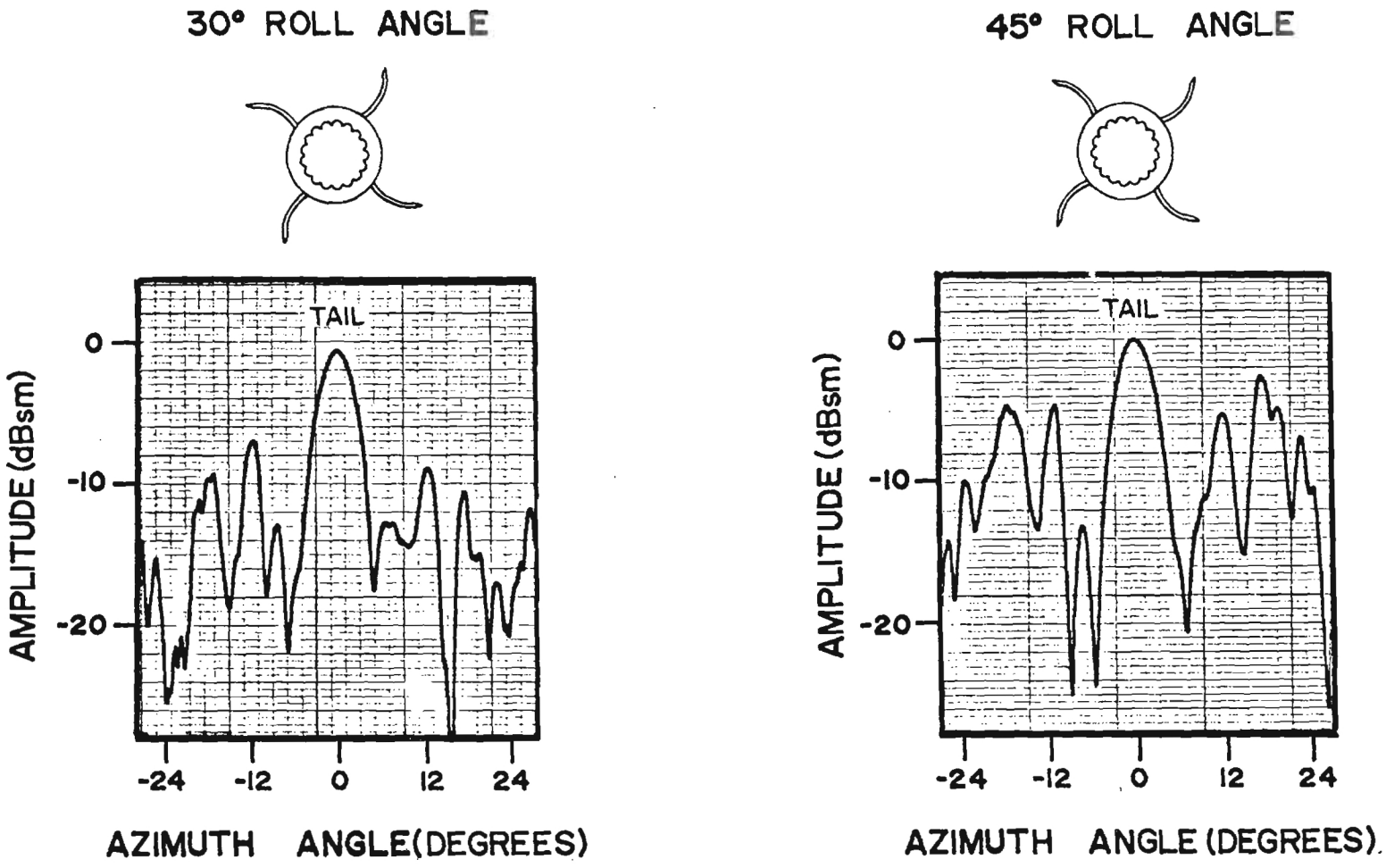

Figure 2. Compact Range RCS Measurements of The Zuni Rocket Tail Section (Rear View) at 30° Roll Angle (Left) and 45° Roll Angle (Right), 10.0 GHz, and Horizontal Polarization.

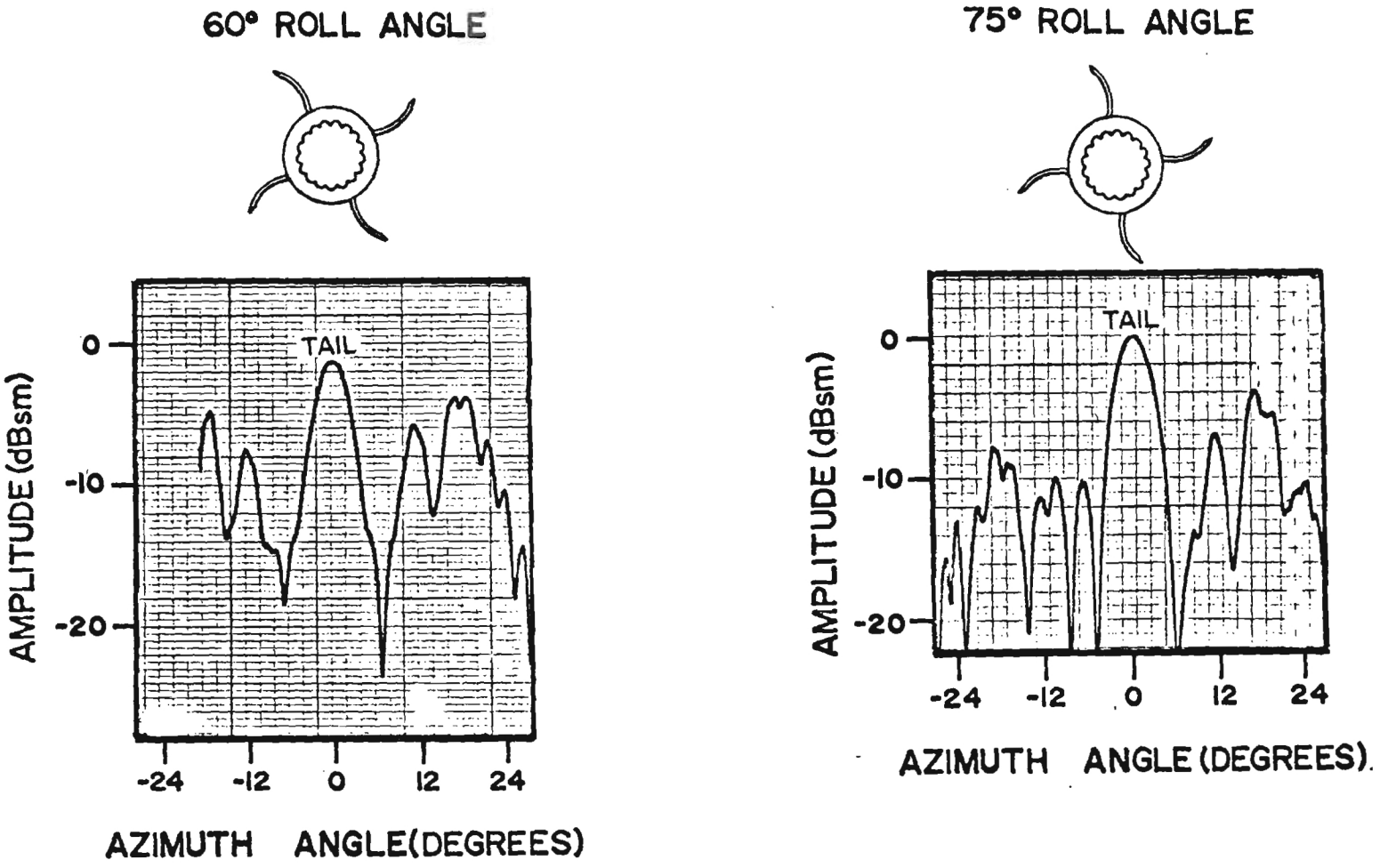

Figure 3. Compact Range RCS Measurements of The Zuni Rocket Tail Section (Rear View) at 60° Roll Angle (Left) and 75° Roll Angle (Right), 10.0 GHz, and Horizontal Polarization.

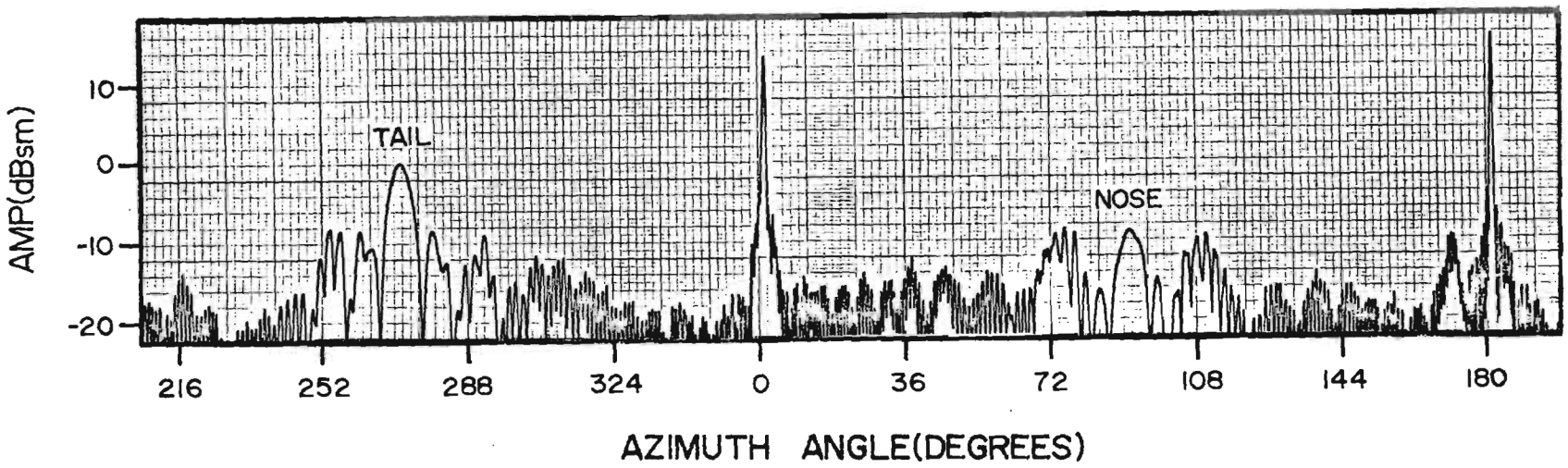

Figure 4. Compact Range RCS Measurements of the Zuni Rocket (360° Azimuth Rotation) at 0° Roll Angle, 10.0 GHz, and Horizontal Polarization

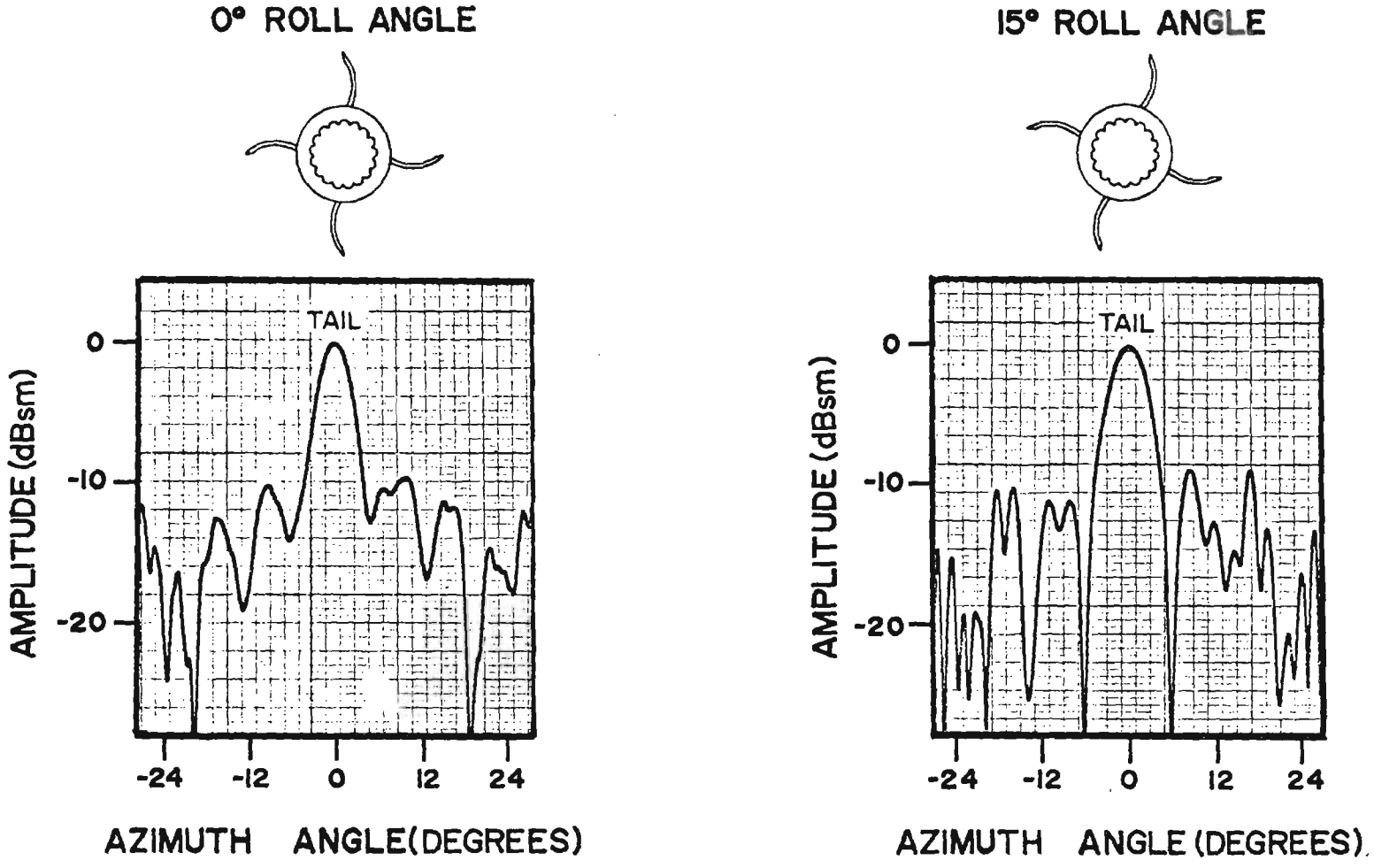

Figure 5. Compact Range RCS Measurements of The Zuni Rocket Tail Section (Rear View) at 0° Roll Angle (Left)and 15° Roll Angle (Right), 10.0 GHz, and Vertical Polarization.

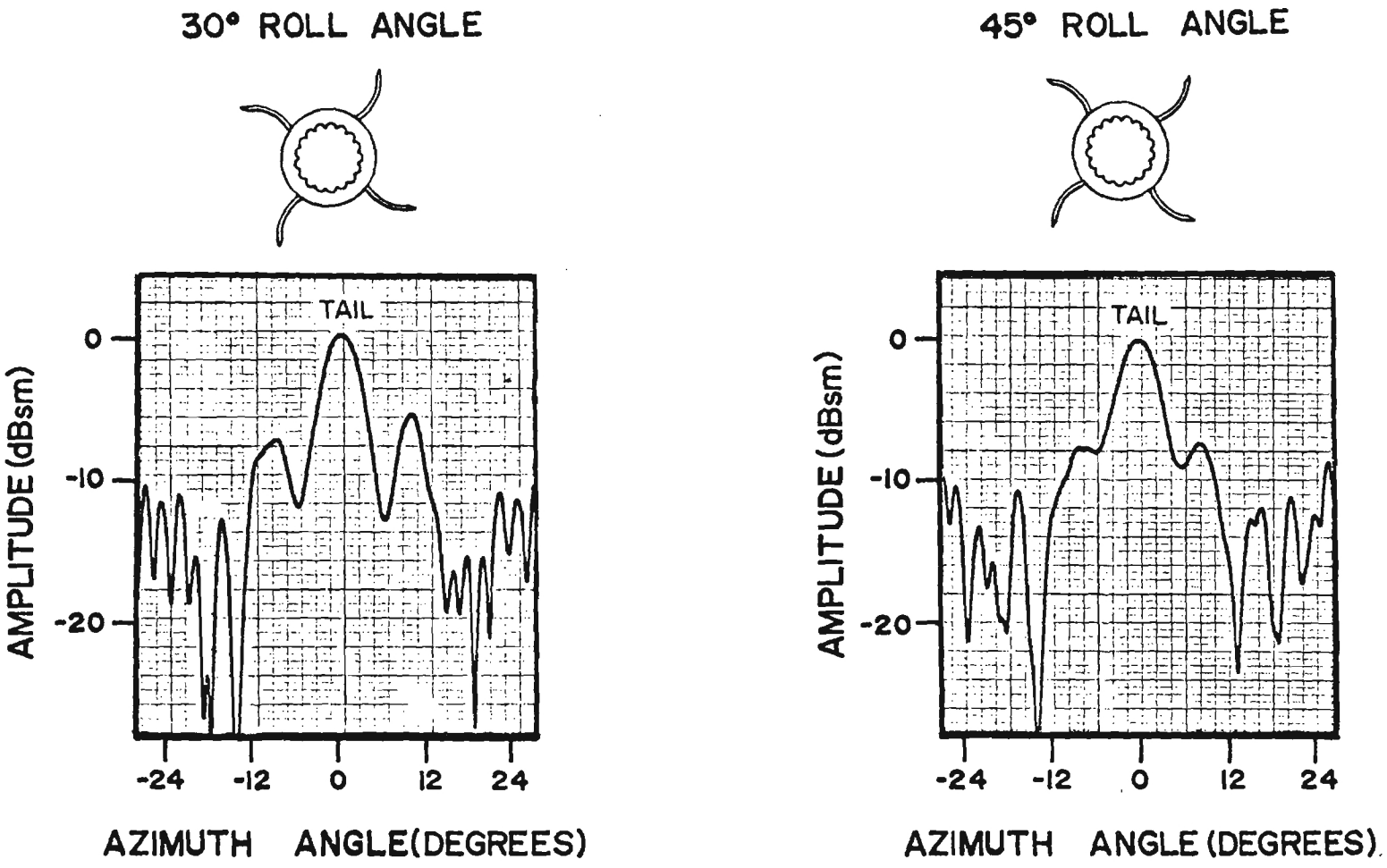

Figure 6. Compact Range RCS Measurements of The Zuni Rocket Tail Section (Rear View) at 30° Roll Angle (Left) and 45° Roll Angle (Right), 10.0 GHz, and Vertical Polarization.

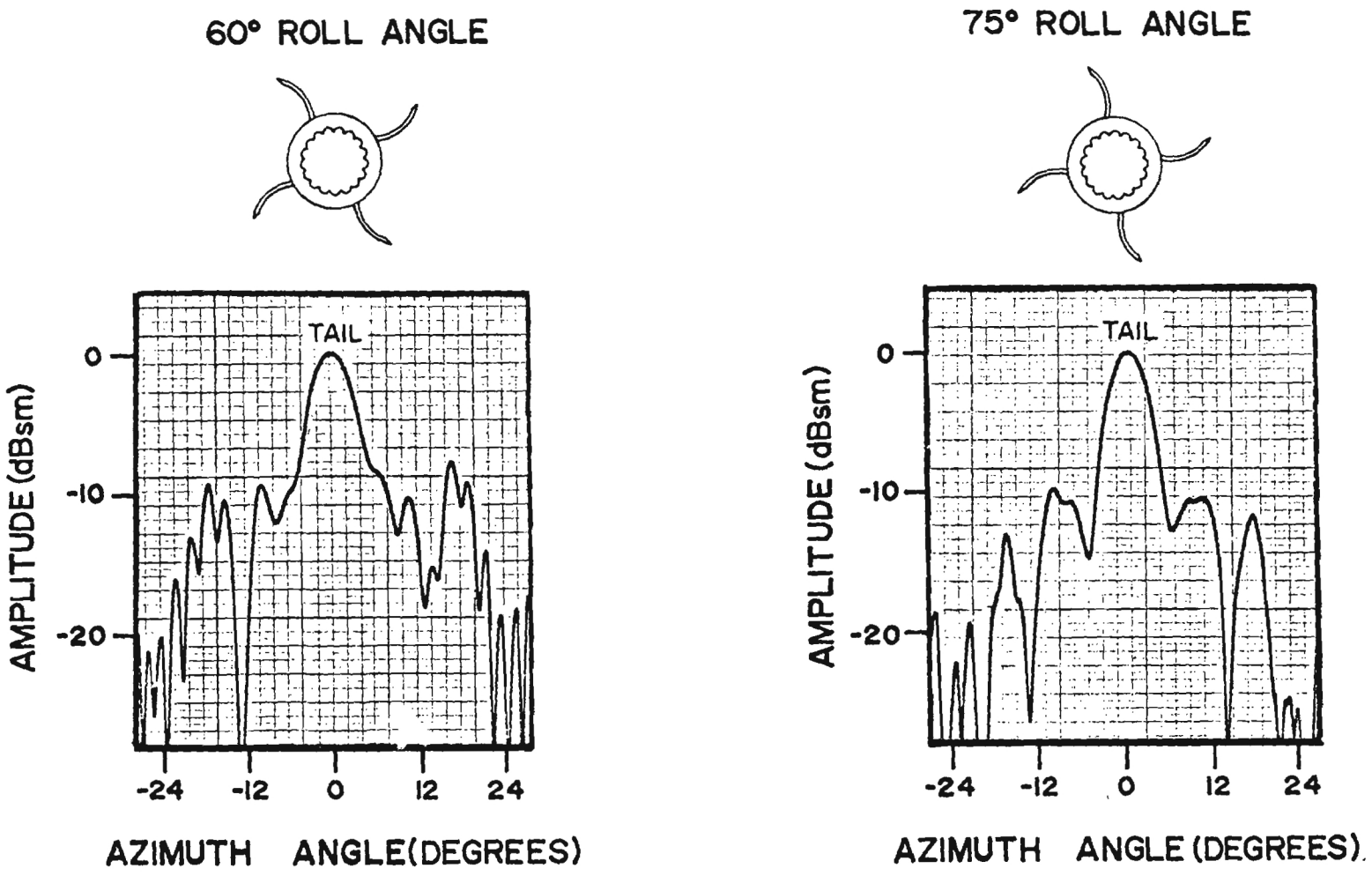

Figure 7. Compact Range RCS Measurements of The Zuni Rocket Tail Section (Rear View) at 60° Roll Angle (Left) and 75° Roll Angle (Right), 10.0 GHz, and Vertical Polarization.

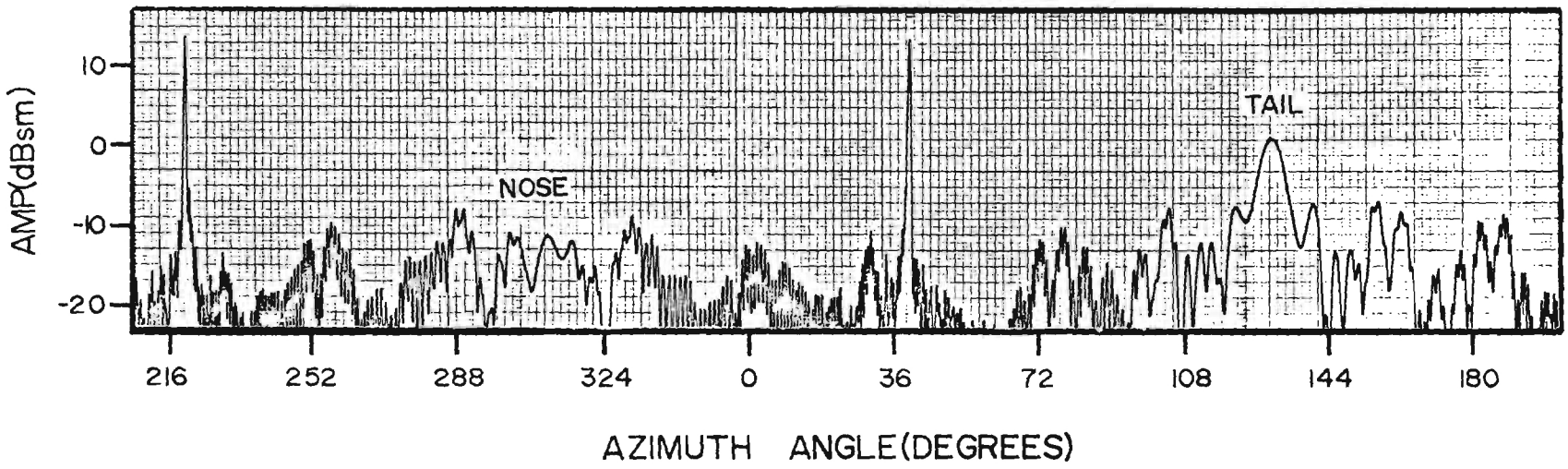

Figure 8. Compact Range RCS Measurements of The Zuni Rocket (360° Azimuth Rotation) at 0° Roll Angle, 10.0 GHz, and Vertical Polarization.

A-2940

Cost Information

The following charges have been incurred against the contract during period 1 June through 30 June, 1981.

	Expended	Encumbered
Personal Services (PS)	$ 1,205.01	$ -0-
Materials and Supplies	439.74	(91.60)
Travel	127.65	-0-
Overhead (@ 76% of PS)	879.66	-0-
Retirement (@ 10.51% of PS)	133.30	-0-
TOTAL	2,785.36	$ (91.60)

The breakdown of personal services is as follows:

	Dollars	Approximate Man Hours
Principal Research Scientists/Engineers	$ -0-	0
Senior Research Scientists/Engineers	528.31	27
Research Scientists II/Engineers II	-0-	0
Research Scientists I/Engineers I	-0-	0
Technicians/Draftsmen	253.60	26
Students	388.66	70
Secretarial/Clerical/Other	34.44	5
TOTAL	1,205.01	128

The current financial status of the contract is as follows:

	Budget As Proposed	Expended	Free Balance
Personal Services (PS)	$ 23,412.37	$ 2,330.75	$ 21,081.62
Materials and Supplies	3,923.42	684.66	3,238.76
Travel and Shipping	1,734.00	249.42	1,484.58
Computer	-0-	-0-	-0-
Overhead	17,42[illegible]6	1,701.45	15,724.51
Retirement	1,587.25	248.07	1,339.18
Encumbered	-0-	-0-	-0-
TOTAL	$ 48,083.00	$ 5,214.35	$ 42,868.65

FUNDING

Based on present full funding, the funding and equivalent man hours are sufficient to complete the task. Approximately 11 % of the proposed task has been completed.

A-2940

Monthly Technical Report No. 3
and
Monthly Cost and Performance Report No. 3

Report Period
July 1-July 31, 1981

DYNAMICALLY AIMED FREE FLIGHT ROCKET TASK

D.J. Kozakoff

Contract No. DAAH01-81-D-A003
Delivery Order No. 0016
EES Project A-2940

Effective Date: 4/23/81
Expiration Date: 9/30/81

Prepared for

U.S. Army Missile Command
Attn: DRDMI-ICBB/Lukens
Redstone Arsenal, Alabama 35809

Prepared by

Georgia Institute of Technology
Engineering Experiment Station
Atlanta, Georgia 30332

WORK PERFORMED DURING THIS REPORT PERIOD

Performance tradeoffs of various sensors have continued. A trip was made to MICOM to discuss trajectory data with the contract technical monitor.

Full scale Ku-band RCS measurements were performed. The resulting data are being factored into the tradeoff study.

PROBLEMS ENCOUNTERED

No problems were encountered during this period.

WORK TO BE PERFORMED IN THE NEXT REPORT PERIOD

Finalize sensor trades and identify a baseline sensor design. Work on the final report will begin.

Cost Information

The following charges have been incurred against the contract during period July 1 -July 31, 1981

	Expended	Encumbered
Personal Services (PS)	2,244.90	
Materials and Supplies	13.00	
Travel	108.12	
Overhead (@ 75% of PS)	1,683.68	
Retirement (@ 11.11% of PS)	217.33	
TOTAL	4,267.03	0

The breakdown of personal services is as follows:

	Dollars	Approximate Man Hours
Principal Research Scientists/Engineers	0	0
Senior Research Scientists/Engineers	802.50	375
Research Scientists II/Engineers II	1,092.28	64
Research Scientists I/Engineers I	0	0
Technicians/Draftsmen	0	0
Students	270.70	44
Secretarial/Clerical/Other	79.42	11
TOTAL	2,244.90	156.5

The current financial status of the contract is as follows:

	Budget As Proposed	Expended	Free Balance
Personal Services (PS)	14,292.37	4,575.65	9,716.72
Materials and Supplies	2,723.42	697.66	2,025.76
Travel and Shipping	750.00	357.54	392.46
Computer	0	0	0
Overhead	10,646.96	3,3385.13	7,261.83
Retirement	1,587.25	465.40	1,121.85
Encumbered	0	0	0
FUNDING	30,000.00	9,481.38	20,518.62

Based on present full funding, the funding and equivalent man hours are sufficient to complete the task. Approximately 32 % of the proposed task has been completed.

A-2940

Monthly Technical Report No. 4

and

Monthly Cost and Performance Report No. 4

Report Period
August 1 - August 31, 1981

DYNAMICALLY AIMED FREE FLIGHT ROCKET TASK

D.J. Kozakoff

Contract No. DAAH01-81-D-A003
Delivery Order No. 0016
EES Project A-2940

Effective Date: 4/23/81
Expiration Date: 9/30/81

Prepared for

U.S. Army Missile Command
Attn: DRDMI-ICBB/Lukens
Redstone Arsenal, Alabama 35809

Prepared by

Georgia Institute of Technology
Engineering Experiment Station
Atlanta, Georgia 30332

WORK PERFORMED DURING THIS REPORT PERIOD

Radar tradeoff studies have progressed. In addition, evaluation of laser and IR trackers have been factored into the study. A trip was made to Redstone Arsenal to discuss progress with the contract technical monitor.

PROBLEMS ENCOUNTERED

No problems were encountered during this period.

WORK TO BE PERFORMED IN THE NEXT REPORT PERIOD

The objectives for the following month are to tie together the results of all the individual sensor category tradeoffs. From the data base, an optimum sensor definition for the DAFFR application will emerge.

A-2940

Cost Information

The following charges have been incurred against the contract during period August 1-August 31, 1981

	Expended	Encumbered
Personal Services (PS)	$7,294.65	0
Materials and Supplies	214.62	0
Travel	352.09	0
Overhead (@ 75% of PS)	5,442.21	0
Retirement (@ 11.11% of PS)	778.64	0
TOTAL	$14,082.21	0

The breakdown of personal services is as follows:

	Dollars	Approximate Man Hours
Principal Research Scientists/Engineers	$ 210.72	8
Senior Research Scientists/Engineers	3,980.40	186
Research Scientists II/Engineers II	971.47	57
Research Scientists I/Engineers I	836.55	61
Technicians/Draftsmen	966.73	106
Students	75.40	12
Secretarial/Clerical/Other	253.65	34
TOTAL	$7,294.65	464

The current financial status of the contract is as follows:

	Budget As Proposed	Expended	Free Balance
Personal Services (PS)	$14,292.37	$11,870.30	$2,422.07
Materials and Supplies	2,723.42	912.28	1,811.14
Travel and Shipping	750.00	709.63	40.37
Computer	0	0	0
Overhead	10,646.96	8,827.34	1,819.62
Retirement	1,587.25	1,244.04	343.21
Encumbered	0	0	0
FUNDING	$30,000.00	$23,563.59	$6,436.41

Based on present full funding, the funding and equivalent man hours are sufficient to complete the task. Approximately78.5% of the proposed task has been completed.

PROJECT NO. A–2940

DYNAMICALLY AIMED FREE FLIGHT ROCKET SENSOR STUDY

GEORGIA INSTITUTE OF TECHNOLOGY

A Unit of the University System of Georgia
Engineering Experiment Station
Atlanta, Georgia 30332

1981

September 1981

FINAL REPORT FOR PERIOD 23 April – 30 September 1981

Prepared for

U.S. ARMY MISSILE COMMAND
Advanced Sensors Directorate
Redstone Arsenal, Alabama 35809

Contract No. DAAH01–81–D–A003
Delivery Order 0016

FINAL TECHNICAL REPORT

Project A-2940

DYNAMICALLY AIMED FREE FLIGHT ROCKET SENSOR STUDY

September 1981

D.J. Kozakoff, J.M. Newton, P.P. Britt, L.C. Bomar,
and J.J. Gallagher

Contract No. DAAH01-81-D-A003
Delivery Order 0016

U.S. Army Missile Command
Advanced Sensors Directorate
Redstone Arsenal, Alabama 35809

Prepared by

Georgia Institute of Technology
Engineering Experiment Station
Atlanta, Georgia 30332

Unclassified

SECURITY CLASSIFICATION OF THIS PAGE *(When Data Entered)*

REPORT DOCUMENTATION PAGE		READ INSTRUCTIONS BEFORE COMPLETING FORM
1. REPORT NUMBER A2940	2. GOVT ACCESSION NO.	3. RECIPIENT'S CATALOG NUMBER
4. TITLE *(and Subtitle)* DYNAMICALLY AIMED FREE FLIGHT ROCKET SENSOR STUDY		5. TYPE OF REPORT & PERIOD COVERED Final Report 23 April - 30 Sept. 1981 6. PERFORMING ORG. REPORT NUMBER
7. AUTHOR*(s)* D.J. Kozakoff, J.M. Newton, P.P. Britt, L.C. Bomar and J.J. Gallagher		8. CONTRACT OR GRANT NUMBER*(s)* DAAH01-81-D-A003 Delivery Order 0016
9. PERFORMING ORGANIZATION NAME AND ADDRESS Engineering Experiment Station Georgia Institute of Technology Atlanta, Georgia 30332		10. PROGRAM ELEMENT, PROJECT, TASK AREA & WORK UNIT NUMBERS
11. CONTROLLING OFFICE NAME AND ADDRESS U.S. Army Missile Command Redstone Arsenal, Alabama 35809 Project Technical Monitor: H. Buie		12. REPORT DATE September, 1981 13. NUMBER OF PAGES 94
14. MONITORING AGENCY NAME & ADDRESS*(if different from Controlling Office)*		15. SECURITY CLASS. *(of this report)* Unclassified 15a. DECLASSIFICATION/DOWNGRADING SCHEDULE

16. DISTRIBUTION STATEMENT *(of this Report)*

17. DISTRIBUTION STATEMENT *(of the abstract entered in Block 20, if different from Report)*

18. SUPPLEMENTARY NOTES
The views and conclusions contained in this document are those of the authors and should not be interpreted as necessarily representing the official policies, either expressed or implied, of the U.S. Army Missile Command.

19. KEY WORDS *(Continue on reverse side if necessary and identify by block number)*
Unguided projectile, Zuni rocket, signatures, microwave and millimeter wave radars, Laser trackers, IR trackers, DAFFR.

20. ABSTRACT *(Continue on reverse side if necessary and identify by block number)*
This document contains analyses of sensor approaches which can be implemented to gather trajectory data from a single shot test round from the DAFFR rocket launcher. These data permit subsequent adjustment to the launcher to correct for the effects of surface winds on trajectory, thereby improving CEP accuracy of subsequent rounds.

DD FORM 1 JAN 73 1473 EDITION OF 1 NOV 65 IS OBSOLETE

Unclassified

SECURITY CLASSIFICATION OF THIS PAGE *(When Data Entered)*

Table Of Contents

List of Figures

List of Figures (cont'd)

List of Figures (cont'd)

List Of Tables

1.0 Introduction

The known dispersions of unguided rocket artillery indicate 85% of the ultimate (CEP) error in hitting the target are due to uncertainties in surface winds up to an altitude of about 2 km. The purpose of the sensor described herein is to track and record position and velocity data of a single shot DAFFR (Dynamically Aimed Free Flight Rocket) registration round such that the aiming error could be quantified and corrected within 10 seconds of launch. As a result, the CEP for subsequent rounds fired in ripple fire or salvo would be greatly enhanced.

In this study, a number of different sensor types were investigated and traded off in terms of performance. These include laser, passive infrared (IR), and microwave and millimeter wave (MMW) radars. The tradeoffs included consideration at atmospheric and rocket plume effects. In addition, radar cross section (RCS) measurements on a full scale Zuni rocket model were accomplished to quantify the vehicle RCS signature. For tradeoffs herein, frequencies of interest were taken to be 10,17, 35 and 94 GHz, all of which fall in the well known atmospheric windows.

There are a number of qualitative factors which apply to all sensor categories:

1) The sensor is to be mounted on the rocket launcher so that tracker viewing from rear aspect must track through the turbulent plume.

2) The sensor must have no moving parts. This restriction, coupled with the fact that surface winds could cause significant deflections from its calculated trajectory, requires the sensor have an instantaneous field of view (FOV) of at least $\pm$ 5 degrees.

3) The physical space available for a sensor on the launcher lies within a diameter of approximately 24-inches.

As a result of this study a baseline X-band coherent-on-receive pulsed radar evolved. Signal budget calculations indicate a minimum required transmit power of 1 kW peak. The availability of low cost

pulsed magnetrons should allow DAFFR radar implementations of at least 10 kW peak to provide an adverse weather safety margin.

The report organization herein systematically treats each sensor category. In section 2.0, trajectory data which impacts sensor field-of view (FOV) requirements are discussed. Sections 3.0 through 5.0 discuss radar; section 3.0 presents calculated and measured radar cross section (RCS) data, section 4.0 factors these data into radar signal margin budgets, and section 5.0 develops specifications of the baseline radar. Sections 6.0 and 7.0 discuss laser and IR trackers, respectively.

2.0 PROJECTILE FLIGHT DYNAMICS

2.1 Trajectory and Location Basket at Burnout

It is the purpose of the DAFFR tracker to provide position and velocity vector information on a Zuni rocket. These data can then be compared with an ideal profile so that the rocket launcher may be re-aimed to account for flight errors. Paramount in the tracker design requirements are that the unit be physically small yet produce high track accuracy in all types of weather.

Since the tracker will be exposed to extremely high vibration and shock levels, delicate mechanical and electrical systems are deemed inappropriate. Therefore, critically aligned optics and gimbaled antenna are not desirable. This then dictates that a "starring" type tracker be employed. The critical parameter in this design is that wind acting upon the free flight rocket can cause it to drift up to five degrees away from the boresight axis. Consequently, the beamwidth of the tracker must be broad enough to accept these drifts, yet the beam cannot be made arbitrarily large since degradation of the trackers accuracy would result.

Trajectory data is necessary so that required sensor FOV's and signal Budgets based on sensor-to-projectile range during flight can be formulated. In Appendix A computed DAFFR rocket trajectories for a no-wind condition are summarized for various launch angles. At burnout (1.89 seconds), the range from launch encompasses 634 to 732 meters for launch angles running from 45 to 35 degrees, respectively. For this study a minimum tracking range of 1600 m is adopted, which corresponds to about 3.4 seconds into flight. The maximum axial velocity with respect to the sensor is about 665 m/s.

Table 1 contains projectiles angular displacements from the nominal launch angle (QE line) for various cross wind velocities; the parameters are illustrated in Figure 1. These data are given for 1.2, 1.89 and 3.00 seconds after launch.

Table 1

ROCKET POSITION VERSUS LAUNCH ANGLE AND WIND SPEED [3]

QE (Deg.)	WIND SPEED (Knots)	DISPLACEMENT ANGLES RELATIVE TO QE LINE								
		@ 1.20 sec			@ 1.89 sec (BURNOUT)			@ 3.00 sec		
		ΔEl	ΔAz.	ΔT	ΔEl	ΔAz.	ΔT	ΔEl	ΔAz.	ΔT
10	10	1.59	1.04	1.90	2.14	1.42	2.56	2.64	1.55	3.06
10	20	1.57	2.08	2.60	2.12	2.81	3.52	2.62	3.08	4.04
20	10	1.52	1.05	1.85	2.05	1.42	2.49	2.53	1.56	2.97
20	20	1.50	2.07	2.56	2.03	2.81	3.47	2.51	3.08	3.98
30	10	1.41	1.05	1.75	1.90	1.42	2.37	2.35	1.56	2.82
30	20	1.39	2.07	2.49	1.88	2.80	3.37	2.33	3.08	3.86
40	10	1.25	1.05	1.63	1.69	1.42	2.21	2.09	1.57	2.61
40	20	1.23	2.06	2.40	1.67	2.79	3.25	2.07	3.06	3.69
45	10	1.15	1.05	1.55	1.56	1.42	2.11	1.93	1.56	2.48
45	20	1.13	2.05	2.34	1.54	2.77	3.17	1.91	3.05	3.59
45	30	1.12	3.01	3.21	1.52	4.06	4.33	1.89	4.46	4.84

Note: These data are based on a crosswind to flight direction.

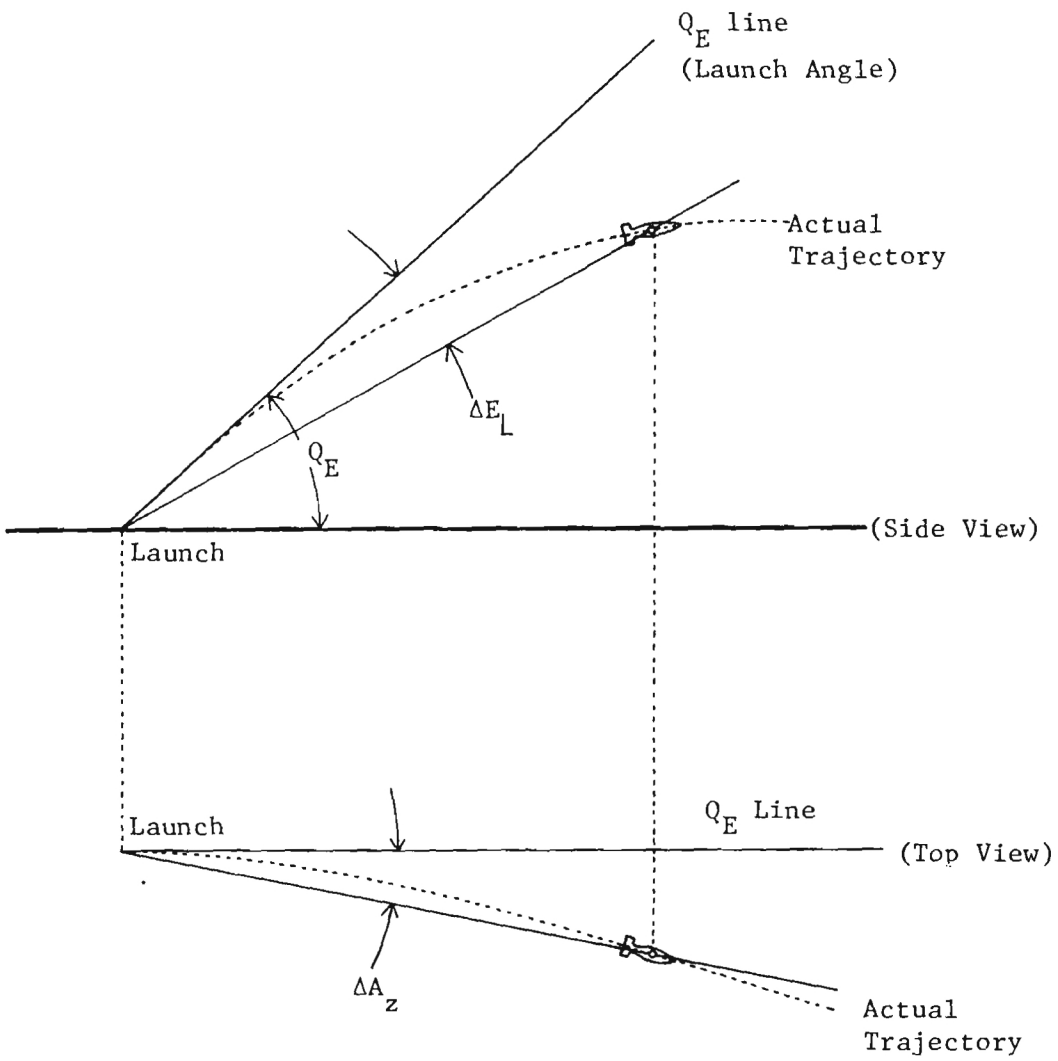

$$\Delta T = \sqrt{\Delta A_z^2 + E_L^2}$$

Figure 1. Definition of Trajectory Parameters

Here, $\Delta E1$ and ΔAz are the elevation and azimuth displacements from the line-of-sight vector, respectively; ΔT is the total angle. From the data in Table 1, it is apparent that line-of-sight angle changes can be large, especially for high wind speeds. Indeed for a wind speed of 30 knots and a launch angle of 45 degrees, angular errors of almost $\pm$ 5 degrees are calculated for a 3 second flight time. Other data (not shown), predict worst case angular errors of 11 degrees in a 70 knot wind. However, the likelihood of a DAFFR being launched in a 70 knot wind is very small. A more realistic wind speed is 20 to 30 knots.

Based on the dispersions resulting from wind, a projectile location basket can be defined via methods previously developed [1,2]. Here, the probability of projectile deviation r from the nominal line of sight* is given by

$$p(r) = \frac{r}{2\pi\sigma^2} \int \exp\left[\frac{-r^2}{2\sigma^2}\right] d\theta \qquad (1)$$

From the available data base, the variance is derived using the formula:

$$\sigma^2 = 0.7213\ \Delta^2 \qquad (2)$$

where the parameter Δ as a function of wind velocity and radial distance r from sensor is shown in Table 2.

The analysis herein indicates that under the worst case conditions, a ±5 degree angular error is anticipated which encompasses the projectile location basket at the largest range of interest (i.e., about 3 km.) An ungimballed sensor would only need to provide an instantaneous field-of-view (FOV) of at least 10 degrees (total) in order to accommodate this situation.

*Note: r is measured normal to line-of-sight vector

Table 2

EMPIRICALLY DERIVED RELATION BETWEEN VARIANCE AND WIND VELOCITY

		For R = 1600 m		
Wind Velocity (knots)	Δ/R	Δ (m)	σ (m)	σ^2 (m^2)
30	0.0845	135.16	113.71	12,930.
20	0.0627	100.25	84.34	7,113.
10	0.0433	69.25	58.26	3,394.

2.2 Measurement Requirements

Based on the projectile trajectory data discussed in the prior subsection, and the location baskets which result from up to 30 knots surface winds, a compilation of sensor measurement requirements were adopted for this study; these are shown in Table 3. In addition, sensor performance must meet these minimum requirements under all adverse weather and battlefield conditions.

While acquisition and tracking prior to burnout is desirable, it is not mandatory for accomplishment of the measurement goals herein, assuming acquisition can be accomplished immediately after burnout and projectile is tracked to at least 2 km. However, the rocket plume effects on the various sensor types are a consideration. Field measurements of Zuni rocket plume effects on radars operating at 10, 35 and 95 GHz have been recently completed by Georgia Tech [4] and will be discussed in a subsequent subsection.

Table 3.

DAFFR TRACKER MEASUREMENT REQUIREMENTS

Instantaneous FOV

- Az: $\pm$ 100 mrad, min.
- El: $\pm$ 100 mrad, min.

Accuracy

- Az: $\pm$ 2 mrad
- El: $\pm$ 2 mrad
- Range: 10 m
- Range Rate: 5 m/sec

Track

- Range: 1600 m (minimum)
- Velocity: 750 m/sec
- Accel: 600 m/sec^2

Physical Volume Limitations

- 2 ft max linear dimension
- 2-3 cu ft total volume

3.0 PROJECTILE RCS SIGNATURE

3.1 General

The MICOM-directed-requirements to evaluate radar sensors operating at 10, 17, 35 and 95 GHz necessitated the availability of accurate RCS data for signal budget calculations. It was found that the required data base for a Zuni type rocket did not exist. Hence, Georgia Tech developed the required data base via a combination of measurements and calculations.

The availability of a compact range RCS facility operating through Ku-band, permitted RCS measurements of a full scale Zuni rocket at 10 and 16 GHz. However, since a millimeter wave RCS measurements facility was not available for Zuni rocket RCS characterization at 35 and 95 GHz, these data had to be obtained via theoretical techniques.

3.2 Measured RCS Data

To accomplish Zuni rocket RCS signature characterization, a full scale projectile model was fabricated in the Georgia Tech model shop; an actual Zuni rocket nozzle and fin assembly were provided by MICOM. A photograph showing the model in the compact range measurements facility is shown in Figure 2.

A complete summary of the measurement method and resultant data base appear in Appendix B. The primary data of interest corresponded to $\pm$ 5 degrees about tail aspect, however, measurements were obtained for $\pm$ 24 degrees about tail aspect. X-band measurements were performed for both vertical and, subsequently, horizontal polarization. Missile roll angles running from 0 through 75 degrees in 15-degree increments were measured to examine null structure detail off tail aspect.

The typical X-band data obtained indicate a peak RCS value of 0 dBsm. At the worst case $\pm$ 5-degree aspect off the tail (as determined in the previous section), the RCS was about -10 dBsm. This value is used in all subsequent signal budget estimates. Examination of the null structure within the $\pm$ 5 degrees tail aspect in the data of Appendix B suggested projectile RCS enhancement may not be necessary at X-band because of the narrowness of the nulls.

A small amount of measurement data were also obtained at Ku-band (16 GHz). The peak tail aspect RCS data was +4 dBsm at Ku-band compared to 0 dBsm at X-band. The main lobe RCS pattern was found to be significantly narrower at Ku-band than X-band, i.e. 8 degrees null-to-null beamwidth compared to 11 degrees.

The null structure of the Ku-band data indicate -25 dB nulls falling with the $\pm$ 5 degrees off tail aspect angles of interest. Therefore, projectile RCS enhancement is most likely required at Ku-band to provide a suitable target return for radar tracking.

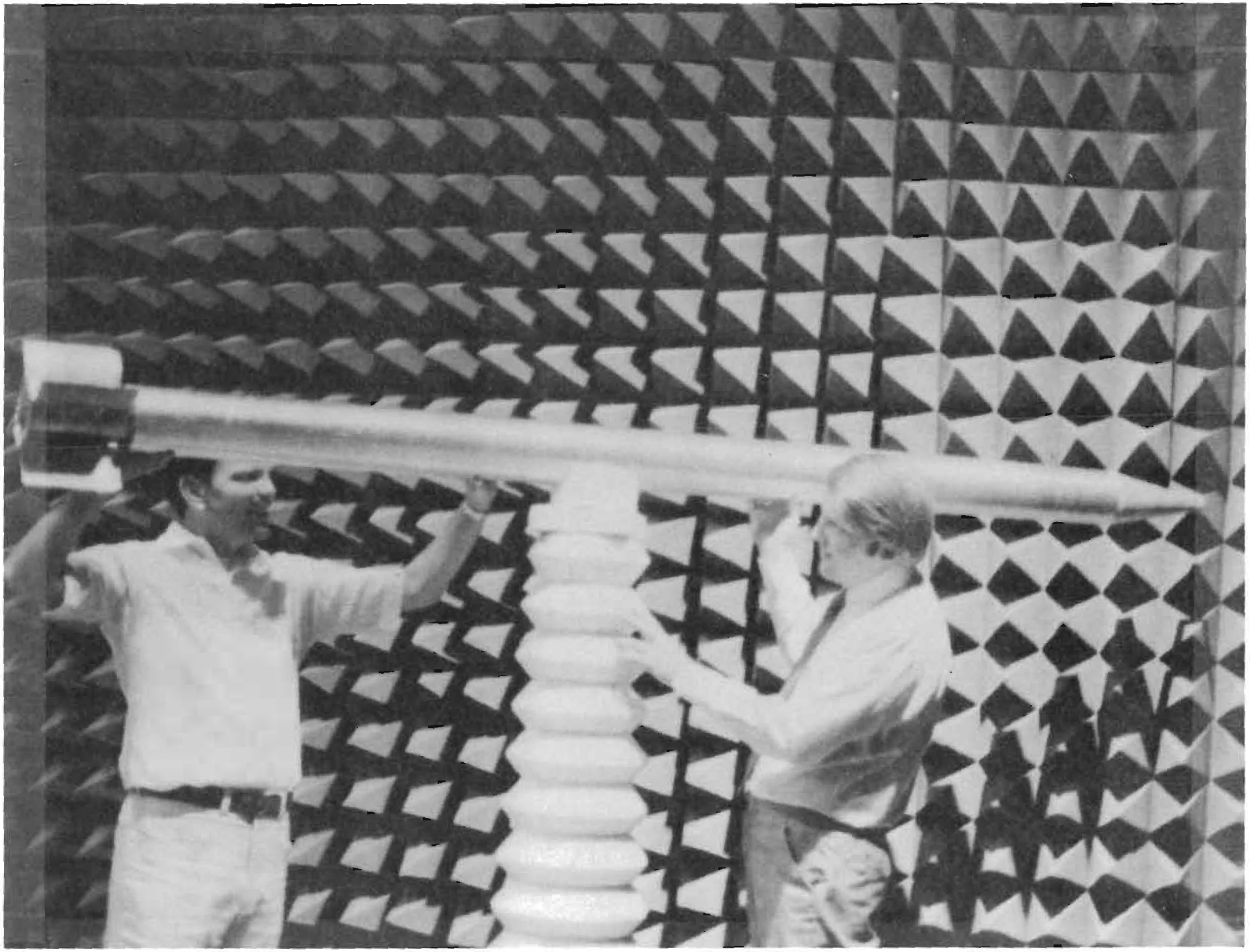

Figure 2. Full Scale Zuni Rocket During RCS Measurements.

3.3 Computed RCS Data

The radar cross-section of the rear aspect of the Zuni rocket was measured at 10 and 16 GHz and computed at 35 and 95 GHz. The rear aspect of the Zuni was modeled for RCS determination. It was initially thought that the tail fins, cylindrical body, and rocket rear would need to be included in this model, but examination of RCS data indicated that acceptable agreement could be obtained by simply modeling the Zuni rear as an annulus. The inside dimension of the annulus was chosen to be the exhaust diameter. The outside diameter of the annulus was taken to be the diameter of the rocket.

The RCS of a simple annulus is given by [6]:

$$\sigma = \frac{\lambda^2 \cos^2\theta}{\pi} \left[(ka_2)^2 \frac{J_1(2ka_2\sin\theta)}{(2ka_2\sin\theta)} - (ka_2)^2 \frac{J_1(2ka_1\sin\theta)}{(2ka_1\sin\theta)} \right] \quad (3)$$

where λ = free-space wavelength

k = $2\pi/\lambda$

θ = incidence angle

a_1 = rocket radius

a_2 = rocket exhaust radius

J_1 = Bessel function

Evaluation of this function for incidence angles less than 20 degrees shows excellent correspondence with measured data. This agreement is shown in Figure 3 for the 10 GHz RCS data. Figure 4 shows how the rear aspect RCS of the Zuni rocket changes with frequency and incidence angle.

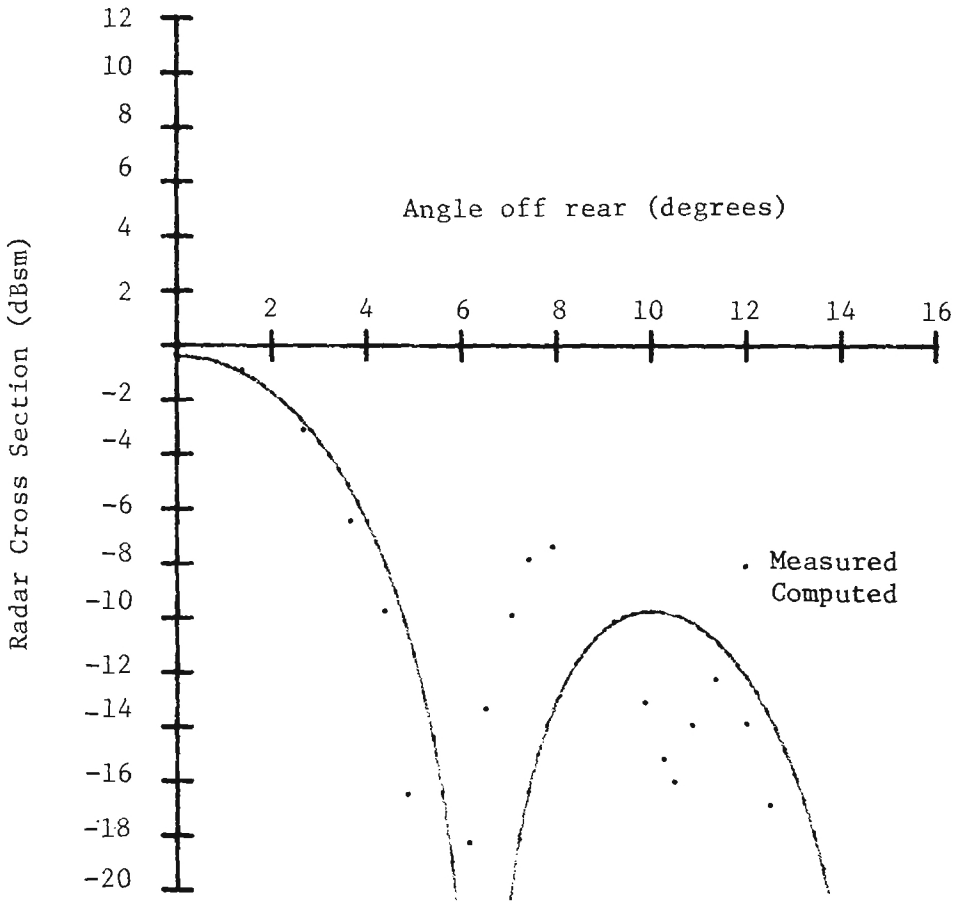

Figure 3. Comparison of Computed and Measured X-Band RCS Data.

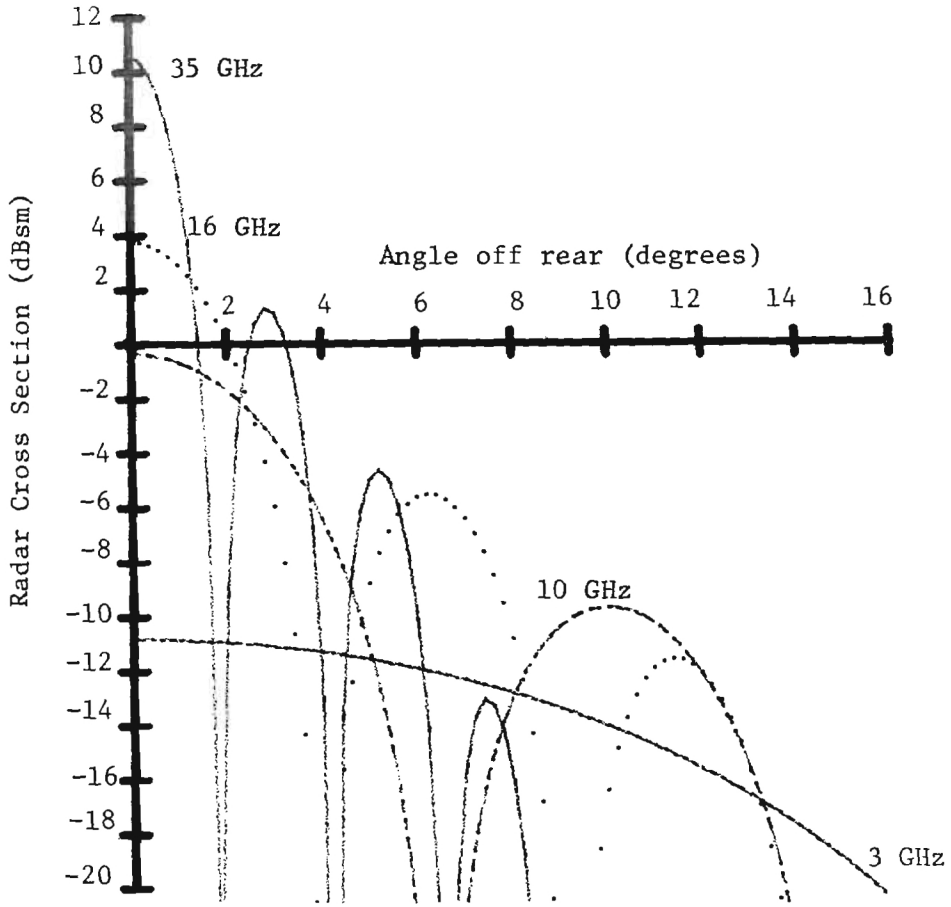

Figure 4. Computed RCS Summary About Tail Aspect

4.0 Microwave and Millimeter Wave Radar Considerations

4.1 Atmospheric Effects

The clear atmosphere progagation losses for 10 GHz, 6 GHz, 35 GHz and 94 GHz all fall within atmospheric "windows" as illustrated in Figure 5. However, the total transmission losses are monotonically increasing with frequency. These losses are roughly as follows:

10 GHz	0.02 dB/km
17 GHz	0.06 dB/km
35 GHz	0.15 dB/km
94 GHz	0.45 dB/km

When the effects of rain are added to the clear weather propagation losses, the losses become very appreciable especially with increasing frequency. For instance, Figure 6 depicts one-way rain attenuation for a 5 mm/hr rate. The worst case data indicates the values shown in Table 4.

The effects of snow fall on atmospheric propagation are illustrated by the data in Figure 7. Here, the attenuation increases with increasing frequency, but the total attenuation in dB/km due to snowfall will be generally less than due to rain. For the data shown, the two-way atmospheric losses due to the snowfall of 1 mm (liquid)/hr represent something in the order of 0.02 dB/km at 10 GHz to a high of about 7 dB/km at 94 GHz.

For radar signal budgets to appear in the next section, Table 5 presents equations that have been produced by examining the two-way radar signal loss for various rain rates. These equations account for attenuations from all sources including radar backscatter, but do not directly give the rain backscatter values. Values for rain backscatter are given in Table 6. Data for various fog densities are given in Table 7. Backscatter from the rain and fog is not anticipated to be a problem for a radar tracker since its effects may be eliminated by setting the acceptable range of radar Dopplers higher than the anticipated Doppler return from the water droplets.

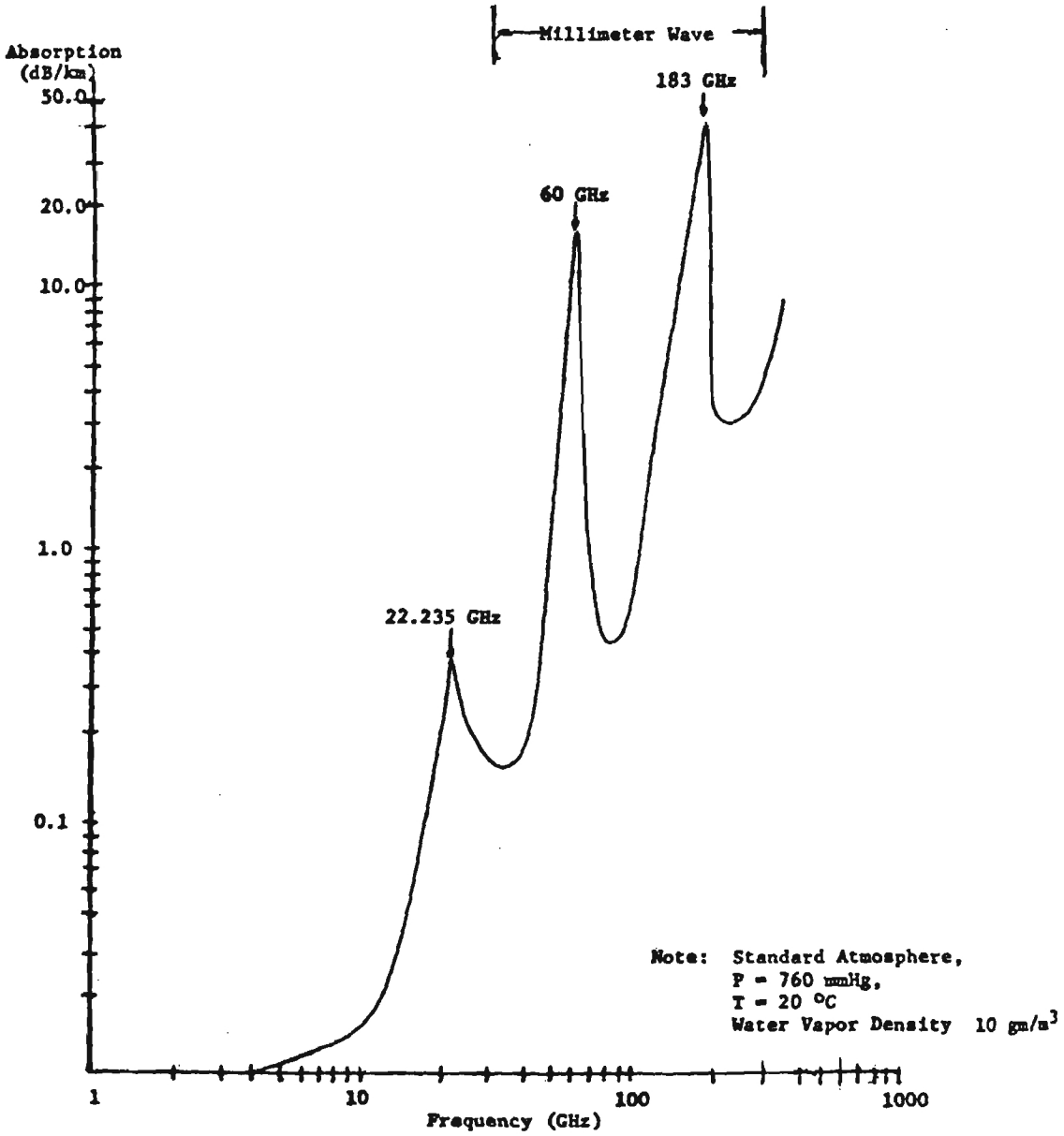

Figure 5. Sea Level Atmospheric Absorption [5].

Table 4

WORST CASE RAIN ATTENUATION FOR 5 mm/hr RAIN RATE

Frequency	One-Way (dB/km)	Two-Way (dB/km)
10 GHz	0.2	0.4
17 GHz	0.45	0.9
35 GHz	1.20	2.40
94 GHz	4.5	9.0

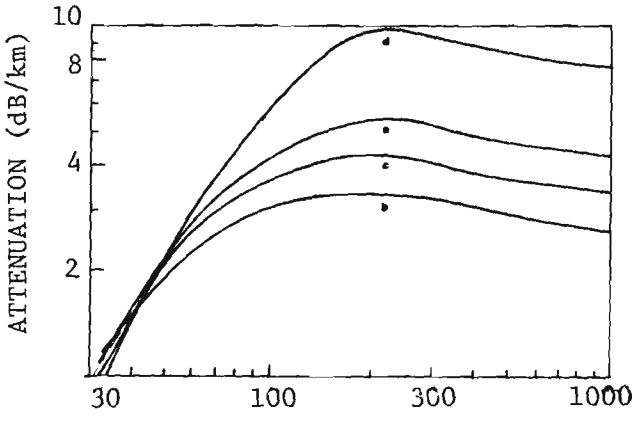

Figure 6. Rain Attenuation For Various Drop Size Distributions At A Rainfall Rate Of 5 mm/hr. [4]

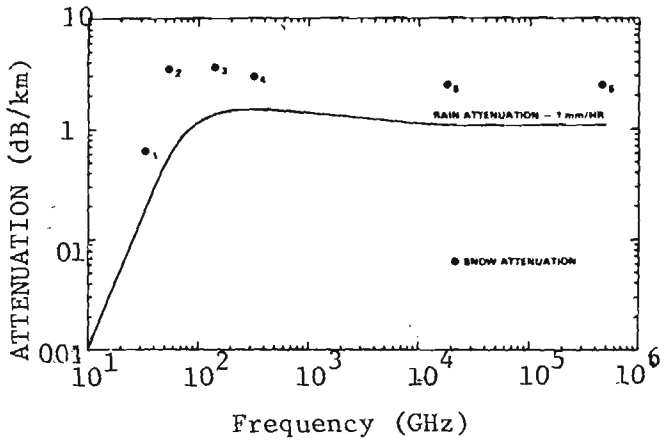

Figure 7. Snow Attenuation Versus Frequency [4]

Table 5

ATMOSPHERIC ATTENUATION (dB/km) AS A
FUNCTION OF FREQUENCY AND RAIN RATE (mm/hr)

Frequency	Equation
10 GHz	$\text{Loss}\left(\frac{\text{dB}}{\text{km}}\right) = 2[0.013 + 0.00919\ RR^{(1.16)}]$
16 GHz	$= 2[0.045 + 0.039\ RR^{(1.124)}]$
35 GHz	$= 2[0.080 + 0.273\ RR^{(0.985)}]$
95 GHz	$= 2[0.22 + 1.60\ RR^{(0.640)}]$
140 GHz	$= 2[0.30 + 1.60\ RR^{(0.70)}]$

Table 6

RAIN BACKSCATTER COEFFICIENT (m^2/m^3)

Frequency (GHz)	Rainfall Rate (mm/hr)		
	1	4	16
9.375	1.03×10^{8}	8.5×10^{-8}	6.9×10^{-7}
16	1.4×10^{-6}	1.1×10^{-5}	9.5×10^{-5}
35	2.2×10^{-5}	9.2×10^{-5}	4.3×10^{-4}

Table 7

ATTENUATION RATE SEA LEVEL (dB/km)

	10 GHz	35 GHz	70 GHz	94 GHz
Clear Air ($7.5\ gH_2O/m^3$)	0.018	0.12	0.7	0.4
FOG				
Light ($0.01\ g/m^3$)	0.0186	0.126	0.722	0.435
Thick ($0.1\ g/m^3$)	0.024	0.18	0.92	0.75
Dense ($1.0\ g/m^3$)	0.078	0.72	2.90	3.90

4.2 Rocket Plume Effects

The attenuation of the DAFFR exhaust plume is an important radar consideration. The chemical composition of the rocket exhaust is shown in Table 8. It is observed that major elements are aluminum oxide, carbon monoxide and hydrochloric acid. These compounds are not known to have resonances in the frequency regions of interest which indicate severe attenuations will not be experienced. The largest single compound in the plume (aluminum oxide) has also been shown to be a very low loss material in the microwave and millimeter wave regions. However, this compound has a dielectric constant somewhere between 8 and 10 which could lead to significant scattering of the tracking signal.

A data base quantifying the plume attenuation effects of the DAFFR rocket plume does not exist in the technical literature. However, Georgia Tech recently participated in a set of rocket plume attenuation measurements performed during Zuni rocket launches at Redstone Arsenal using an advanced instrumentation grade multi-channel receiver operating at 10, 35 and 95 GHz. These measurements were performed in September 1981.

Measurements made through the plume at right angles to the trajectory (i.e. cross plume paths) indicated only low values of attenuation. Nominal values measured were 0.5 dB (10 GHz), 0.3 dB (35 GHz) and 0.1 dB (95 GHz). Tracking paths through greater lengths of the plume geometry will yield resultingly higher attenuations, however, these are expected to still be relatively small compared to atmospheric adverse weather effects. A complete summary of the plume measurements and estimates of total plume attenuation will appear in the Georgia Tech final report [4].

Table 8

COMPOSITION OF ROCKET MOTOR EXHAUST [14]

CHEMICAL	GRAMS PRODUCED PER 100 GRAMS OF PROPELLANT
AlCl	0.01118
$AlCl_2$	0.05611
$AlCl_3$	0.00955
Al	0.00843
Al_2O_3	33.96397
CO	21.95053
CO_2	2.83523
Cl	0.10561
Fe	0.01801
FeCl	0.00327
$FeCl_2$	1.57580
$Fe(OH)_2$	0.00322
H	0.01419
HCl	20.24216
H_2	2.07671
H_2O	8.79125
NO	0.00107
N_2	8.22263
OH	0.02171
	99.99963

4.3 Signal Margin Calculations

The calculation of the signal margin realizable in tracking the Zuni rocket is impacted directly by three factors: radar design, atmospheric attenuation and scattering, and the radar cross section of the rocket.

The radar cross section of the Zuni rocket has been measured (see Appendix B) and found to be about 0 dBsm at 10 GHz and +4 dB at 16 GHz. These values were obtained for signals reflected directly off the rear of the rocket. Rotation of the rocket caused the RCS to drop rapidly falling below -10 dBsm for rotation angles greater than 5 degrees at 10 GHz and 3 degrees at 16 GHz. Due to the likelihood of aspect angles greater than these, some type of RCS enhancement is probably needed for frequencies above 10 GHz. The conformal array proposed by Ball is one technique for achieving the RCS improvement needed. This system is designed to produce an RCS of approximately -6 dBsm at 10 GHz. Therefore, the signal margin calculations in this subsection will assume a rocket RCS of -6 dBsm.

The tracking error of a monopulse type radar is given by [13]:

$$\sigma_t = \frac{\Theta_B}{K_m\sqrt{S/N}} \qquad (4)$$

Where Θ_B = 3dB beamwidth of the antenna pattern
K_m = difference error slope ($K_m \cong 1.57$)
S/N = receiver signal-to-noise ratio

Additionally, the RMS tracking error due to target glint is given by:

$$\sigma_g = \frac{0.35\ L_x}{R} \text{ radian} \qquad (5)$$

Where L_x = physical length of target (m)
R = range to target (m)

This expression was derived for a target consisting of scatters uniformly distributed over the target. Other scatter distributions give a constant value that varies between 0.2 and 0.35. For this report a constant value of 0.3 is assumed. In the present case it may be shown that the glint error is insignificant and that the track error due to noise is predominant. Indeed, for a rocket 500 meters from the tracker, the glint error is less than 0.0003 radians - the specific total track error is 0.002 radians. Examination of equation (4) with an assumed antenna beamwidth of 12 degrees, an error slope parameter of 1.57, and a desired track error of 0.002 radians shows that a signal-to-noise ratio of at least 37 dB is needed. Note that this value is independent of range since the desired track accuracy is independent of range. Assuming a tracker having the parameters shown in Table 9, Figure 8 shows the projected track range for a target having a 0.25 m^2 radar cross sections.

From these data it may be seen that for the 1 kW transmitter, only the 10 GHz systems can track the rocket to 1600 meters. Taking into account worst case atmospheric losses shown prior in Table 4, the 10 GHz system will also track in adverse weather. Satisfactory operation of radius operating above X-band will require considerably greater transmit power than 1 kW to overcome the atmospheric losses. For instance, worse case atmospheric losses at 95 GHz were shown to be over 9 dB/km; thus over $\pm$ 18 dB of increased transmit power is required to provide a suitable margin for adverse weather.

Table 9

ASSUMED RADAR TRACKER PARAMETERS

Frequency 10, 16, 35, 95 GHz

Single Pulse Detection

1000 watts peak transmit power

Bandwidth 500 kHz

PRF 75 kHz

Pulse Duration 2 usec (300 meter blind range)

Staring system (no gimbal)

Antenna Gain = 24 dBi

Receiver Noise Figure 10 dB

S/N ratio 37 dB

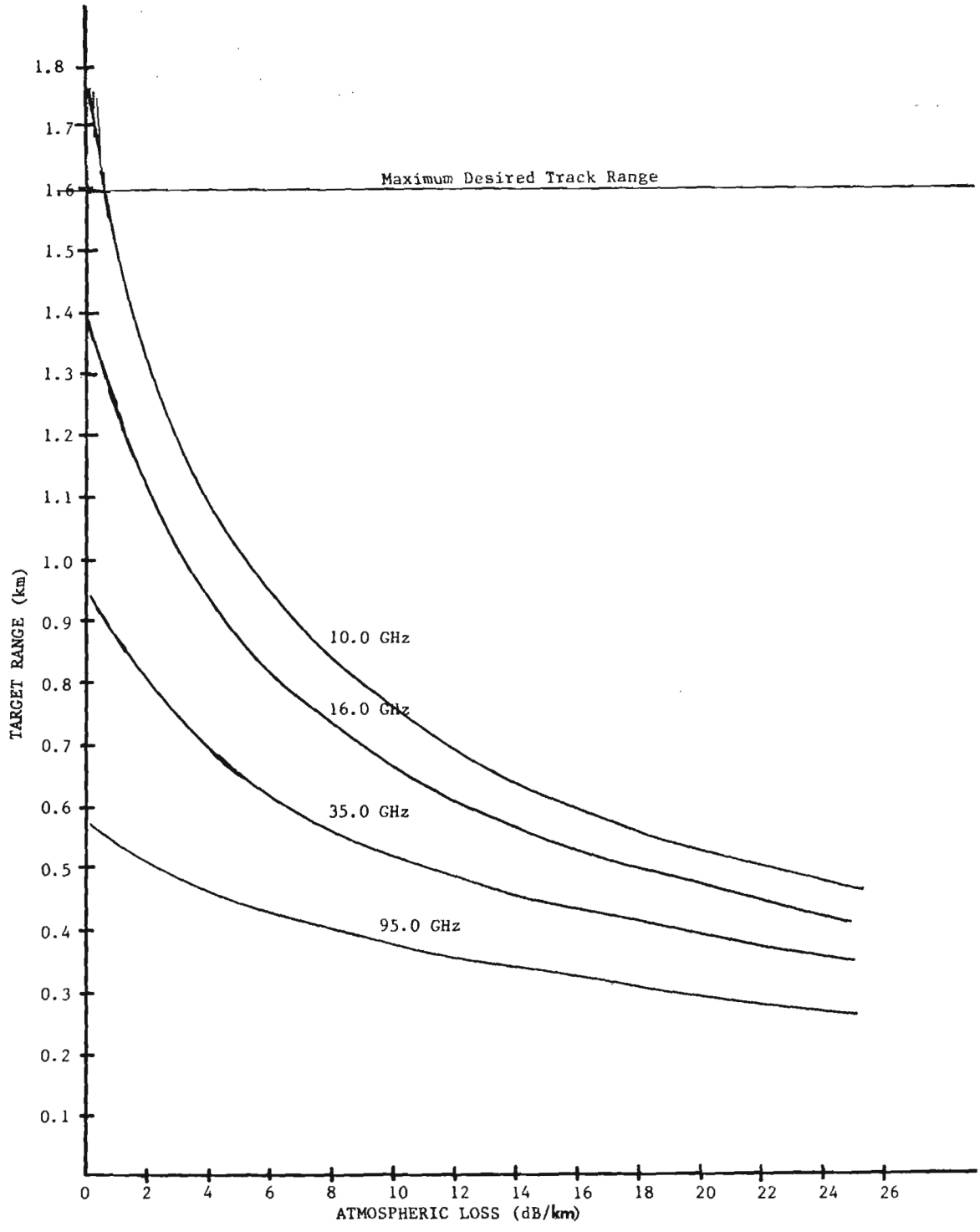

Figure 8. Zuni Projectile Track Range Versus One Way Atmospheric Loss.

5.0 Radar Hardware Considerations

5.1 System Tradeoffs

The radar system required to provide the desired range and cross range information for the free flight rocket is relatively straightforward. The radar system could be developed in one of several pulse or CW configurations. The basic measurement requirements for the radar system are:

Range coverage	0 to 3 km
Range accuracy	1 meter
Cross range accuracy	1 milliradian
Velocity	no specific requirements

The characteristics of the rocket that is to be tracked are:

Velocity	400 to 600 m/s (at 1-2 km range)
Radar cross section	1.0 m^2 (nominal)

The following discussions consider the merits and limitations of the most applicable radar configurations.

Pulsed Magnetron System

The noncoherent pulsed magnetron transmitter/receiver is the simplest and most cost effective of the applicable radar systems. The transmitter consists of a medium power, short pulsed, fixed frequency magnetron. The modulator and power supply are small and can be configured for rugged operation. The noncoherent pulsed magnetron radar has the capacity to measure range but has no ability to discriminate from land or rain clutter. In a coherent-on-receive configuration, the effects of stationary clutter can be cancelled. In this case, a sample of the transmitter is used to injection lock a coherent reference (COHO) which "remembers" the phase of the transmitter signal. This COHO is then used as the coherent reference in the down conversion of the received target echo. This technique would allow the target returns to be processed in the doppler domain so that MTI performance could be achieved. The short pulse required in this application (~ 100 nseconds) makes the injection locking of the COHO more difficult but an MTI improvement of 15 to 20 dB

can be easily obtainable. Care must be taken in the development and timing of the transmitter pulses to insure that blind speed or blind ranges do not occur for the target ranges and velocities anticipated for this application. The receiver local oscillator and COHO are the limitations on performance and the receiver implementation is considerably more complex than that of the noncoherent system.

Coherent Pulsed Amplifier

The best MTI performance is obtained by using a fully coherent transmitter and receiver. Implementation of this configuration requires the use of a stable, low noise, CW oscillator (STALO) which is up-converted with an IF frequency (COHO) and this sum frequency is amplified by a cross field amplifier or traveling wave tube amplifier. The CW STALO provides the coherent reference for the first down conversion and the COHO serves as the coherent IF reference used to convert the IF to baseband and Doppler. MTI clutter cancellation techniques can be applied to discriminate the desired moving targets from rain and other clutter returns. A fully coherent transmitter/receiver system should yield MTI improvements of 20 to 40 dB. The fully coherent system is more complex and expensive than either the noncoherent radar or the coherent-on-receiver radar.

CW Doppler Radar

An unmodulated CW radar directly measures only velocity (and angle with a monopulse receiver). Further study and analysis, using variations of Kalman filtering techniques, would be required to determine the accuracy of impact prediction using only the velocity and angle time histories in the ballistic equation.

A continuous wave radar system can also be used to extract the target range in the presence of clutter. The pure CW transmission contains no information for ranging, hence, additional modulation or processing must be required. A simple method of determining the range to the target with the CW transmission is to use integration of the velocity (Doppler). This requires that the range be known at one time and future estimates are determined by integrating velocity and adding to the range reference. The

Doppler (velocity) could be acquired as the rocket exits the launcher and integrated forward to predict the rocket range.

Modulation of the CW signal could take the form of a phase or frequency modulation of the CW signal. Since the target signals are offset from the clutter returns in frequency due to the Doppler shift, the range can be measured by correlating the return signals. Considerably more complexity is added by the modulation of the CW waveform. Care must be given to use a waveform code that has a sufficiently long range ambiguity, yet yields the resolution or accuracy required for the range measurement.

A second CW approach is to transmit two (or three) simultaneous RF frequencies. The velocity can be measured directly with either frequency and by observing the Doppler returns of the two frequencies from the same target, the range to the target can be calculated. The range can be shown to be related to the phase difference between the two return echoes. The Doppler shift allows the radar to operate in the presence of clutter and velocity can be determined unambiguously. The two RF frequencies must be selected to provide for an unambiguous range interval and still be able to provide an accurate measure of range. This usually results in the need for a third RF frequency which can be used to provide a "fine" range measurement but has a short range ambiguity. Hence, a coarse range/fine range measurement is required.

In all CW cases, the problem of antenna isolation and system degradation due to noise sidebands of the transmitter result in consideration of a two antenna system. In addition, when operated in the presence of strong clutter, the system may still be degraded due to the equivalent reduction of the antenna/receiver isolation. In addition, the complexity of the correlator to system in the case of the phase coded system or the spectrum analysis of the multifrequency system is significantly greater than that required by the MTI technique of the pulsed system.

Antenna Considerations

A number of applicable techniques could be used to obtain the cross range deviation of the rocket. A closed loop tracking system that follows

the target mechanically in angle or a fixed mounted antenna that generates errors due to the target location in angle could be implemented. Conical scan or monopulse could be applied to either scheme.

The closed loop tracking configuration allows the use of a narrow beam, high gain antenna since the antenna boresight is always maintained on the target. This results in very high tracking accuracy and angle measurement. Angle measurements are determined by position pickoff on the antenna gimbals. However, the use of the high gain antenna requires that some method be implemented for acquisition of the target in azimuth and elevation. In addition, there are many mechanical moving parts required and position accuracy is subject to mechanical wear and pickoff calibration.

The fixed mounted antenna requires the use of a lower gain, wide beamwidth antenna. The beamwidth is chosen so that the target stays within the antenna field of view. The angle off boresight is determined by calibration of the antenna error slope. The fixed mounted antenna has no moving mechanical parts and the acquisition problem is simple. The accuracy of the angle measurements is not as good as for a tracking system but may be acceptable depending upon the application.

Angle processing can be accomplished by the use of conical scan or monopulse. The conical scan technique is the simplest and least expensive, but also less accurate. The conical scan mechanics is a mechanical system with many moving parts, rotary joints and subject to wear and degradation. The monopulse is mechanically fixed and not susceptable to mechanical wear. The conical scan system and monopulse both generate an angle error response for off boresight targets but the conical scan system is more difficult to linearize. In addition, the effects of target scintillation and glint are likely to be much more degrading to the measurements in a conical scanner.

5.2 Preferred Approach

The radar system configuration preferred for the free flight rocket sensor is a pulsed magnetron, coherent-on-receive radar. This configuration provides the desired measurement accuracy in range and angle and permits the operation of the system in the presence of land clutter and rain. The radar will use currently available X-band components and well established signal processing techniques.

The basic radar block diagram is shown in Figure 9. The radar uses a medium power magnetron oscillator as the RF source. The RF energy is transmitted through the duplexer and radiated by the antenna. A sample of the transmitter is coupled from the magnetron to an RF mixer which combines this sample with a stable local oscillator (STALO). The output is an IF pulse (100-250 MHz) with a pulse width equal to the RF pulse. This IF pulse is then mixed with the coherent IF reference (COHO) to produce a phase reference value. The COHO is used to down-convert the received IF signals to baseband Doppler. The phase reference value is used to correct the target return prior to MTI processing. The Doppler signals are processed in a two pulse digital MTI canceller and the output processed in a range tracker to extract the range measurement.

The radar transmitter has a 50 kW magnetron transmitter with a pulse length of 100 nanoseconds and pulse repetition rate staggered approximately between 11.4 and 9.1 kHz. The single pulse signal to noise ratio for this system would be approximately [13]

$$S/N = \frac{P_t G^2 \lambda^2 \sigma}{(4\pi)^3 R^4 kTBFL} \qquad (6)$$

where,

P_t = Peak transmit power (W)

G = Antenna power gain (dimensionless)

λ = Wavelength (m)

σ = RCS (m^2)

R = Range (m)

k = Boltzman's constant = 1.38×10^{-23} J/K

T = Effective antenna temperature = 290°

B = Receiver noise bandwidth (Hz)

F = Front end receiver noise factor (dimensionless)

L = System loss factor (dimensionless)

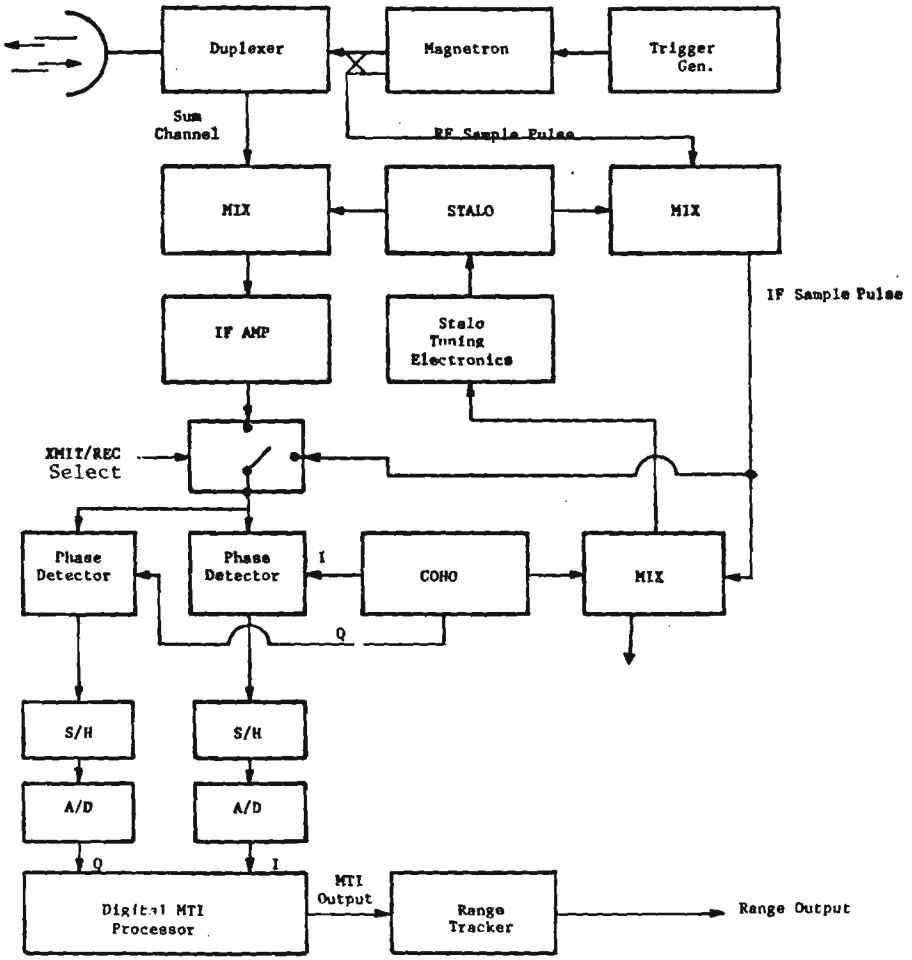

Figure 9. Basic Radar Block Diagram

For

P_t = 50,000 W
G = 316.22 (25 dB)
λ = 0.03 m
σ = 0.1 m^2
B = 14 x 10^{-6} Hz
L = 2.51 (-4 dB losses)
F = 4.0
R = 2000 to 3000 m

then S/N = + 24 dB (@ 2000 m)
= + 17 dB (@ 3000 m)

The standard deviation of the range measurement for a split gate range tracker in terms of pulse length τ for $B\tau = 1.4$ is [13]:

$$\sigma_r = \frac{\tau}{2.5\sqrt{2\ S/N}}, \qquad (7)$$

Where σ_r is in units of seconds. At 2000 meters the range measurement accuracy on a single pulse is:

$$\sigma_r = \frac{100 \times 10^{-9}}{2.5\sqrt{2\ (252)}} = 1.79 \times 10^{-9} \text{ sec (0.25 meters)} \qquad (8)$$

Similarly, at 3000 m, it can be shown σ_r corresponds to 0.6 meters. Consequently, there is sufficient range accurate measurement to at least 3000 meters. The measurement accuracy can be further enhanced by integrating over a number of pulses.

The launch angle of the rocket is sufficient to insure that the main antenna beam does not intercept ground clutter. However, the clutter may well enter through the antenna sidelobes. An estimate of ground clutter power is made via the formula [13]

$$P_c = \frac{P_t\ G_{sl}^2\ \lambda^2}{(4\pi)^3\ R^4} (\sigma^\circ\ Ac) \qquad (9)$$

where,

G_{sl} = Average Antenna Sidelobe Gain (dimensionless)

σ° = Ground Clutter Coefficient (m^2/m^2)

A_c = Clutter area $\simeq (R\theta)(c\tau/2)$

c = 3×10^{-8} m/s

τ = Pulsewidth (s)

θ = Sidelobe HPBW (radians)

Using the values,

R = 2000 m

G_{sl} = 0 dB = 1 (average sidelobe)

σ° = -15 dB (m^2/m^2) = 0.0316

P_t = 50,000 W

one obtains, $P_c \simeq$ - 81 dBm. Hence the clutter power is approximately 12 dB lower than the signal return from the rocket at a range of 2000 meters. Consequently, additional processing would probably be required to meet the measurement accuracy. Also, it should be noted that normalized radar cross sections of clutter can rise considerably above -15 dB m^2/m^2 in certain cases.

Another source of clutter would be from rainfall within the clutter cell containing the rocket. The backscatter power from rainfall at X-band is approximated as [13]

$$P_R = \frac{P_t G^2 \lambda^2}{(4\pi)^3 R^4} (\sigma_v V_R) \qquad (10)$$

where, σ_r = Normalized rain backscatter coefficient (m^2/m^3)

$V_R = (\pi/4)(R\theta)^2 (c\tau/2)$

Using the previous radar parameters and with an assumed $\sigma_v \simeq 10^{-6}$ for 10 mm/hr rain [13], then $P_R \simeq$-67 dBm. This clutter power returned from the rain cell is approximately 15 dB higher than the target reflected. Hence, additional processing may be necessary to achieve the required measurement accuracy.

In order to overcome the returns from rainfall and clutter, an MTI clutter canceller/filter will be implemented. This processor will have the benefit of reducing the low requirency clutter fluctuations while passing the higher Doppler frequencies due to the target. The improvement factors for a two pulse or three pulse canceller are estimated as [13]:

$$I_1 = 2\left(\frac{f_r}{2\pi\sigma_c}\right)^2 \qquad \text{(two pulse canceller)} \tag{11}$$

$$I_2 = 2\left(\frac{f_r}{2\pi\sigma_c}\right)^4 \qquad \text{(three pulse canceller).} \tag{12}$$

The improvement factor is dependent upon the clutter spectral spread σ_c and the radar system prf. The rocket being tracked has a velocity that varies from approximately 600 m/s to 450 m/s. This would correspond to Doppler frequencies of 40 kHz and 30 kHz, respectively. In order to get the most MTI improvement the prf should be kept high. The range ambiguity ($c\tau/2$) should be kept sufficiently large to prevent extraneous targets from entering the desired range interval. A prf of less than 15 kHz would provide an unambiguous range interval greater than 10 km and should be sufficient for this application.

The Doppler spread of the target is sufficiently large (10 kHz) that at least two prf's will be necessary to insure that the target does not fall into a null in the canceller frequency response. The selection of the two prf's will depend on the exact doppler frequencies for the specific application. An example would be to use the frequencies of 11.43 kHz and 9.14 kHz. The single pulse canceller response for each prf is shown in Figure 10 (a) and 10 (b) as well as the resultant response for the staggered prf in 10 (c). Further smoothing of the response can be achieved by the addition of other prf's. The resulting MTI improvement that can be obtained for a two pulse canceller then becomes (for rain clutter)

$$I_1 = 2\left(\frac{f_r}{2\pi\sigma_c}\right)^2 \tag{13}$$

$$I_1 = 23.8 \text{ dB}$$

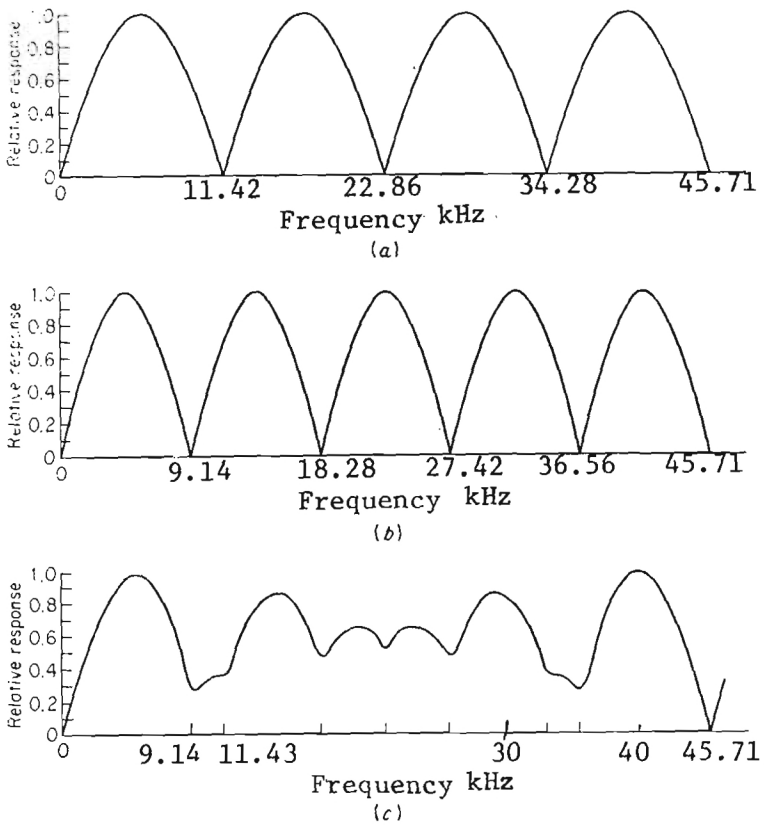

MIT Canceller frequency response
a) Single delay 1 prf = 11.42 kHz
b) Single delay prf = 9.17 kHz
c) Staggered pulse between (a),(b)

Figure 10. Single Pulse Canceller Response

where

f_r = 9.14 kHz

σ_v = standard deviation of clutter spectrum = 2.0 m/s for rain

$\sigma_c = 2\sigma_v/\lambda$ = 133 Hz (rain)

For a three pulse canceller the improvement would become [13]:

$$I_2 = 2\left(\frac{f_r}{2\pi\sigma_c}\right)^4 \tag{14}$$

$$I_2 = 44.6 \text{ dB}$$

A three pulse digital MTI canceller is not a difficult processor and, in fact, can be implemented in a small electronic package. At this level of processing gain, the true practical limitation will depend on the transmitter, STALO, and COHO stability. An MTI improvement of 15 to 20 dB should be sufficient to overcome the effects of rain and land clutter and is also well within the hardware and processor stabilities obtainable.

The magnetron transmitter will be required to produce either a 50 kW peak power [or a 5 kW peak power, depending on system requirements], with a 100 nanosecond pulse width at a nominal 10 kHz prf. Currently available tubes, such as the Litton 4J52A (50 kW) or Litton 2J42 (5 kW) would meet these requirements. The tube would require 14 to 16 kv at 15 amps (pulsed) for 50 kW operation (or 6 kV at 5.5 amps for 5 kW operation).

The radar receiver, duplexer, mixers, IF amplifiers are all conventional X-band components and are easily obtainable. The STALO and COHO will have a direct effect on the MTI performance and will require care in the selection and operation to insure that the desired 20 dB improvement will be achieved.

The 50 kW transmitter receiver would require about 900 W of 400 Hz power and occupy less than 2 ft^3. (The 5 kW transmitter would need about 250 W of dc power and occupy less than 1 ft^3.)

Antenna and Angle Measurements

The measurement of cross range or off boresight angle errors is best accomplished by use of a monopulse antenna. Conical scan technique requires closed loop gimballed tracking and is degraded by target amplitude and

scintillation. The antenna configuration is a standard 4 horn, 3 channel processor that will generate orthogonal error components (azimuth and elevation) for target returns off the boresight axis of the antenna. The antenna will be fix mounted such that the antenna boresight is aligned with the rocket launcher. The beamwidth of the antenna will be selected to be sufficiently wide to keep the rocket within the field-of-view during the first 3 km of the mission. The angle errors generated in the two axes will be calibrated so that a precise measurement of off axis angle can be determined.

The antenna beamwidth that will keep the rocket within the antenna field of view has been tentatively selected as 10 degrees in azimuth and elevation (a 9 inch in diameter aperture at X-band). The angle measurement accuracy of this off axis error measurement is approximated as [13]:

$$\sigma_\theta = \frac{0.58\,\theta}{\sqrt{\left(\frac{(S/N)^2}{1 + S/N}\right)\left(\frac{prf}{B_s}\right)}} \tag{15}$$

where

σ_θ = rms angle noise

θ = half power beamwidth

S/N = single pulse signal to noise ratio

prf = pulse repetition rate

B_s = tracking bandwidth

The rms angle noise is plotted in Figure 11 as a function of target range for the system discussed with a 50 kW transmitter and a 0.1 m^2 target. The resultant angle errors are less than 0.1 meters for a 1 Hz bandwidth at 3000 meters of slant range which is well within the desired 1 meter cross range accuracy. This performance would also result from a 5 kW transmitter and 1 m^2 target RCS. Thus, since measured X-band tail aspect RCS is in the order of 1 m^2, a nominal 5 kW peak transmit power is recommended for a baseline design.

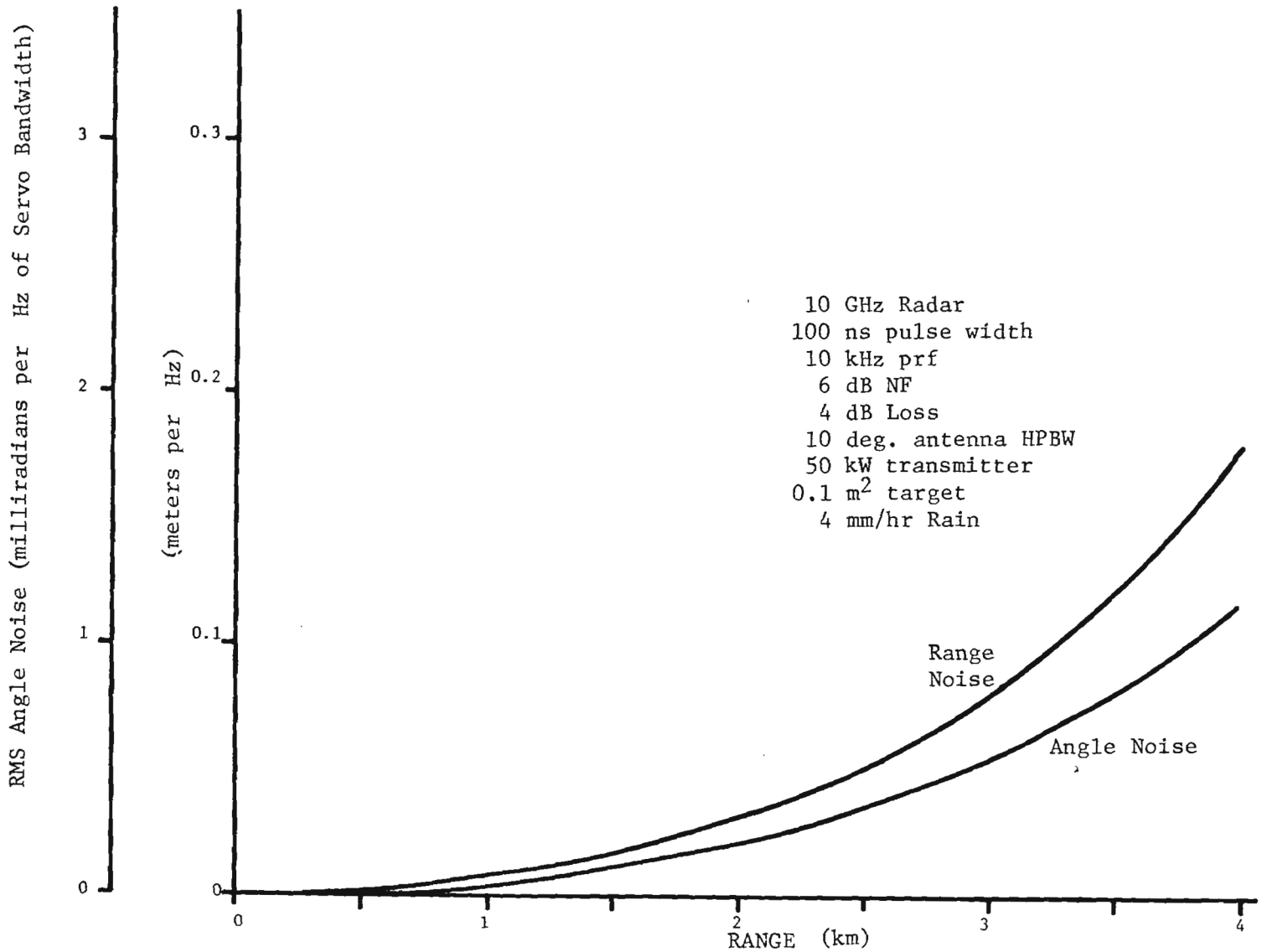

Figure 11. RMS Angle Noise Versus Target Range

6.0 Laser Trackers

The use of electro-optical techniques for DAFFR tracking could be performed by either passive IR systems or a laser radar. Studies of a laser-aided FLIR technique indicate the DAFFR system would not profit from the use of this particular tracker [5]. The use of a laser tracker is considered and shown to be capable of performing the tracking task well beyond burn-out under ideal conditions. However, the operation of the tracker under adverse battlefield conditions is of importance to the DAFFR system. In the case of a laser tracker, both envelope-detection and heterodyne-detection modes are possible. The heterodyne detection mode can provide considerable improvement in sensitivity and, when used with narrow-band optical filters, provides discrimination against unwanted thermal background.

Before analyzing the performance of the laser tracker, one can consider several important qualitative factors:

1) The laser sensor is to be mounted on the rocket launcher so that the tracker viewing from the rear aspect must see through the turbulent plume.

2) The sensor must be mounted on the launcher with no mechanical moving parts. This restriction, coupled with the fact that surface winds could deflect the rocket from its calculated trajectory, requires that the field of view be at least 160 milliradians.

3) The physical space available for a sensor on the launcher lies within a diameter of approximately 24 inches.

4) Plume effects on the laser system include attenuation due to the hot gases and particulate matter such as aluminum oxide, scattering by the particles, and turbulence effects resulting not only from the plume directly but along the path of trajectory. The turbulence effects could result in angle of arrival discrepancies in the tracking signal.

5) As a result of the mounting position on the launcher, severe shock will be experienced by the sensor. This could result in considerable misalignment and/or damage of the optical components. This effect of mechanical vibration and shock is extremely critical for the performance of a superheterodyne laser tracking radar. Alignment of the received signal and the local oscillator in laser systems is also important and often difficult to maintain on the most stable platforms. Because of limitations on envelope-detection capability for laser radar, the heterodyne laser radar would be the most likely to be employed. Thus, the importance of vibration/shock effects is evident.

6) The laser that is most practical for Zuni rocket tracking is the CO_2 laser. To produce necessary high peak power at 10.6 μm, a physically large CO_2 laser is required. If a TEA CO_2 laser were employed PRF would also be low, disallowing signal averaging that might be required under adverse weather requirements. Alternatively, the YAG:Nd^{3+} or Ruby laser might be considered, as both have high peak power capabilities. However, atmospheric effects more severe than at 10.6 μm and lower PRF than achievable by the CO_2 laser lessen the probability of the use of the Ruby laser and YAG:Nd^{3+} laser.

To evaluate the laser sensor, it is important to examine some of the above factors in greater detail. The most important effect to be evaluated is the environment in which these sensors would operate. Among the factors that must be examined are clear air effects, hydrometeorites (rain and fog), dust, explosions, smokes and aerosols and surface wetting effects.

During heavy precipitation or occurrence of fog, both optical systems (active and passive) are adversely affected. Figure 12 shows a gross

picture of attenuation by atmospheric gases, rain and fog; fog for low visibility conditions at laser wavelengths can become appreciable. On the other hand, most rainfalls that can be expected, will result in an attenuation of less than 10 dB/km. These effects are summarized in Table 10, where the effects of fog are seen to be very high at 10 μm, and attenuation in rain peaking in the 3-5 mm region. For a radiative fog with the severe condition of 30 meters visibility which does occur in Europe, the attenuation might be as high as 373 dB/km.

In addition to the rain attenuation effects, rain backscatter presents serious effects at both mm and IR wavelengths. This can set a threshold of signal return above which the target must be observed. Figure 13 demonstrates the calculated rain backscatter coefficient as a function of frequency with the few experimental points that exist included. As in the microwave and millimeter wave systems, Doppler discrimination can be employed to minimize backscatter signals in the case of superheterodyne systems.

An effect that can be expected during rain or fog is the wetting of surfaces (windows, lenses, antennas, etc.). Transmission through a layer of water presents a serious problem which increases in magnitude as wavelength decreases. Figure 14 shows the transmission coefficient as a function of the water layer thickness. In addition to the attenuation effect of surface wetting, wet surfaces of the rocket can reduce contrast if the passive system were to depend entirely on detecting the rocket body.

Recent tests on propagation through dust and debris resulting from explosions have demonstrated the seriousness of these effects on weapon systems and sensors. It can be concluded that airborne soil particles can seriously degrade the transmission of EO and IR radiation through the atmosphere [10]. The effect on millimeter and longer wavelengths has been shown to be considerably less, but one might consider that properly executed firing of explosives could reduce or eliminate the

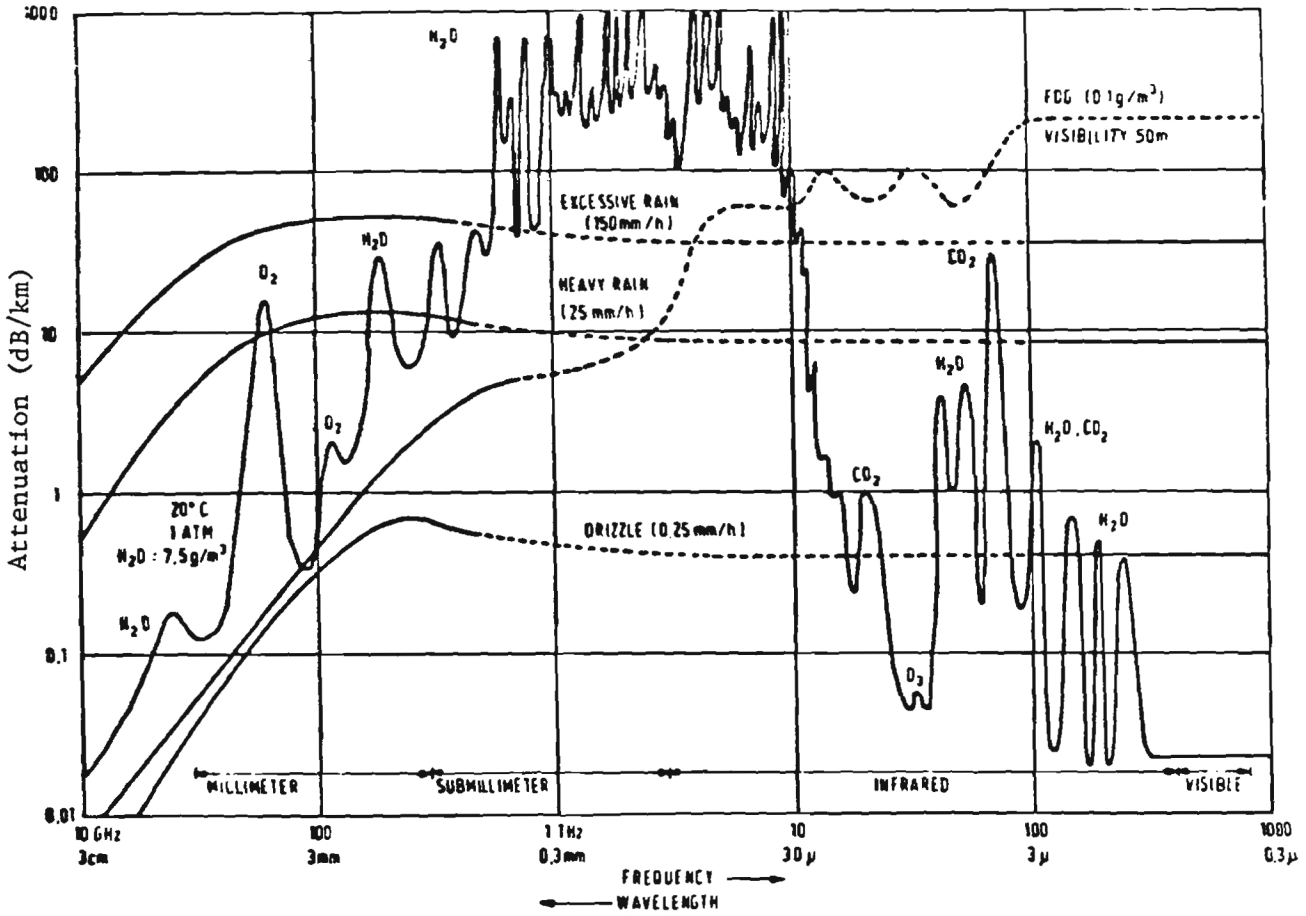

Figure 12. Attenuation by Atmospheric Gases, Rain and Fog [6]

Table 10

SUMMARY OF PROPAGATION DATA [7]

Attenuation, α(dB/km)
Water Density, $\rho(g/m^3)$

	α Clear Rel. Humidity = 100%		α Fog				α Fog			α Rain			α Cloud	
			Radiative Fog				Advection Fog			mm/hr			Fair	
	T = 32°F	68°F	R_V = 400m	200	100	30	400	200	100				Weather	Nimbo-
λ (μm)	ρ = 4.8	17.4	ρ = 0.014	0.038	0.11	0.71	0.063	0.18	0.4	1	4	10	Cum.	Strat.
1				80		500							95	570
4													120	640
10.6	0.3	1.2	7	20	58	373	17	63	140	1	2.6	6	50	500
337	50	185	0.6	1.5	4.3	28	2.5	7.1	15.8	1	3	7	3	20
724	10	37	0.3	0.9	2.6	17	1.0	4.3	9.6	1	3	7	2	7
880	7	24	0.3	0.7	2.0	14	1.2	3.5	7.9	1	3	7	1.5	6
1300	2	6	0.2	0.5	1.4	9	0.8	2.3	5.1	1	3	7	0.8	4
2300	1	3	0.1	0.2	0.6	4	0.4	1.0	2.2	1	3	8		2
3200	0.2	0.9	0.1	0.2	0.5	3.2	0.3	0.8	2	1	3	8		1.5

Notes: (1) for α_{CLEAR} at other Rel. Hum., scale down from 100% given

(2) for a fog situation, $\alpha_{TOTAL} = \alpha_{CLEAR}$ (RH = 100%) + α_F (likewise for clouds)

(3) for a rain situation, $\alpha_{TOTAL} = \alpha_{CLEAR}$ (RH = 100%) + α_R

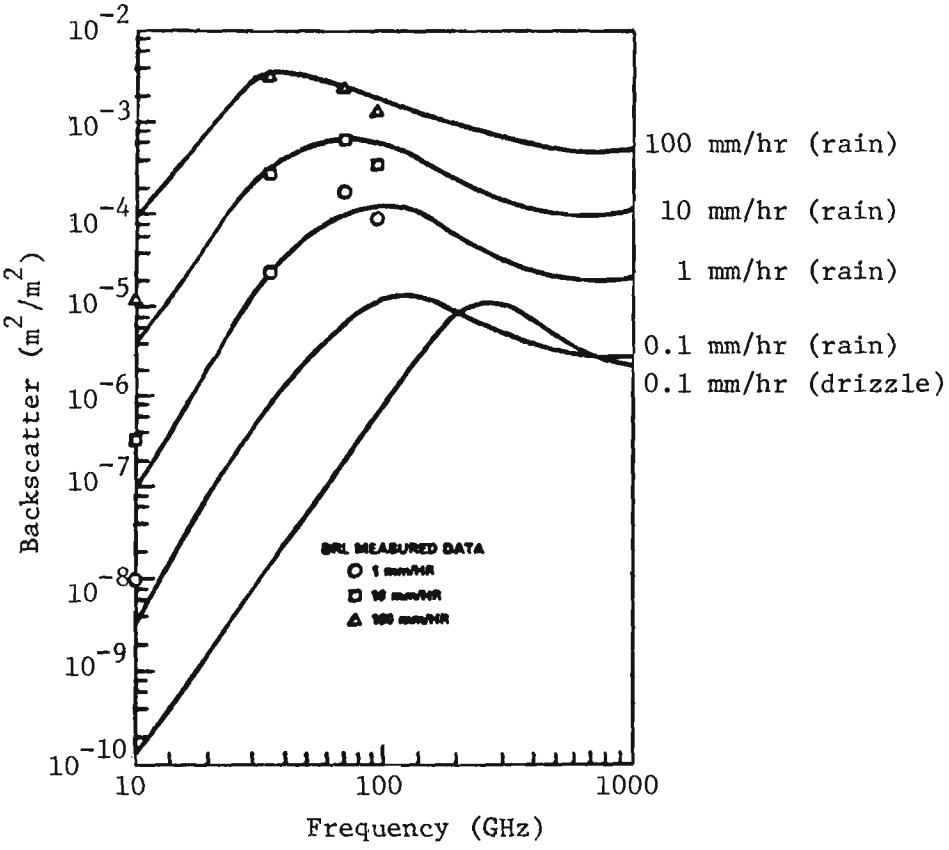

Figure 13. Calculated and Measured Rain Backscatter Coefficient Versus Frequency [8]

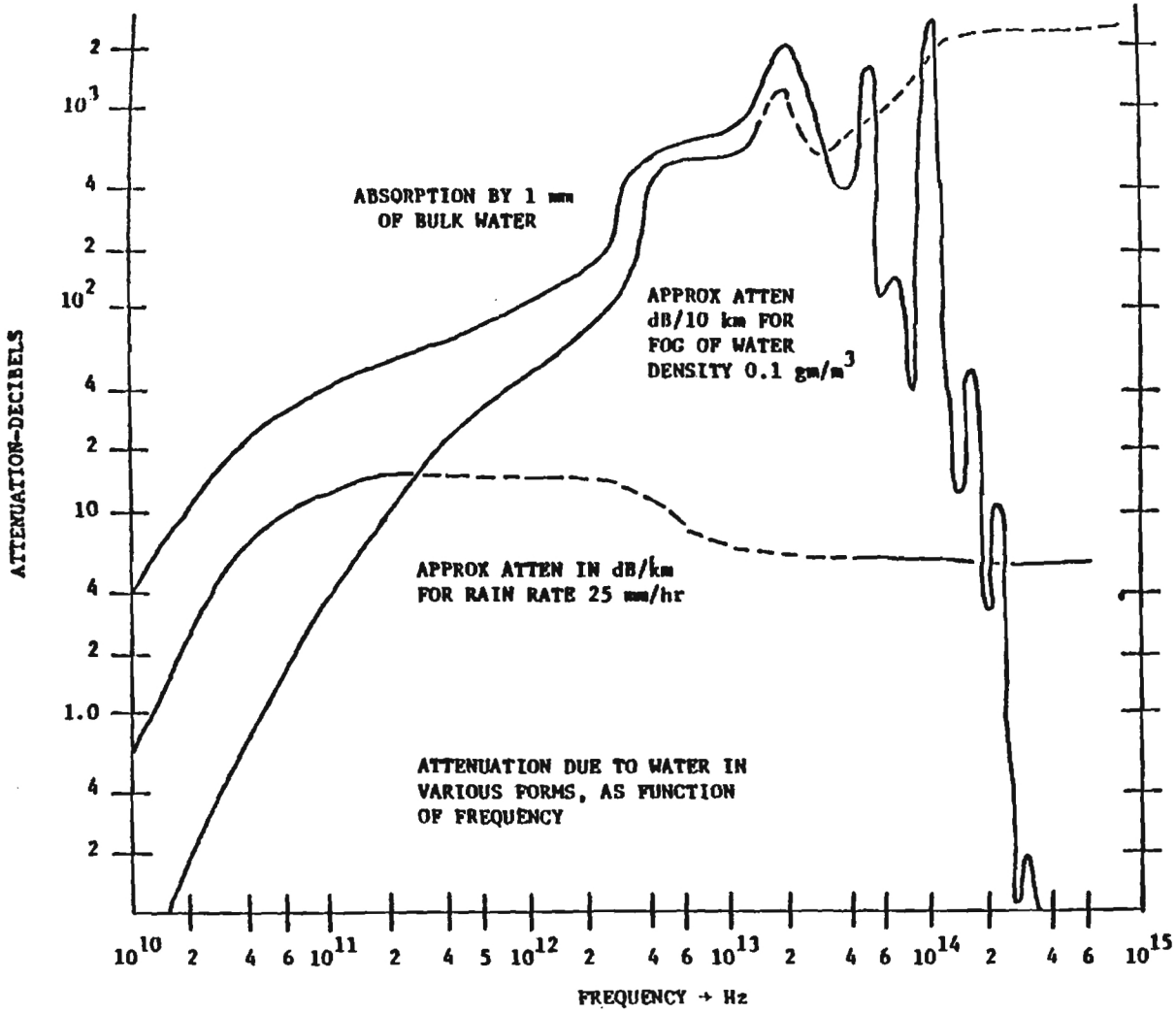

Figure 14. Comparison of Attenuation By Water In Various Forms; The Integrated Thickness Of Water On The Transmission Path Is 1 mm In All Cases [9].

effectiveness of the tracking sensor at all wavelengths. It is, however, the long term presence of dust, dirt or debris blown into the air that are the most realistic degrading effects for laser systems. The following discussion demonstrates the degradation caused by battlefield activities such as dust and debris clouds generated by explosions or vehicular activities.

Measurements of the optical and millimeter wave attenuation due to the dust has been presented by Lindberg [10] for the Dirt-I tests, as shown in Figure 15. The particular event is a barrage of three firings of four 166-mm howitzers in a span of approximately 55 seconds. The appearance of five spikes (rather than three) for the 94 GHz system is a result of the fact that not all howitzers fired simultaneously and a delay occurred for some rounds. The time lapse for each millimeter attenuation was less than 5 seconds, with peak attenuations typically less than -15 dB. As the large debris fell out of the transmission path, the 94 GHz attenuation rapidly decreased and no effect was evident from the remaining dust or from that raised from vehicles. On the other hand, the optical transmissions were seriously degraded for minutes. Optical attenuation exceeded -15 dB for approximately two minutes, and was equal to or exceeded 10 dB for almost three minutes. (It should be noted that the propagation length was 2 km but the 12 rounds were probably confined to less than 100 meters of this path). A report by Seagraves and Duncan [11] has combined the results of vehicular dust tests, debris from firing of TNT charges, and howitzer shots to show the percentage of time that the measured transmittance was less than a particular value. The results of tests on transmission through dust raised by a vehicle shown in Figure 16 and 17 indicate that, for the pathlength employed, the transmittance was reduced to approximately 40% for time on the order of 10 seconds. Thus, one would have to minimize even his own vehicular motion before or during the firing of a register round. Figure 18 illustrates similar data but through battlefield smoke.

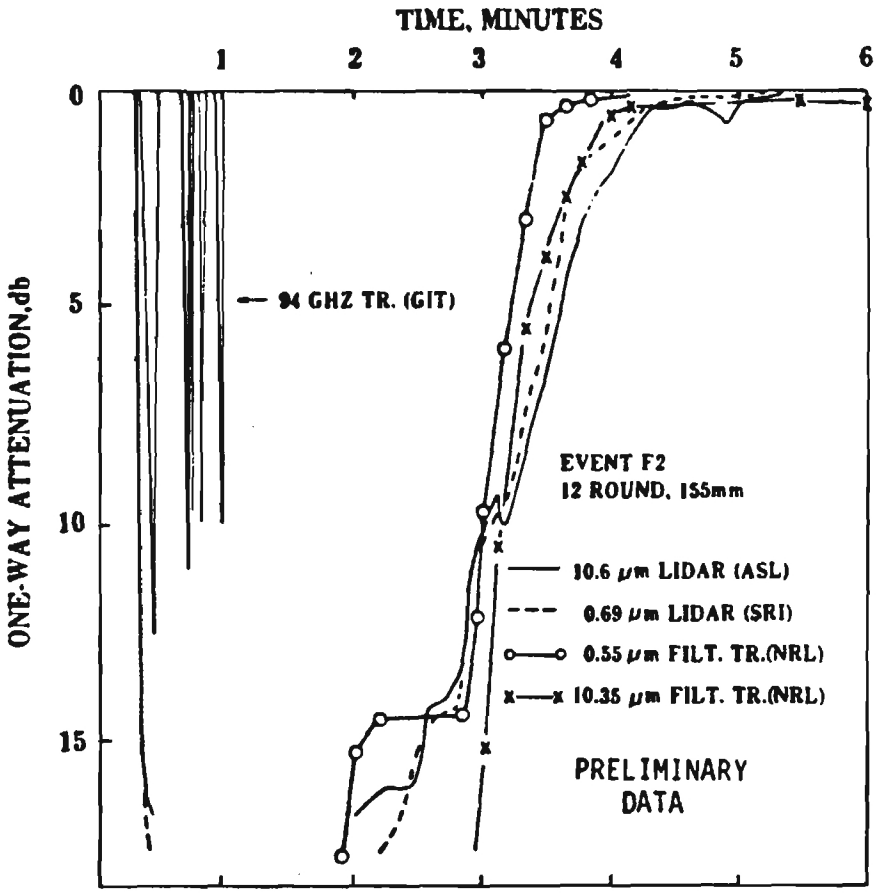

Figure 15. Intercomparison Of Attenuation Due to Dust At Several Wavelengths Over The 2 km Path For Event F - 2 [10].

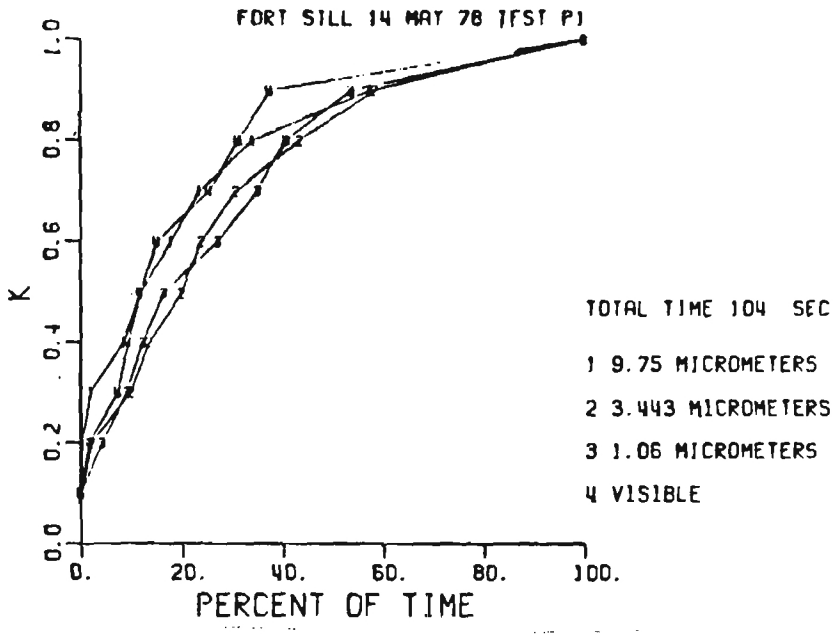

Figure 16. Percent Of Time Measured Transmittance Was Less Than K, Fort Sill Test P1 [11]

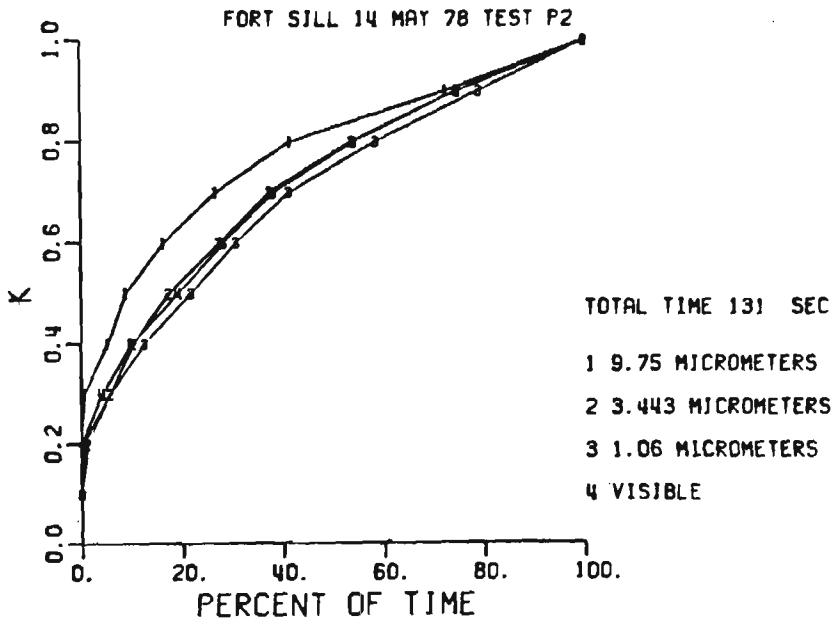

Figure 17. Percent Of Time Measured Transmittance Was Less Than K, Fort Sill Test P2 [11]

TABLE 11

COMPARATIVE SUMMARY OF AEROSOL ATTENUATION (dB/km) EFFECTS [12]

Aerosol	Optical	Infrared 10.6 μm	400 GHz 730 μm	340 GHz 880 μm	220 GHz 1.3 mm	140 GHz 2.1 mm	100 GHz 3 mm	35 GHz 8.6 mm
Fog T = 10 C V ~ 100 m W = 0.3 g/m³	~204	~200	~4	~3.6	3	2.25	1.4	~0.1
Vehicular dust	Large (L)	Significant (S)	Negligible (N)	N	N	N	N	N
Rain 10 mm/hr	5.2	~5.2	7.4	7.8	8.3	8.7	8.7	2.6
Snow 10 mm/hr (H_2O)	>>5.2	>>5.2	~3.7 dry ≳7.4 wet	~3.9 dry ≳7.8 wet	~4.1 dry ≳8.3 wet	~4.4 dry ≳8.7 wet	~4.4 dry ≳8.7 wet	~1.3 dry ≳2.6 wet

In this section, we have discussed mainly the atmospheric effects upon laser radars. The IR effects have been considered from the viewpoint of 10.6 μm, the wavelength of the CO_2 laser. The effects would be greater at shorter wavelengths, for example at 1.06 μm where the YAG:Nd^{3+} laser operates or at 0.6943 μm where the Ruby laser operates. Thus, fog and smoke attenuation would be greater at the shorter wavelength, and rain attenuation would be comparable with 10.6 μm plume effects. Reflection from aerosol particles within the plume could further reduce the transmission to and from the missile body. As a result, the CO_2 laser would be the leading candidate for a DAFFR sensor.

The CO_2 coherent radar employing superheterodyne detection can be shown to be appropriate during clear weather applications. Investigations of the use of CO_2 system for terrain avoidance systems for low-flying aircrafts and helicopters have shown that a 10 W laser with 40,000 Hz pulses per second can detect very small obstacles (e.g. wires) at 1 km ranges. This system or an equivalent one would be suitable for a clear air rocket tracker. However, inclement weather would render this system ineffective.

As a result of these considerations, a laser tracker is not appropriate for the DAFFR system.

A comparative summary of aerosol attenuation effects has been given by Gamble [7] with results similar to those discussed above. Table 11 presents this summary. Data for snow are not complete as yet, but the table indicates that for snow IR attenuation is much greater than that at longer wavelengths.

In geographical regions where low-lying clouds can occur in the path of the missile trajectory, the laser tracker can be seriously affected; clouds can be considered equivalent to heavy fog. The data for heavy fog shown in Table 11 are applicable to the low-flying cloud condition.

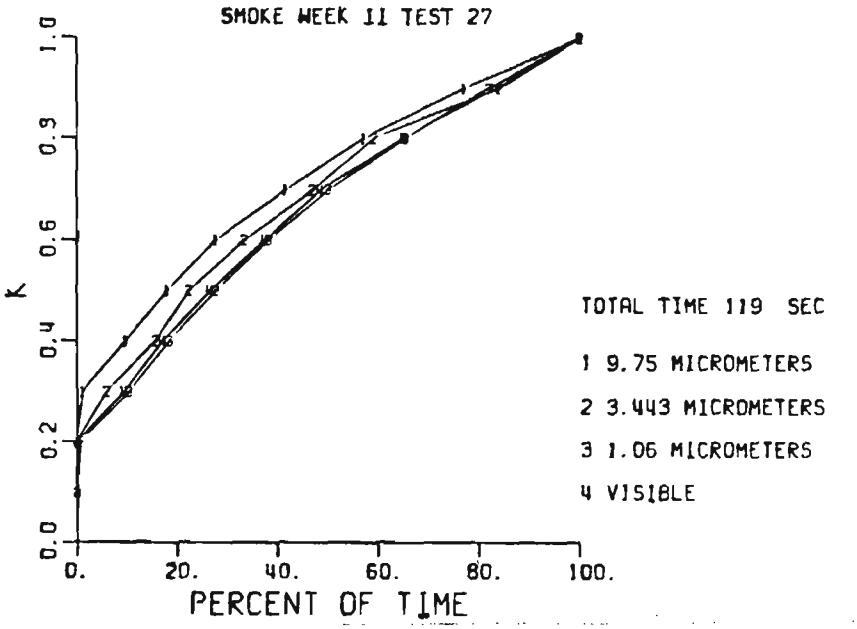

Figure 18. Percent Of Time Measured Transmittance Was Less Than K, Smoke Week II Test 27 [11]

7.0 Passive IR Tracker

Passive IR trackers have been employed in the past as clear weather trackers of missiles. Recently, as part of the DAFFR System Program, Texas Instruments has recently performed an investigation of Zuni Rocket Thermal Signature Characterization using an 8-12 μm FLIR; Appendix B documents some data from these tests. The measurements were performed under clear weather conditions. The TI rough draft of their Final Report [12] indicates that the use of an IR sensor in conjunction with a digital tracker to determine rocket trajectory for ballistic correction is feasible. However, further investigation of this system is necessary before it can be considered a primary candidate for the DAFFR System. This section will discuss several aspects of the use of an IR sensor which were either not addressed by the TI report or which, though addressed, appear to be incomplete. Most of these topics are related to the battlefield environment in which the sensor must operate. The adverse weather and battlefield conditions briefly described in Section 6.0 apply equally to the passive IR system. In addition, other aspects of the environment must be investigated; the EOSAEL Reports discuss some of these topics [13].

TI computed excess signal for each point in the flight. Figure 19 is a graph of what is referred to as the allowable "additional" atmospheric extinction coefficient that can be tolerated before rendering the signature untrackable. TI has not included the change in relative humidity between that which existed during the flights and 100% humidity which would exist during rain and fog, for instance. Although the increased contribution due to water vapor at 100% RH is small compared to that of fog and rain, with a small working margin, this can add to a reduction of range. It should be noted that the allowable attenuation coefficient curve begins at approximately 650 m. This is due to the fact that, at shorter ranges, the rocket is obscured by the extended plume source radiation. Thus, with a FLIR system, no information on the rocket trajectory is available before

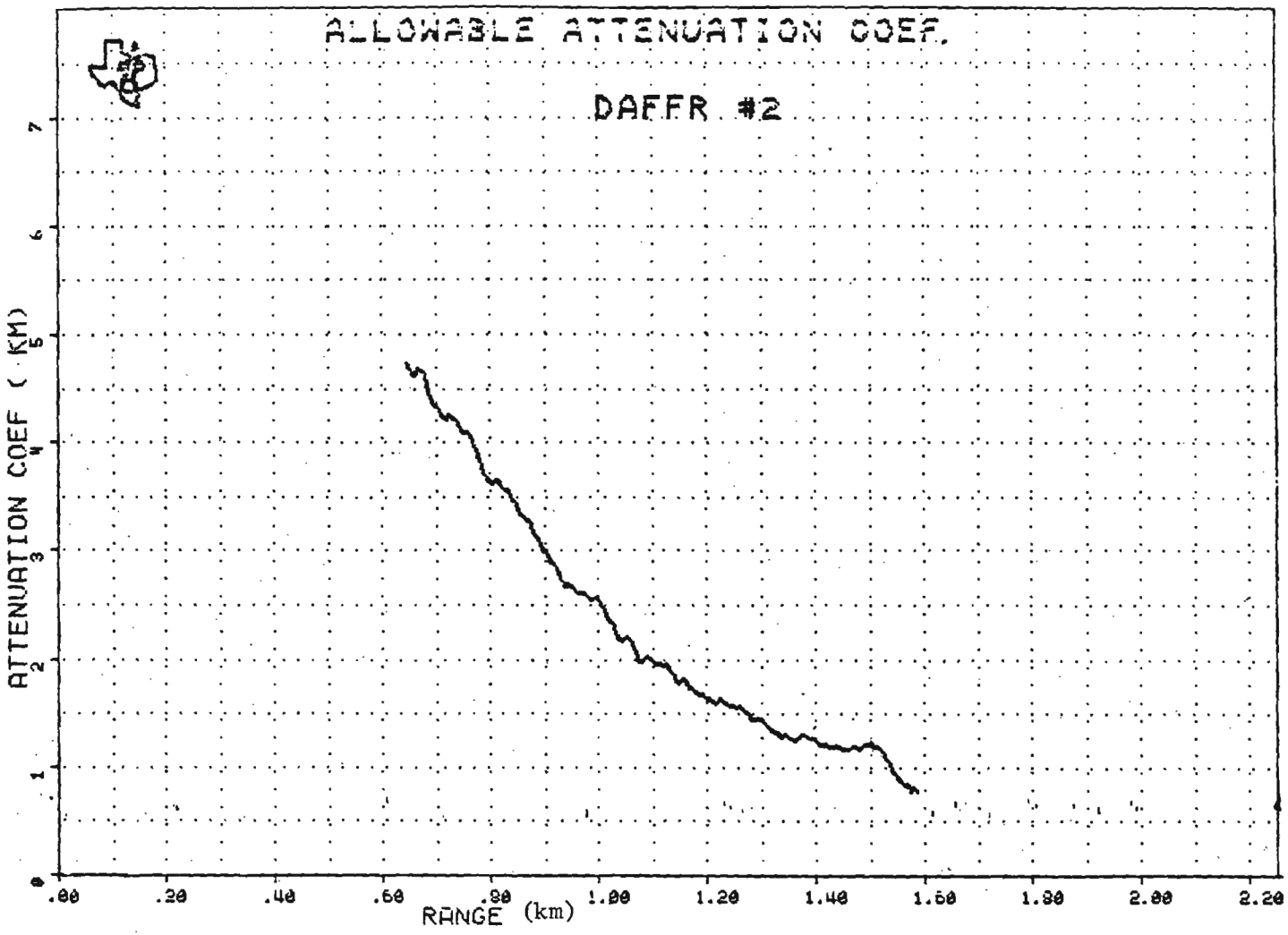

Figure 19. Allowable Attenuation Coefficient [12]

650 m (actually slightly in access of 700 m for launch angles of 35° and 40°).

The effects of atmospherics on IR transmission are summarized in Table 12. However, all the data presented prior in section 6.0 directly apply. A more detail discussion related specifically to the IR propagation is discussed below.

Fog and Haze

TI has employed the following relation for the attenuation coefficient of fog or haze in the region of 8-12 μm:

$$K(8\text{-}12) = \exp(-1.65 + \ln [k(vis)]) \quad (16)$$

where

$$K(vis) = \text{visible attenuation} = 3.912/R_{vis} \quad (17)$$

and

$$R_{vis} = \text{visibility range in km} \quad (18)$$

This fog corresponds to the radiative fogs discussed in Section 6.0 It is seen from Tables 10 and 11 in that section that an advection fog attenuates at a much higher value. Thus, an advection fog in conjunction with the extended plume radiation would not permit observation of the rocket at all. While referring to Section 6.0, one should note the effects of 100% RH at 68°F (20°C) compared to a

Table 12

EFFECTS OF PROPAGATION PHENOMENA ON IR SENSOR

Effect	IR (8-12 μm)
1. Clear Air	Insignificant
2. Rain	Small attenuation for passive system; backscatter can set a signal threshold for active systems.
3. Surface Wetting	Can cause very large signal reduction when optics surfaces are wetted.
4. Fog	Significant attenuation; fogs with visibilities $\leq$ 500 m will attenuate strongly.
5. Dust and Debris from Explosions	Explosions and vehicles cause sufficient dust/debris levels to attenuate signals for several minutes.
6. Smokes	Cause some attenuation for short range only when concentrations are high.
7. Snow	Needs further exploring to determine if reduction of transmittance is large enough to cause system to be ineffective.

standard atmosphere can result in an increase of 1.1 dB/km, equivalent to 100 m reduction for the R_{vis} considered by TI.

In the European theatre, fogs occur quite often particularly during winter months and many of these are more of the nature of an advection fog than of a radiative fog. Fogs of much shorter visibility than 500 m occur frequently in this region.

When calculating fog attenuation for a slant angle trajectory such as that followed by the Zuni rocket, it is important to include in the calculations the effects of the vertical profile model for fog [e.g. page 21 of The Electro-Optical Systems Atmospheric Effects Library, Vol.1, ASL-TR-0047, Dec. 1979]. This effect has been found to be important for such systems as the Copperhead, Hellfire and Airborne E-O Surveillance System and, as shown below, can be significant for DAFFR systems. It has recently been shown that fogs are much denser at altitudes of 100 or 200 meters than at ground level, implying that slant range transmission can be significantly lower than horizontal path transmission at the surface. The interim model used in E-O SAEL provides a means for predicting the visible extinction coefficient through a 50 m thick layer as a function of the visible extinction coefficient at the bottom of the layer. The relation can be applied sequentially to consecutive layers to the top of the fog (usually assumed to be on the order of 1000 m). The altitude of 1000 m corresponds to a range along a Zuni rocket trajectory of 1470 m over which a fog of much greater attenuation than at ground level will exist. If we take the fog considered in the TI report, it can be shown that within the first few hundred meters altitude, the attenuation can far exceed the ground value which has been used for the projected FLIR operation. The ASL report shows that the actual change through a 50-meter layer is given by the formula:

$$K = \exp[-2.64(\log k_o)^2 + 6.63 \log k_o - 0.46] \qquad (19)$$

This is employed to compute the profile at 0.55 μm. Here,

$$k_o = 3.912/R_{vis} \qquad (20)$$

The scaling law, given above from the TI report, is used to compute the profile of k(8-12). The result is that, for the fog used by TI, the range is reduced to approximately 900 m compared to the value of 1200 m given in the TI report. This would allow a window for observation of approximately 200 m between 700 m (burn-out) and 900 m, approximately 0.2 second of flight time. This would not provide sufficient information for the DAFFR system. The result does not include effects of 100% RH, battlefield explosions, dust and dirt and a possible contrast transmittance effect (to be discussed later).

On the basis of the discussion given here, the use of the passive IR sensor for DAFFR applications does not provide satisfactory tracking during fog conditions that can be expected in Europe.

Snow

In discussing the effects of snow on an IR sensor for DAFFR, new data obtained from the SNOW measurements made in January, 1981 in Vermont should be used. The relation given by TI can represent the effect, however. The extinction coefficient is given by:

$$K(8\text{-}12) = \exp(0.114 + 0.993 \ln K_{vis}) \qquad (21)$$

where

$$K_{vis} = 3.912/R_{vis} \text{ as before.} \qquad (22)$$

R_{vis} is given as 100 m, corresponding to a light snow fall. Then,

$$K_{vis} = 3.912/0.1$$

$$= 39.12 \text{ km}^{-1} \quad (23)$$

so that

$$K(8\text{-}12) = 4.34 \text{ km}^{-1} \quad (24)$$

This is the result obtained by TI, and it shows that, with plume obscuration of the rocket to 700 m, it is not possible to use the FLIR for snow falls with R_{vis}<1000 m. Other factors mentioned under the fog discussion would also apply to this situation.

Rain

The case for using the FLIR in rain at a rainfall rate of man/hours agrees with numbers obtained previously, but factors mentioned under fog could contribute further to shortening the tracking range.

Smokes

The coefficients given by TI for WP, HC and Fog Oil in the 0.55 μm and 8-12 μm regions do not correspond to the numbers which we find in E-O SAEL. The values which are given in Table 3-1, p. 23 of ASL-TR-0047 (also p. 60 of ASL-TR-0048) are:

Smoke	0.4 - 0.7 μm	8 - 12 μm
WP, PWP	3.1C	0.36C
HC	3.3C	0.13C
Fog Oil	7.06C	0.25C

The following FLIR tracking ranges are obtained for conditions of interest:

Obscurant	FLIR RANGE
WP, PWP with 100 m vis	$\lesssim$ 400 m
HC smoke with 25 m vis	$\lesssim$ 450 m
Fog Oil smoke with 25 m vis	$\lesssim$ 550 m

With these coefficients and under the visibility conditions given, the FLIR could not operate in the DAFFR system. Possibly other more recently determined smoke coefficients exist, which we do not have available. It is also assumed that uniform smoke concentrations exist along the entire trajectory path. Data are needed on slant path transmission through smoke and on the lessening of smoke as a function of altitude.

Clouds

No consideration has been given to cloud attenuation and, as shown in Section 6.0, clouds have attenuation characteristics similar to heavy fog in the IR spectral region. Low-lying clouds which can occur in the mountains and passes of Western Germany could seriously affect the operation of a DAFFR system employing any IR sensor. Clouds lying as low as 0.5 km to 1.0 km could obscure the path of transmission for ranges from 940 m to almost 2000 m, which cover the major portion of the observing range of the FLIR. In a personal conversation with Don Snider of ASL, he indicated that M. Heaps of ASL is developing algorithms for low-lying clouds in Europe based upon ballon measurements made by Jim Lindberg of ASL.

TURBULENCE EFFECTS AND CONTRAST TRANSMITTANCE EFFECTS

In what might be considered the "conventional" application of FLIRS, atmospheric effects are considered as causing attenuation only. Since the FLIR is an ac-coupled device, background and any atmospheric effects not occurring at frequencies exceeding the low frequency cutoff of the FLIR system are considered as dc-level. In a dynamic system such as experienced in a Zuni flight, rapidly changing spatial effects and turbulence can result in a highly degrading environment, which further enhances the transmission effects of smoke, fog, rain, plume exhaust products, clouds, smoke and battlefield. Atmospheric turbulence effects can result in several adverse propagation effects which, under conditions which can occur along a trajectory of a Zuni rocket, should have power spectrum components at frequencies above the FLIR low-frequency cutoff. As a result, angle of arrival discrepancies can occur so that the rockets apparent position would fluctuate because of the turbulence in the path from the rocket to the sensor. Bulk refractive effects can cause erroneous determinations of the rocket position. Turbulence effects can also cause spatial variations of plume hot spots remaining behind the missile so that, if they intercept the field of view to the rocket, a contrast transmittance reduction can occur as the FLIR scans the scene. In adverse conditions, the disturbance of the atmosphere by the rocket can result in further contrast reduction of emission, reflection of radiation or other turbulence-induced effects within the intervening medium.

8.0 Conclusions and Recommendations

In this study a wide range of possible sensor candidates were investigated for tracking the DAFFR vehicle; a relative performance summary is shown in Table 13.

While a laser tracker can be made to work under fair weather conditions, the adverse atmosphere effects must preclude its operation. An IR sensor is somewhat less vulnerable to the atmospheric effects than a laser, however, a passive IR system requires a separate microwave Doppler velocimeter since the IR system will not provide range/velocity data. The requirement of being an autonomous sensor would not be satisfied. Other factors to consider relative to an IR sensor are:

1) The DAFFR system requirements include the acquiring of the missile signature immediately after launch and tracking through the motor burnout. An IR system cannot perform these functions because of obscuration by the plume.
2) Effects resulting from launcher dynamics, e.g. vibration and shock, might influence the IR optics more adversely than the microwave or millimeter wave sensors since ruggedness of FLIR is not typically as great as that of the long wavelength devices. Protection for lens from the rocket blast and residual rocket materials is necessary. Aluminum oxide particulates could seriously degrade the FLIR optics over a period of several firings, as could battlefield dust and debris in general.
3) Gimbal or moving mirror parts are not to be used as indicated in the DAFFR requirements. The moving mirror of the FLIR does not meet this requirement and must be ruggedized to survive the many rocket blasts experienced by a launcher. The other systems (mm/microwave/laser) were evaluated as staring systems and would profit from the use of a scanning apparatus.
4) Cryogenic cooling of the FLIR must be maintained in the field. Improved miniaturized cryostatic techniques should aleviate this problem, but, in prolonged operation, cryogenic liquid supplies will have to be maintained.

Table 13

SENSOR RELATIVE PERFORMANCE SUMMARY

	SATISFACTORY PERFORMANCE IN ADVERSE ATMOSPHERE													
SYSTEM	RAIN*	FOG	HAZE	SMOKE	CLOUDS	TURBULENCE EFFECTS	HIGH HUMIDITY	CRYOGENIC COOLING REQUIREMENT	RANGE MEASUREMENT CAPABILITY	SATISFACTORY TRANSMISSION THRU PLUME	GIMBAL REQUIREMENT	SATISFACTORY ANGULAR RESOLUTION	MEETS PACKAGING REQUIREMENT	TARGET SIGNATURE AUGMEN. NEEDED
10 GHz Radar	YES	YES	YES	YES	YES	YES	YES	NO	YES	YES	NO	YES	YES	NO
17 GHz Radar	YES	YES	YES	YES	YES	YES	YES	NO	YES	(TBD)	NO	YES	YES	YES
35 GHz Radar	YES	YES	YES	YES	YES	YES	YES	NO	YES	YES	NO	YES	YES	YES
94 GHz Radar	NO	NO	YES	YES	YES	YES	YES	NO	YES	YES	NO	YES	YES	YES
Infrared	NO	NO	NO	NO	NO	(SIGNIFICANT EFFECTS)	(SIGNIF. EFFECTS)	YES	NO	NO	NO	YES	YES	NO
Laser	NO	NO	NO	NO	NO	(SIGNIFICANT EFFECTS)	YES	YES	YES	(SIGNIFICANT EFFECTS)	NO	YES	YES	YES

*5 mm/hr

Radar considerations indicated an X-band pulsed system with a minimum of 1 kW can provide Zuni rocket tracking to at least 1600 m under all weather conditions and does not require projectile RCS augmentation. A baseline radar hardware implementation was developed in this report.

9.0 References

[1] D.J. Kozakoff and J.M. Schuchardt, "Long Range Projectile Guidance Preliminary Study," Final Report on Project A-2529, prepared for U.S. Army MICOM under contract DAAK40-79-D-0028, Delivery Order 0007, Georgia Tech, Atlanta, Georgia, March 1980.

[2] D.J. Kozakoff, R.L. Hummel and J.M. Schuchardt, "Advanced Study of Long Range Projective Terminal Guidance," prepared for U.S. Army MICOM under contract DAAK40-79-D-0028, Delivery Order 0010, Georgia Tech, Atlanta, Georgia, September 1980.

[3] S.M. Kulpa and E.A. Brown, "Near-Millimeter Wave Technology Base Study: Volume I - Propagation and Target/Background Characteristics," HDL-SR-79-8, U.S. Army Harry Diamond Laboratories, White Oak, Maryland, November 1979.

[4] J.A. Gagliano and J.M. Schuchardt, "DAFFR Test/Zuni Rocket Firing Report," Final Report on Project A-3031, prepared for the U.S. Army Missile Command under Contract DAAH01-81-D-A003, Delivery Order 0027, Georgia Tech, September 1981.

[5] V.J. Corcoran, "Performance of Laser-Aided Forward Looking Infrared Systems (FLIRs)," IDA Paper p. 1163 (1978).

[6] J. Preissner, Paper 48, "The Influence of the Atmosphere on Passive Radiometric Measurements," AGAR Conference, proceedings No. 245 - Millimeter and Submillimeter Wave Propagation and Circuits, edited by E. Spitz, 4-8 September, 1978.

[7] S.M. Kuppa and E.A. Brown, "Near Millimeter Wave Technology Base Study," Report HDL-SR-79-8 (November, 1979).

[8] V.W. Richard, Ballistic Research Laboratories, Memorandum Report 2631, June 1976.

[9] D.C. Hogg and T.S. Chu, "The Role of Rain in Satellite Communications," Proc. IEEE, Vol. 23, pp. 1308-1331 (September 1975).

[10] J.D. Lindberg, "Measured Effects of Battlefield Dust and Smoke on Visible, Infrared and Millimeter Wavelengths Propagation: Preliminary Report and Dusty Infrared Test-I (DIRT-I)," ASL-TR-0021,

[11] M. Seagraves and L. Duncan, Report on Battlefield Contaminants, U.S. Army ECOM, Atmospheric Sciences Laboratory Report, 1980.

[12] "Final Report for Zuni Rocket Thermal Signature Characterization: A Part of the Dynamically Acquired Free Flying Rocket (DAFFR) System," (Preliminary, Texas Instruments (October 1981).

[13] M.I. Skolnik, "Radar Handbook," McGraw Hill Book Company, New York, pp. 25-40, 1970.

[14] Data obtained from "Plan for Demilitarization and Disposal of 227 MM Rocket for the Multiple Launch Rocket System," U.S. Army MICOM, 1981.

Appendix A. DAFFR Trajectory Data Computed by Sperry Rand Corporation

Table A-1. DAFFR Flight Data for a No Wind Launch at 35 Degrees

Time	Down Range (m)	Cross Range (m)	Height (m)	Axial Velocity (m/s)	Cross Velocity (m/s)	Cross Velocity (m/s)	Yaw	Pitch

•RMEMET,VMEMET,GAMY,GAMZ3

T	RMEMET(1)	RMEMET(2)	PMEMET(3)	VMEMET(1)	VMEMET(2)	VMEMET(3)	GAMY	GAMZ
0.	0.	0.	-2.1335000	0.	0.	0.	0.	0.
0.2000000	6.1337118	4.757E-08	-6.2328240	66.819960	3.831E-06	-44.836458	4.761E-08	0.5909993
0.4000000	26.384414	1.058E-04	-19.819888	135.59451	0.0020702	-90.886586	1.268E-05	0.5905015
0.6000000	60.432668	0.0017360	-42.583360	205.93086	0.0167141	-136.68695	6.762E-05	0.5869819
0.8000000	108.96134	0.0064454	-74.472024	279.32794	0.0253260	-182.35837	7.592E-05	0.5783739
1.0000000	172.51355	0.0114134	-115.75641	357.19579	0.0306844	-231.24007	7.212E-05	0.5745796
1.2000000	252.39631	0.0177042	-167.24703	443.36351	0.0265461	-284.61967	5.039E-05	0.5706993
1.4000000	350.48095	0.0250291	-230.03272	539.58752	0.0366654	-343.72179	5.739E-05	0.5680289
1.6000000	468.10479	0.0329963	-304.89502	635.98076	0.0466585	-403.81289	6.193E-05	0.5657189
1.8000000	599.58116	0.0417097	-388.17123	665.85856	0.0467031	-420.79509	5.929E-05	0.5635877
2.0000000	732.14493	0.0503877	-471.74831	658.09236	0.0452444	-413.94510	5.820E-05	0.5614760
2.2000000	862.76974	0.0588702	-553.71496	648.18742	0.0437605	-405.77414	5.722E-05	0.5593279
2.4000000	991.44105	0.0672015	-634.06959	638.57897	0.0423184	-397.81800	5.625E-05	0.5571410
2.6000000	1118.2201	0.0754036	-712.85435	629.25607	0.0410431	-390.06904	5.544E-05	0.5549157
2.8000000	1243.1620	0.0834877	-790.10981	620.20702	0.0400110	-382.51907	5.491E-05	0.5526522
3.0000000	1366.3172	0.0914598	-865.87284	611.38033	0.0392448	-375.13533	5.471E-05	0.5503505
3.2000000	1487.7269	0.0993187	-940.17422	602.75081	0.0387080	-367.90131	5.481E-05	0.5480100
3.4000000	1607.4301	0.1070699	-1013.0435	594.31599	0.0383138	-360.81432	5.511E-05	0.5456309
3.6000000	1725.4658	0.1147122	-1084.5097	586.07319	0.0379552	-353.87137	5.544E-05	0.5432094
3.8000000	1841.8719	0.1222535	-1154.6014	578.01949	0.0375492	-347.06941	5.569E-05	0.5407473
4.0000000	1956.6859	0.1296983	-1223.3465	570.15166	0.0370713	-340.40548	5.583E-05	0.5382429
4.2000000	2069.9446	0.1370509	-1290.7725	562.46616	0.0365558	-333.87672	5.589E-05	0.5356961
4.4000000	2181.6841	0.1443136	-1356.9059	554.95931	0.0360586	-327.48032	5.596E-05	0.5331067
4.6000000	2291.9398	0.1514866	-1421.7732	547.62735	0.0356097	-321.21335	5.609E-05	0.5304745
4.8000000	2400.7463	0.1585710	-1485.3997	540.46654	0.0351938	-315.07269	5.626E-05	0.5277991
5.0000000	2508.1375	0.1655653	-1547.8104	533.47315	0.0347769	-309.05512	5.641E-05	0.5250797
5.2000000	2614.1464	0.1724749	-1609.0297	526.64336	0.0343452	-303.15748	5.652E-05	0.5223158
5.4000000	2718.8053	0.1793007	-1669.0811	519.97331	0.0339147	-297.37672	5.662E-05	0.5195072
5.6000000	2822.1460	0.1860437	-1727.9879	513.45908	0.0335023	-291.70986	5.673E-05	0.5166535
5.8000000	2924.1993	0.1927045	-1785.7724	507.09683	0.0331034	-286.15383	5.685E-05	0.5137544
6.0000000	3024.9944	0.1992844	-1842.4566	500.88202	0.0327047	-280.70514	5.696E-05	0.5108093
6.2000000	3124.5609	0.2057852	-1898.0611	494.80465	0.0323063	-275.35739	5.705E-05	0.5078174
6.4000000	3222.9250	0.2122079	-1952.6060	488.86009	0.0319171	-270.10726	5.715E-05	0.5047795
6.6000000	3320.1126	0.2185532	-2006.1099	483.02938	0.0315355	-264.94357	5.724E-05	0.5016940
6.8000000	3416.1417	0.2248218	-2058.5877	477.27470	0.0311532	-259.84496	5.733E-05	0.4985605
7.0000000	3511.0275	0.2310142	-2110.0522	471.59592	0.0307716	-254.81103	5.741E-05	0.4953782
7.2000000	3604.7851	0.2371309	-2160.5164	465.99433	0.0303945	-249.84216	5.748E-05	0.4921465

Table A-2. DAFFR Flight Data for a No Wind Launch at 39 Degrees

Time	Down Range (m)	Cross Range (m)	Height (m)	Axial Velocity (m/s)	Cross Velocity (m/s)	Cross Velocity (m/s)	Yaw	Pitch
T	RMEMET(1)	RMEMET(2)	RMEMET(3)	VMEMET(1)	VMEMET(2)	VMEMET(3)	GAMY	GAMZ
0.	0.	0.	-2.1336000	0.	0.	0.	0.	0.
0.2000000	5.8269848	4.510E-08	-6.6565314	63.452515	3.634E-06	-49.431455	4.518E-08	0.6618233
0.4000000	25.051248	1.301E-04	-21.631427	128.70696	0.0019631	-100.16720	1.204E-05	0.6613422
0.6000000	57.428537	0.0016464	-46.730739	195.50265	0.0158548	-150.80842	5.421E-05	0.6570496
0.8000000	103.45417	0.0061168	-81.952157	265.30900	0.0240559	-201.61182	7.219E-05	0.6498154
1.0000000	163.82631	0.0108288	-127.62405	339.32398	0.0290770	-255.92481	6.841E-05	0.6461962
1.2000000	239.73242	0.0168043	-184.64473	421.35120	0.0251659	-315.35722	4.782E-05	0.6425037
1.4000000	332.95784	0.0237415	-254.23833	511.96642	0.0349447	-381.15206	5.475E-05	0.6399631
1.6000000	444.78117	0.0313007	-337.28453	604.67844	0.0444445	-448.10945	5.905E-05	0.6377618
1.8000000	569.79548	0.0395697	-429.72462	633.16332	0.0444162	-467.22929	5.645E-05	0.6357305
2.0000000	695.85547	0.0478048	-522.55001	625.83111	0.0429850	-459.87616	5.535E-05	0.6337180
2.2000000	820.08177	0.0558553	-613.63778	616.47154	0.0415134	-451.05739	5.435E-05	0.6316702
2.4000000	942.46432	0.0637639	-702.98655	607.40082	0.0400888	-442.47904	5.335E-05	0.6295851
2.6000000	1063.0613	0.0715512	-790.64344	598.60788	0.0388506	-434.13222	5.254E-05	0.6274631
2.8000000	1181.9259	0.0792272	-876.65376	590.08083	0.0378820	-426.00741	5.205E-05	0.6253045
3.0000000	1299.1075	0.0867962	-961.05862	581.77029	0.0372007	-418.06787	5.193E-05	0.6231092
3.2000000	1414.6464	0.0942591	-1043.8924	573.65290	0.0367515	-410.29565	5.211E-05	0.6208767
3.4000000	1528.5810	0.1016176	-1125.1881	565.72592	0.0364244	-402.68741	5.245E-05	0.6186059
3.6000000	1640.9490	0.1088755	-1204.9781	557.98645	0.0360982	-395.23959	5.279E-05	0.6162960
3.8000000	1751.7877	0.1160384	-1283.2943	550.43130	0.0356961	-387.94860	5.301E-05	0.6139458
4.0000000	1861.1335	0.1231122	-1360.1676	543.05695	0.0352177	-380.81099	5.310E-05	0.6115549
4.2000000	1969.0222	0.1301008	-1435.6285	535.85960	0.0347221	-373.82345	5.314E-05	0.6091232
4.4000000	2075.4888	0.1370055	-1509.7067	528.83534	0.0342697	-366.99265	5.324E-05	0.6066506
4.6000000	2180.5675	0.1438258	-1582.4311	521.98028	0.0338709	-360.29507	5.340E-05	0.6041370
4.8000000	2284.2918	0.1505622	-1653.8300	515.29063	0.0334895	-353.72701	5.359E-05	0.6015816
5.0000000	2386.6944	0.1572169	-1723.9309	508.76255	0.0330915	-347.30474	5.372E-05	0.5989838
5.2000000	2487.8072	0.1637926	-1792.7606	502.39211	0.0326817	-341.01469	5.382E-05	0.5963433
5.4000000	2587.6612	0.1702906	-1860.3452	496.17334	0.0322860	-334.85204	5.394E-05	0.5936597
5.6000000	2686.2857	0.1767113	-1926.7093	490.09506	0.0319103	-328.80845	5.407E-05	0.5909328
5.8000000	2783.7053	0.1830554	-1991.8763	484.15333	0.0315380	-322.88038	5.419E-05	0.5881620
6.0000000	2879.9558	0.1893246	-2055.8689	478.34498	0.0311617	-317.06498	5.430E-05	0.5853469
6.2000000	2975.0548	0.1955203	-2118.7095	472.66678	0.0307919	-311.35908	5.440E-05	0.5824868
6.4000000	3069.0309	0.2016430	-2180.4196	467.11557	0.0304332	-305.76012	5.451E-05	0.5795816
6.6000000	3161.9089	0.2076938	-2241.0202	461.67988	0.0300776	-300.25974	5.461E-05	0.5766307
6.8000000	3253.7077	0.2136735	-2300.5282	456.32098	0.0297208	-294.83209	5.471E-05	0.5736335
7.0000000	3344.4421	0.2195825	-2358.9577	451.03540	0.0293683	-289.47458	5.480E-05	0.5705892
7.2000000	3434.1268	0.2254212	-2416.3227	445.82420	0.0290193	-284.18751	5.489E-05	0.5674971

Table A-3. DAFFR Flight Data for a No Wind Launch at 41°

Time	Down Range (m)	Cross Range (m)	Height (m)	Axial Velocity (m/s)	Cross Velocity (m/s)	Cross Velocity (m/s)	Yaw	Pitch
T	RMEMET(1)	RMEMET(2)	RMEMET(3)	VMEMET(1)	VMEMET(2)	VMEMET(3)	GAMY	GAMZ
0.	0.	0.	-2.1336000	0.	0.	0.	0.	0.
0.2000000	5.6622525	4.378E-08	-6.8691344	61.648147	3.529E-06	-51.638540	4.387E-08	0.6972706
0.4000000	24.337248	9.720E-05	-22.501375	125.02177	0.0019061	-104.62217	1.169E-05	0.6967993
0.6000000	56.788230	0.0015987	-48.722037	189.91989	0.0153960	-157.58876	6.239E-05	0.6926283
0.8000000	100.50488	0.0059411	-85.544249	257.79176	0.0233748	-210.86282	7.018E-05	0.6855954
1.0000000	159.17156	0.0105165	-133.32491	329.75332	0.0282215	-267.79045	6.644E-05	0.6820715
1.2000000	232.94152	0.0163223	-193.00430	409.52477	0.0244311	-330.13985	4.644E-05	0.6784804
1.4000000	323.55527	0.0230560	-265.67237	497.65224	0.0340107	-399.15839	5.331E-05	0.6760098
1.6000000	432.25834	0.0303952	-352.85625	587.83428	0.0432431	-469.42590	5.748E-05	0.6738674
1.8000000	553.79446	0.0394266	-449.70667	615.56203	0.0431818	-499.57850	5.490E-05	0.6718904
2.0000000	676.35265	0.0464248	-546.98365	608.45828	0.0417685	-481.93594	5.381E-05	0.6699317
2.2000000	797.13326	0.0542444	-642.46236	599.38648	0.0403083	-472.85844	5.280E-05	0.6679364
2.4000000	916.12768	0.0619268	-736.14159	590.59875	0.0388986	-463.98403	5.179E-05	0.6659087
2.6000000	1033.3917	0.0694921	-828.07093	582.08398	0.0376948	-455.35323	5.099E-05	0.6638429
2.8000000	1148.9738	0.0769496	-918.29804	573.83028	0.0367529	-446.95577	5.053E-05	0.6617413
3.0000000	1262.9373	0.0843029	-1006.8661	565.78943	0.0361163	-438.75304	5.044E-05	0.6596040
3.2000000	1375.3068	0.0915531	-1093.8113	557.93902	0.0357098	-430.72638	5.066E-05	0.6574302
3.4000000	1486.1250	0.0987017	-1179.1684	550.27623	0.0354122	-422.87214	5.103E-05	0.6552191
3.6000000	1595.4293	0.1057529	-1262.9715	542.79806	0.0350974	-415.18647	5.136E-05	0.6529694
3.8000000	1703.2562	0.1127129	-1345.2539	535.50121	0.0346949	-407.66549	5.155E-05	0.6506803
4.0000000	1809.6415	0.1195877	-1426.0482	528.38204	0.0342186	-400.30553	5.162E-05	0.6483514
4.2000000	1914.6206	0.1263808	-1505.3864	521.43666	0.0337381	-393.10304	5.167E-05	0.6459826
4.4000000	2018.2274	0.1330927	-1583.2996	514.66108	0.0333113	-386.05439	5.178E-05	0.6435739
4.6000000	2120.4959	0.1397230	-1659.8181	508.05140	0.0329363	-379.15576	5.196E-05	0.6411251
4.8000000	2221.4597	0.1462724	-1734.9716	501.60381	0.0325686	-372.40315	5.213E-05	0.6386354
5.0000000	2321.1478	0.1527435	-1808.7898	495.31444	0.0321792	-365.79261	5.226E-05	0.6361042
5.2000000	2419.5944	0.1591390	-1881.2976	489.17522	0.0317829	-359.31732	5.236E-05	0.6335311
5.4000000	2516.8271	0.1654596	-1952.5241	483.17582	0.0314062	-352.96901	5.249E-05	0.6309161
5.6000000	2612.8737	0.1717055	-2022.4934	477.31294	0.0310468	-346.74442	5.262E-05	0.6282586
5.8000000	2707.7611	0.1778777	-2091.2299	471.58340	0.0306860	-340.64036	5.275E-05	0.6255580
6.0000000	2801.5156	0.1839781	-2158.7573	465.98402	0.0303223	-334.65370	5.285E-05	0.6228139
6.2000000	2894.1630	0.1900076	-2225.0989	460.51160	0.0299684	-328.78141	5.296E-05	0.6200259
6.4000000	2985.7284	0.1959670	-2290.2772	455.16298	0.0296243	-323.02045	5.308E-05	0.6171937
6.6000000	3076.2360	0.2018571	-2354.3141	449.92929	0.0292811	-317.36774	5.318E-05	0.6143166
6.8000000	3165.7050	0.2076790	-2417.2277	444.77285	0.0289383	-311.78403	5.328E-05	0.6113942
7.0000000	3254.1499	0.2134331	-2479.0326	439.69829	0.0286007	-306.27719	5.337E-05	0.6084256
7.2000000	3341.5851	0.2191195	-2539.7434	434.67654	0.0282652	-300.84346	5.347E-05	0.6054102

Table A-4. DAFFR Flight Data for a No Wind Launch at 45°

Time	Down Range (m)	Cross Range (m)	Height (m)	Axial Velocity (m/s)	Cross Velocity (m/s)	Cross Velocity (m/s)	Yaw	Pitch
T	RMEMET(1)	RMEMET(2)	RMEMET(3)	VMEMET(1)	VMEMET(2)	VMEMET(3)	GAMY	GAMZ
0.	0.	0.	-2.1336000	0.	0.	0.	0.	0.
0.2000000	5.3115333	4.099E-08	-7.2495472	57.808958	3.304E-06	-55.857585	4.111E-08	0.7682323
0.4000000	22.518711	9.103E-05	-24.164043	117.13087	0.0017851	-113.13334	1.096E-05	0.7677934
0.6000000	52.301025	0.0014974	-52.527176	178.05072	0.0144229	-170.54547	5.850E-05	0.7638716
0.8000000	94.232607	0.0056580	-92.409442	241.78662	0.0219244	-228.55265	6.590E-05	0.7572685
1.0000000	149.26531	0.0098537	-144.22317	309.35917	0.0264123	-290.48906	6.224E-05	0.7539504
1.2000000	218.48229	0.0152998	-208.99994	384.30090	0.0228761	-358.42740	4.353E-05	0.7505765
1.4000000	303.52381	0.0216870	-288.12558	467.10030	0.0320003	-433.62951	5.021E-05	0.7482556
1.6000000	405.56461	0.0284744	-382.64901	551.85781	0.0406593	-510.24659	5.410E-05	0.7462401
1.8000000	519.67019	0.0360012	-487.94606	577.95400	0.0405397	-532.38433	5.159E-05	0.7443799
2.0000000	634.74517	0.0434966	-593.74975	571.32851	0.0391711	-524.33815	5.051E-05	0.7425370
2.2000000	746.16043	0.0508256	-697.64005	562.96052	0.0377455	-514.62486	4.949E-05	0.7406611
2.4000000	859.90906	0.0580274	-799.61619	554.66507	0.0363780	-505.18964	4.849E-05	0.7387507
2.6000000	970.04453	0.0651216	-899.73265	546.73114	0.0352247	-496.02170	4.772E-05	0.7368061
2.8000000	1078.6162	0.0721132	-998.04168	539.04690	0.0343737	-487.10939	4.731E-05	0.7348277
3.0000000	1185.6762	0.0790078	-1094.5906	531.56678	0.0338284	-478.41035	4.730E-05	0.7328154
3.2000000	1291.2566	0.0858060	-1189.4190	524.27027	0.0335025	-469.90471	4.759E-05	0.7307695
3.4000000	1395.3959	0.0925069	-1282.5652	517.15443	0.0332544	-461.58816	4.797E-05	0.7286859
3.6000000	1498.1300	0.0991105	-1374.0666	510.21615	0.0329542	-453.45624	4.828E-05	0.7265565
3.8000000	1599.4940	0.1056467	-1463.9596	503.45158	0.0325503	-445.50459	4.842E-05	0.7244096
4.0000000	1699.5221	0.1120975	-1552.2799	496.85809	0.0320856	-437.72902	4.845E-05	0.7222148
4.2000000	1798.2482	0.1184731	-1639.0625	490.43043	0.0316448	-430.12545	4.851E-05	0.7199823
4.4000000	1895.7050	0.1247733	-1724.3412	484.16499	0.0312720	-422.68968	4.866E-05	0.7177121
4.6000000	1991.9246	0.1309973	-1808.1492	478.05791	0.0309389	-415.41724	4.885E-05	0.7154037
4.8000000	2086.9380	0.1371470	-1890.5184	472.10077	0.0305924	-408.29960	4.901E-05	0.7130563
5.0000000	2180.7740	0.1432254	-1971.4786	466.28278	0.0302215	-401.32645	4.912E-05	0.7106694
5.2000000	2273.4601	0.1492343	-2051.0583	460.60058	0.0298577	-394.49421	4.923E-05	0.7082428
5.4000000	2365.0230	0.1551738	-2129.2854	455.05094	0.0295194	-387.79938	4.937E-05	0.7057762
5.6000000	2455.4886	0.1610441	-2206.1869	449.63070	0.0291888	-381.23837	4.951E-05	0.7032691
5.8000000	2544.8836	0.1668463	-2281.7893	444.33677	0.0288507	-374.80762	4.963E-05	0.7007209
6.0000000	2633.2318	0.1725838	-2356.1193	439.16557	0.0285162	-368.50369	4.974E-05	0.6981313
6.2000000	2720.5579	0.1782554	-2429.1990	434.11516	0.0281948	-362.32319	4.986E-05	0.6954998
6.4000000	2806.8856	0.1838622	-2501.0556	429.19130	0.0278776	-356.26273	4.998E-05	0.6928261
6.6000000	2892.2379	0.1894057	-2571.7117	424.35897	0.0275600	-350.31701	5.008E-05	0.6901096
6.8000000	2976.6340	0.1948866	-2641.1879	419.61449	0.0272471	-344.45757	5.019E-05	0.6873499
7.0000000	3060.0892	0.2003052	-2709.5000	414.93865	0.0269386	-338.67639	5.030E-05	0.6845462
7.2000000	3142.6141	0.2056618	-2776.6636	410.33215	0.0266295	-332.97363	5.039E-05	0.6816978

Appendix B. Zuni Rocket RCS Measurements

Measurement Data

X-Band Data

Full scale X-band (10 GHz) RCS measurements were performed to determine Zuni backscatter signatures over tail aspect angles of interest. Azimuth plane cuts were performed, where the missile roll angle varied over a number of different values. For horizontal polarization, figures B-5 through B-7 plot the azimuth plane RCS over ± 24 degrees azimuth and for roll angles of 0, 15, 30, 45, 60 and 75 degrees. The peak value at tail aspect is approximately 0 dBsm. The data for 0 degrees roll, but for full 360 degree azimuth rotation, is shown in Figure B-8.

For vertical polarization, similar ± 24 degree azimuth data are shown for roll angles of 0, 15, 30, 45, 60, and 75 degrees in Figures B-9 through B-11, respectively. A vertical polarization full 360 degree (principal plane) azimuth cut for zero degrees roll angle is shown in Figure B-12.

Ku-Band Data

A small amount of measurement data were obtained at Ku-Band (16 GHz) that are useful for a relative comparison of RCS signature between the two bands. Figures B-13 and B-14 plot vertical polarization azimuth plane RCS over ± 24 degrees for roll angles of 0, 15, and 30 degrees. No horizontal polarization data were obtained at this time.

Comparing the X-Band and Ku-Band data, several observations are made. The peak tail aspect RCS is 0 dBsm at X-Band compared to +4 dBsm at Ku-Band. Secondly, the main lobe RCS pattern is significantly narrower at Ku-Band than X-Band, i.e. 8 degrees null-to-null beamwidth compared to 11 degrees.

B-1. Measurement Method

Radar Cross section (RCS) measurements were performed using an indoor compact range facility at Georgia Tech. An illustration of the measurement facility is shown in Figure B-1. A block diagram of related equipment is shown in Figure B-2. Here, by use of transmitter feedback in conjunction with a nulling network, room background RCS is nulled out. Typically, -40 to -50 dBsm room background is achievable depending on frequency.

Standard RCS measurement procedures are employed to calibrate the equipment in dBsm via use of reference cylinder. A chart recorder is precalibrated in dBsm. Subsequently, the missile model is placed on an azimuth rotator and rotated through the range of angles of interest.

For Zuni RCS backscatter measurements, an actual rocket tail assembly was obtained (Figure B-3). A rocket nose was fabricated from wood and subsequently painted with an Atcheson Colloids silver base paint to make it conductive; nose detail is shown in Figure B-4. A photograph of the entire full-scale Zuni missile used for these measurements appears as Figure 2 in the main body of the report.

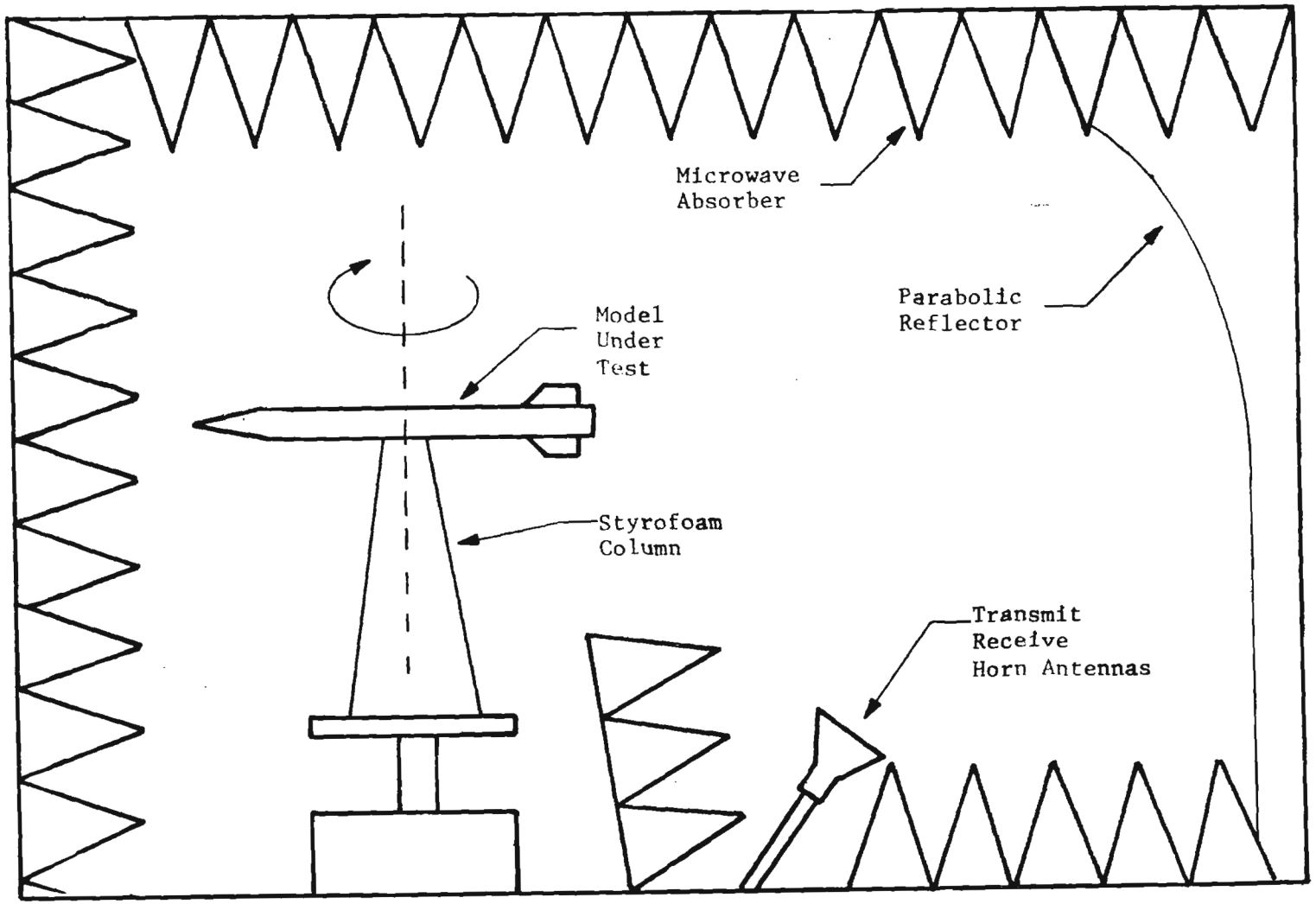

Figure B-1. Compact Range RCS Measurement Facility

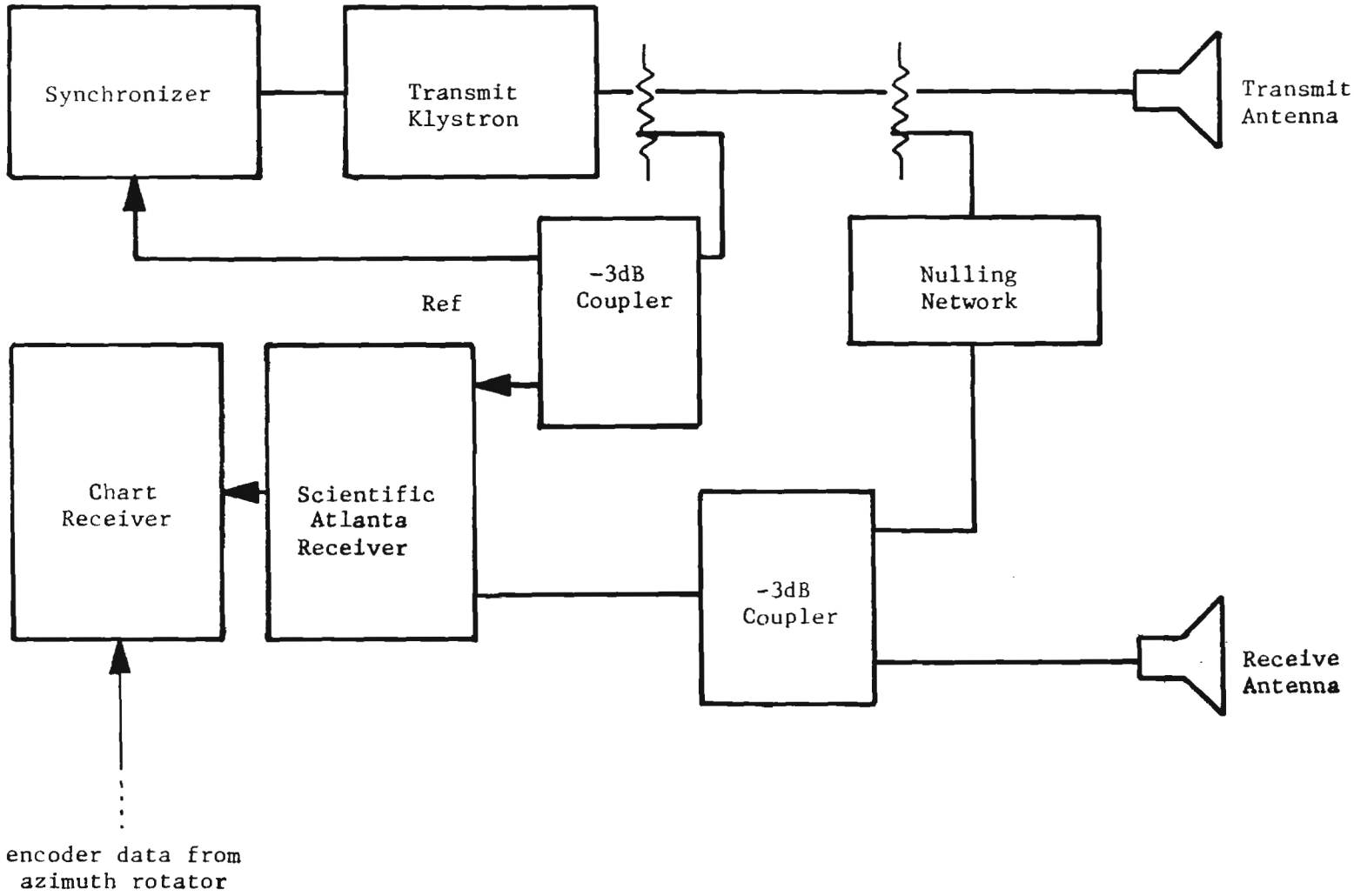

Figure B-2. Equipment Block Diagram

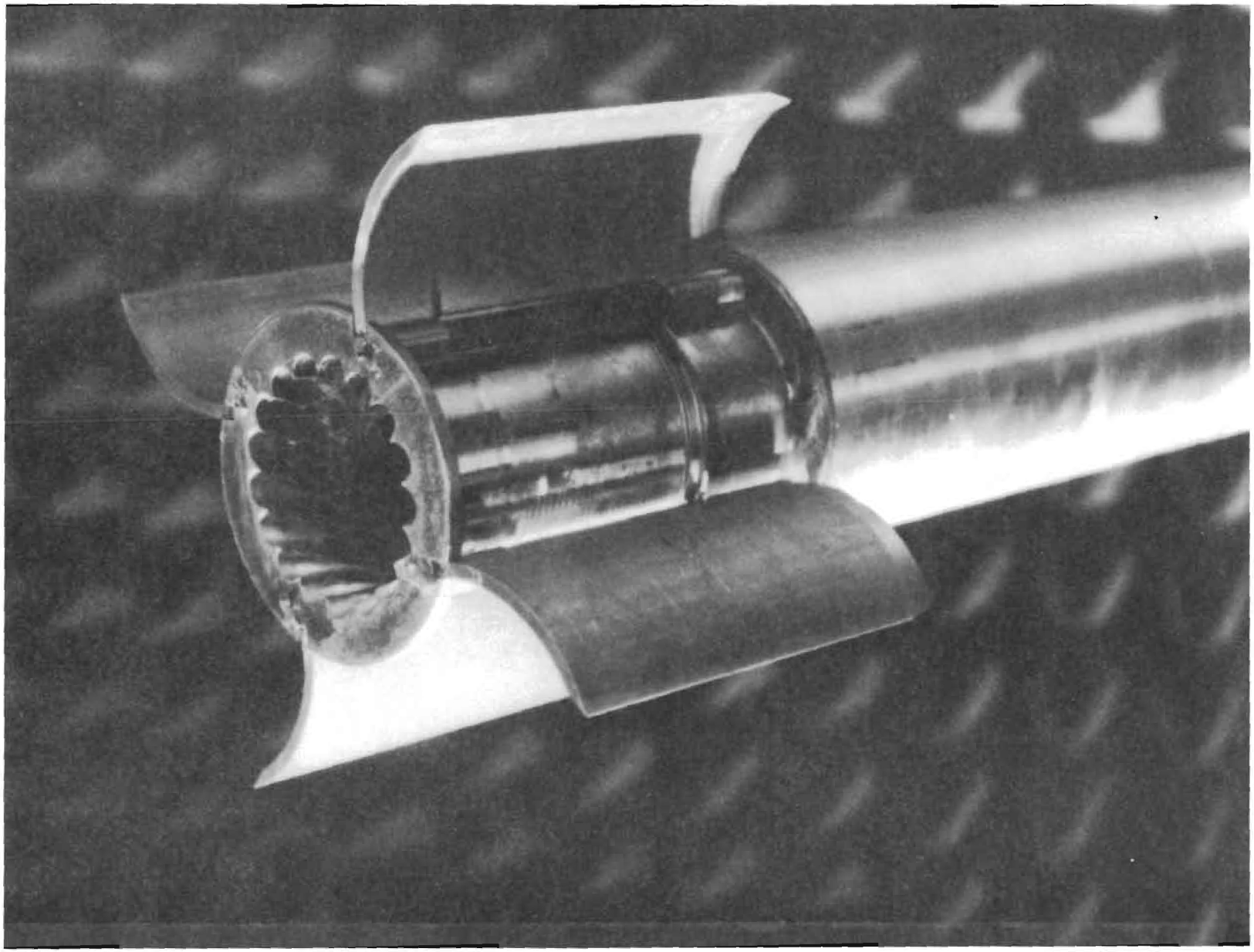

Figure B-3. Actual Zuni Rocket Tail Assembly Used in Model.

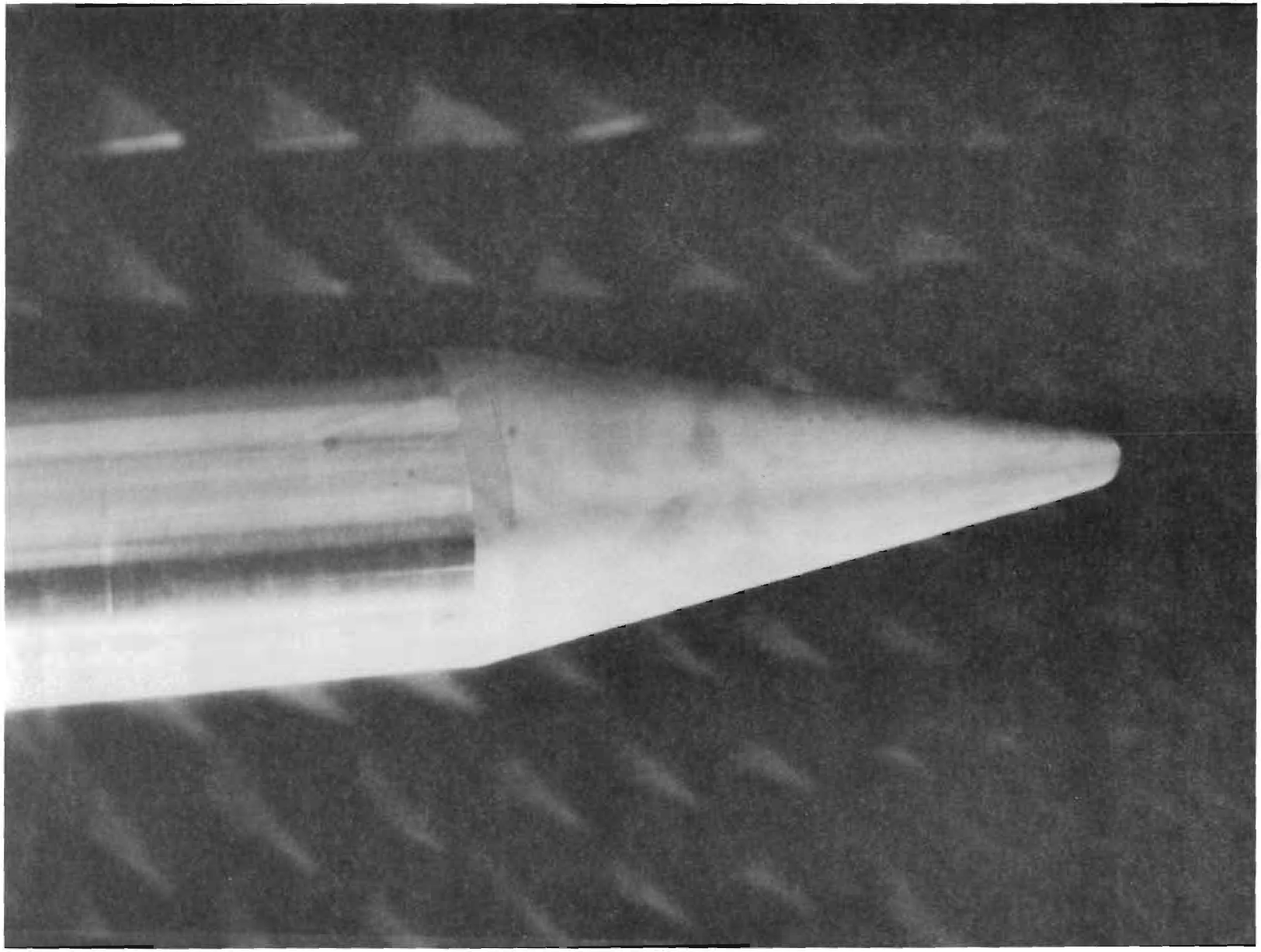

Figure B-4. Model Tip Detail.

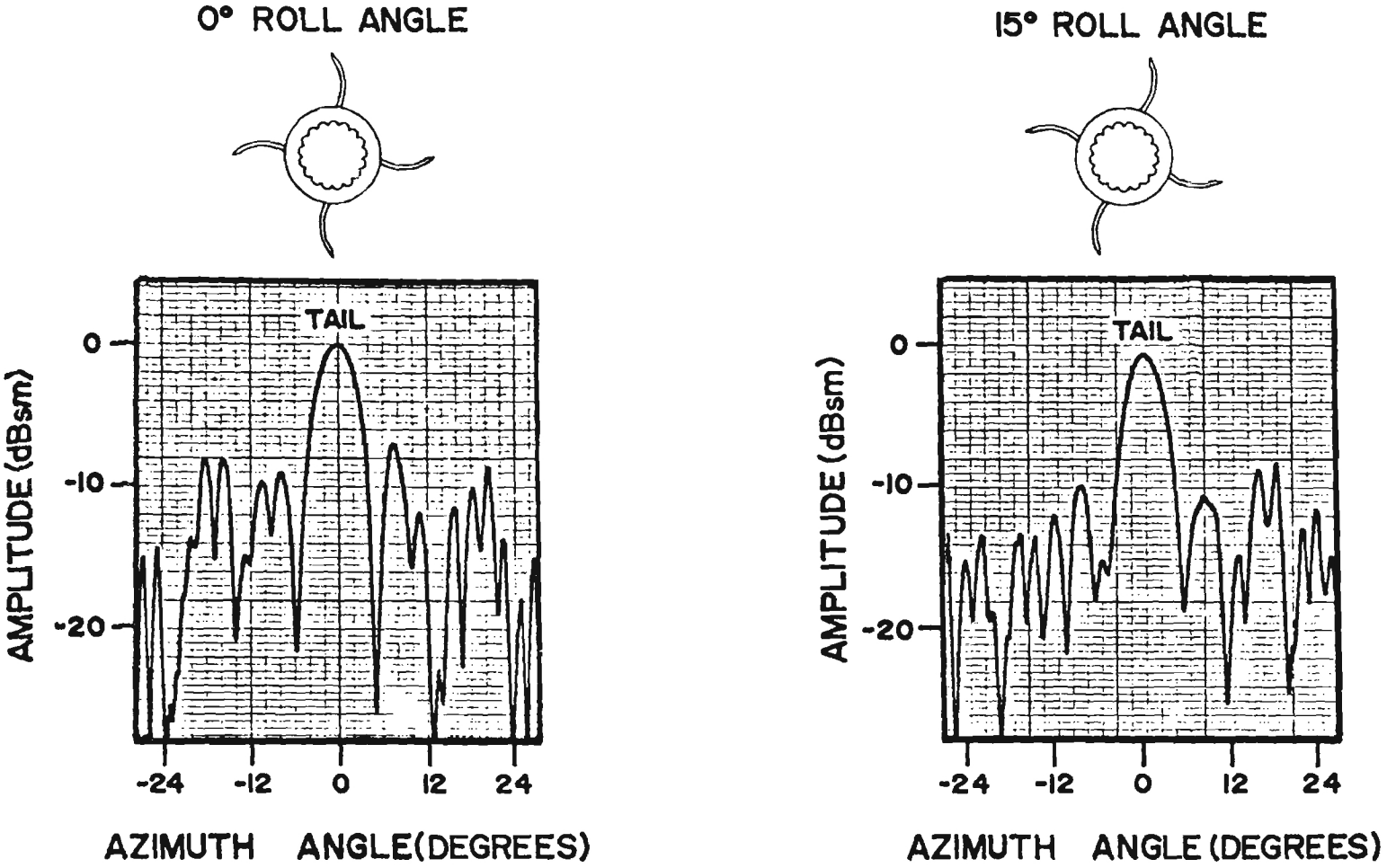

Figure B-5. Compact Range RCS Measurements of The Zuni Rocket Tail Section (Rear View) at 0° Roll Angle (Left) and 15° Roll Angle (Right), 10.0 GHz, and Horizontal Polarization.

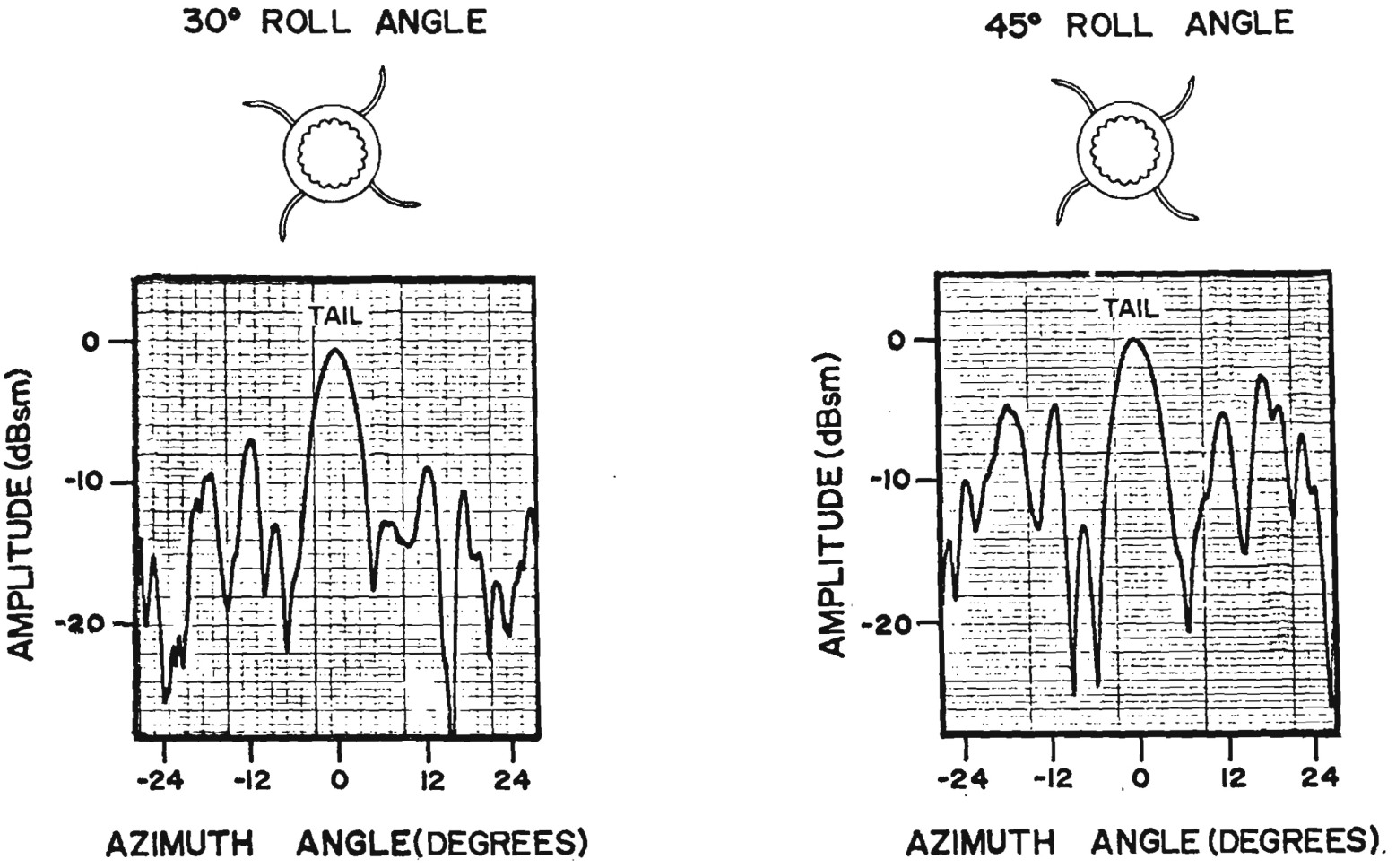

Figure B-6. Compact Range RCS Measurements of The Zuni Rocket Tail Section (Rear View) at 30° Roll Angle (Left) and 45° Roll Angle (Right), 10.0 GHz, and Horizontal Polarization.

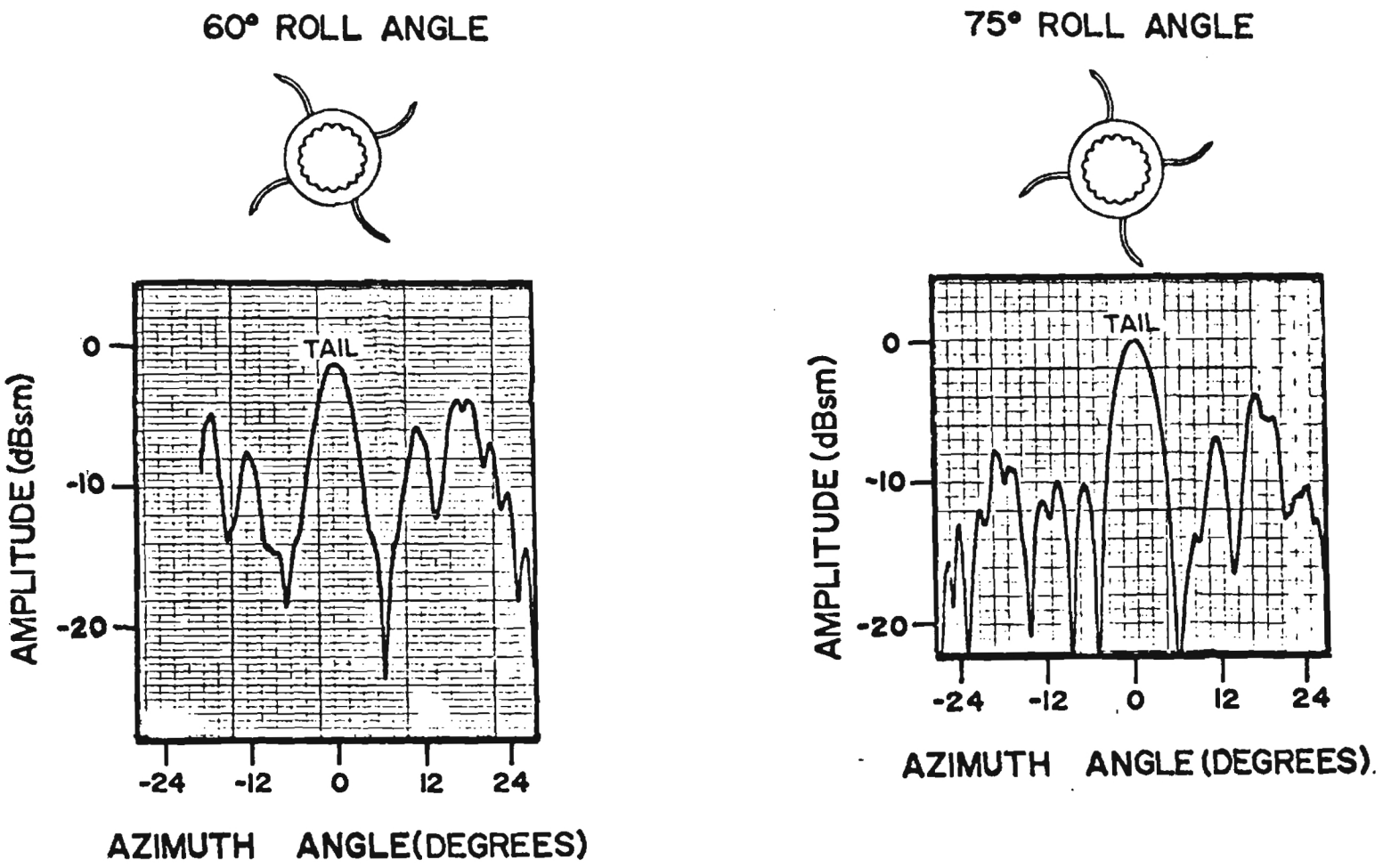

Figure B-7. Compact Range RCS Measurements of The Zuni Rocket Tail Section (Rear View) at 60° Roll Angle (Left) and 75° Roll Angle (Right), 10.0 GHz, and Horizontal Polarization.

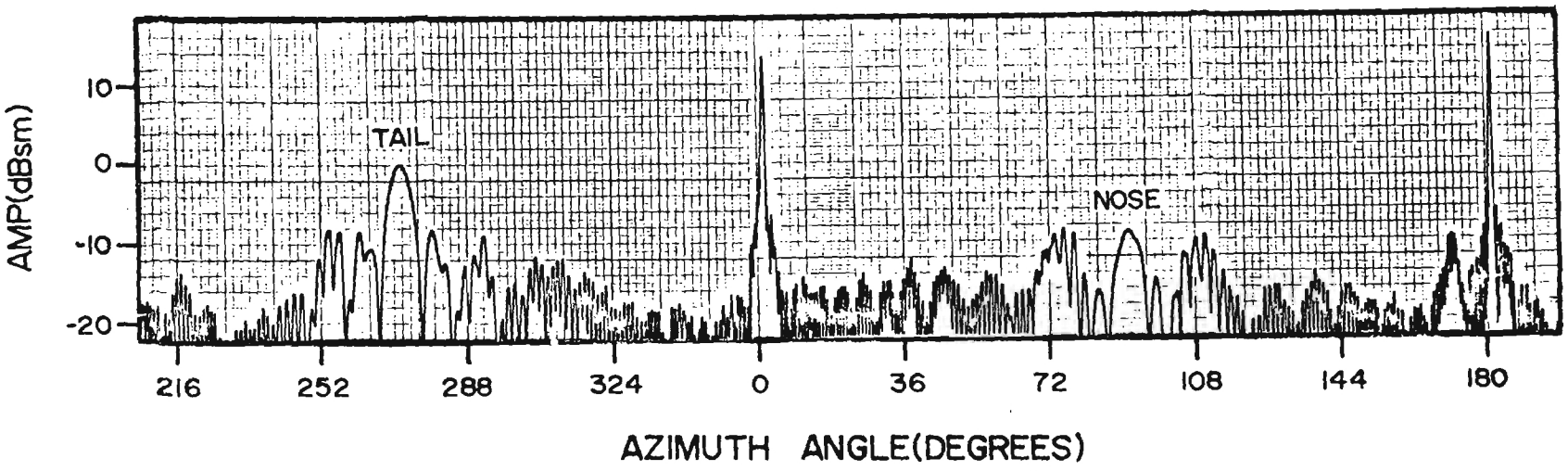

Figure B-8. Compact Range RCS Measurements of the Zuni Rocket (360° Azimuth Rotation) at 0° Roll Angle, 10.0 GHz, and Horizontal Polarization

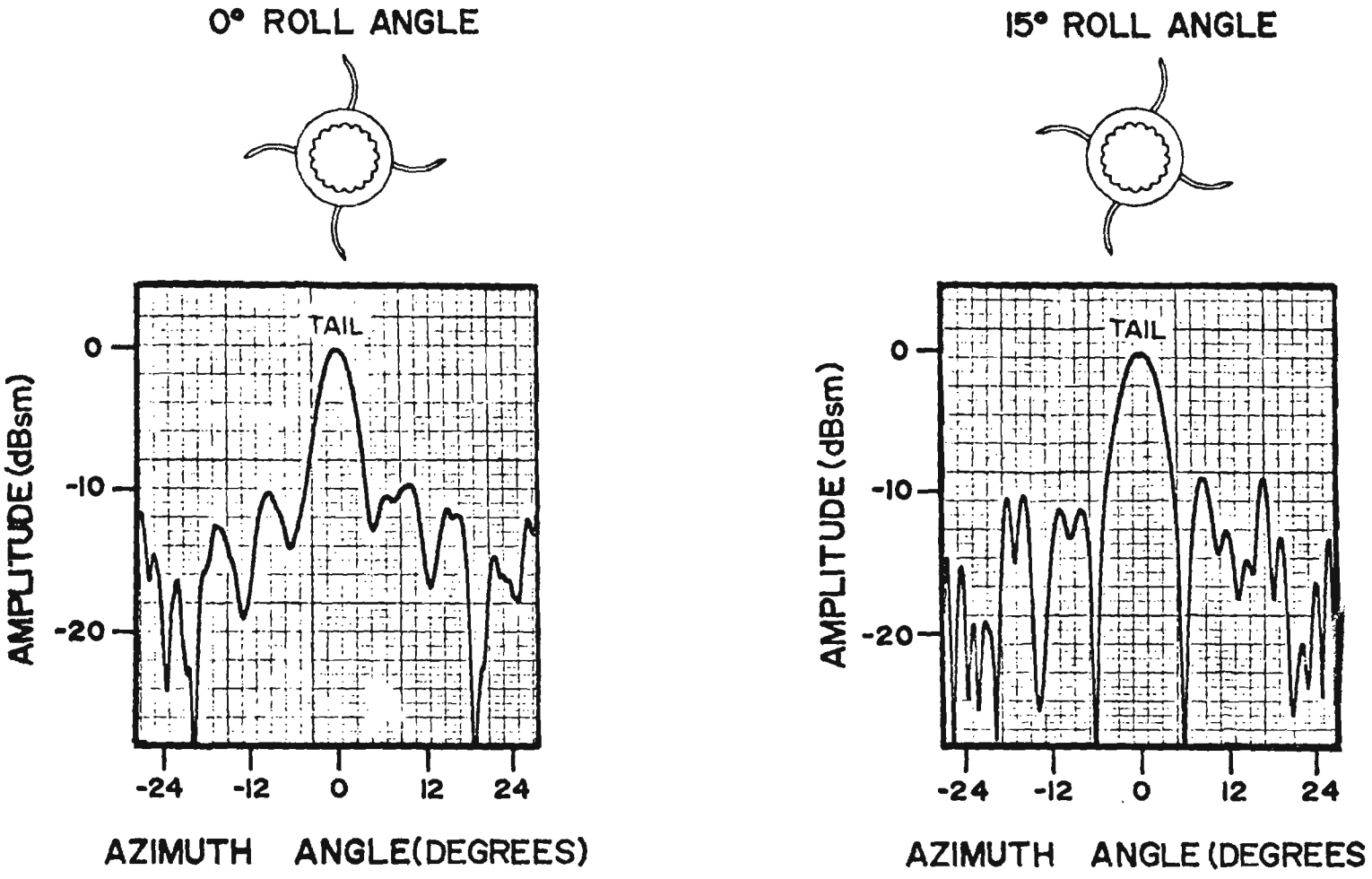

Figure B-9. Compact Range RCS Measurements of The Zuni Rocket Tail Section (Rear View) at 0° Roll Angle (Left)and 15° Roll Angle (Right), 10.0 GHz, and Vertical Polarization.

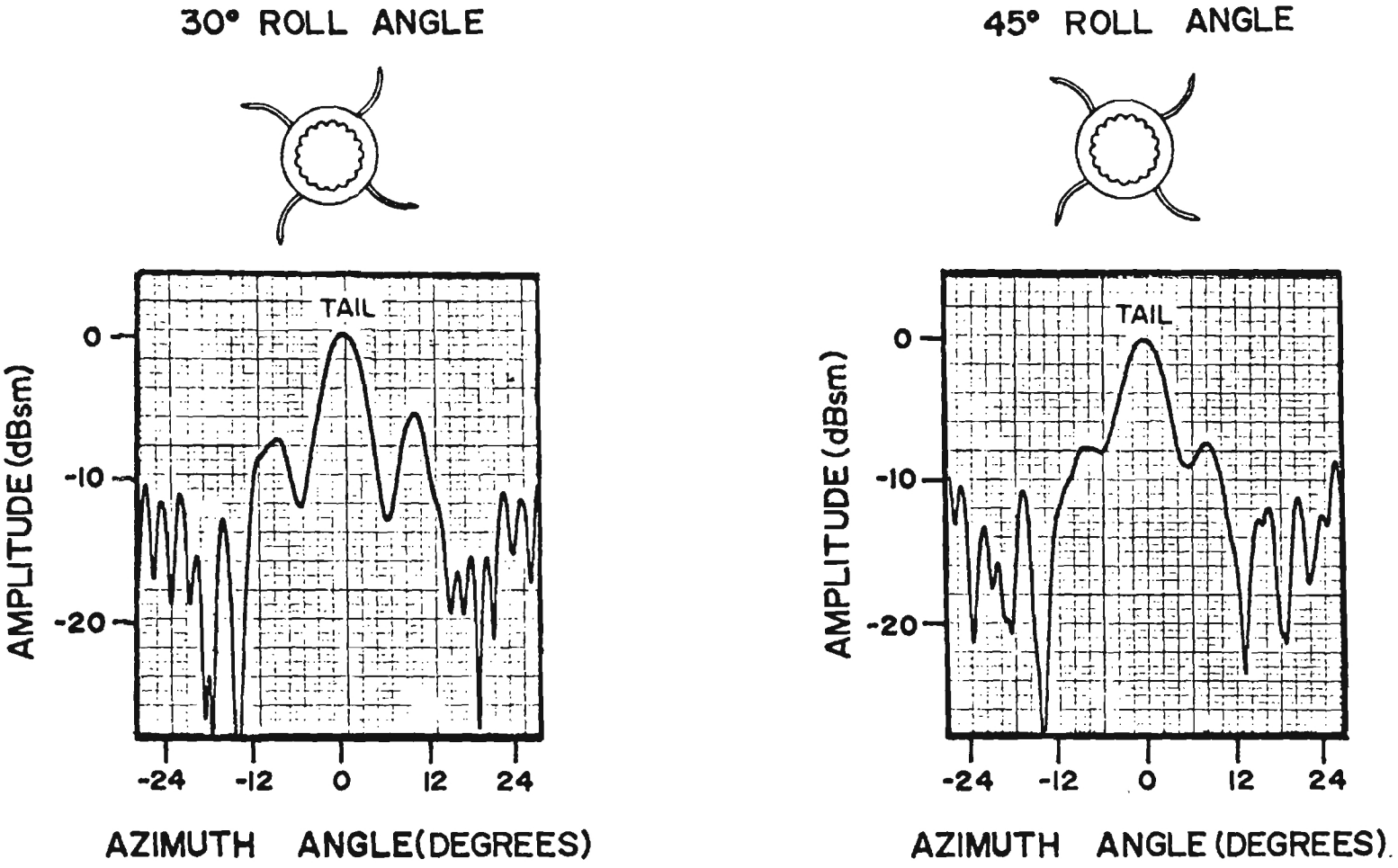

Figure B-10. Compact Range RCS Measurements of The Zuni Rocket Tail Section (Rear View) at 30° Roll Angle (Left) and 45° Roll Angle (Right), 10.0 GHz, and Vertical Polarization.

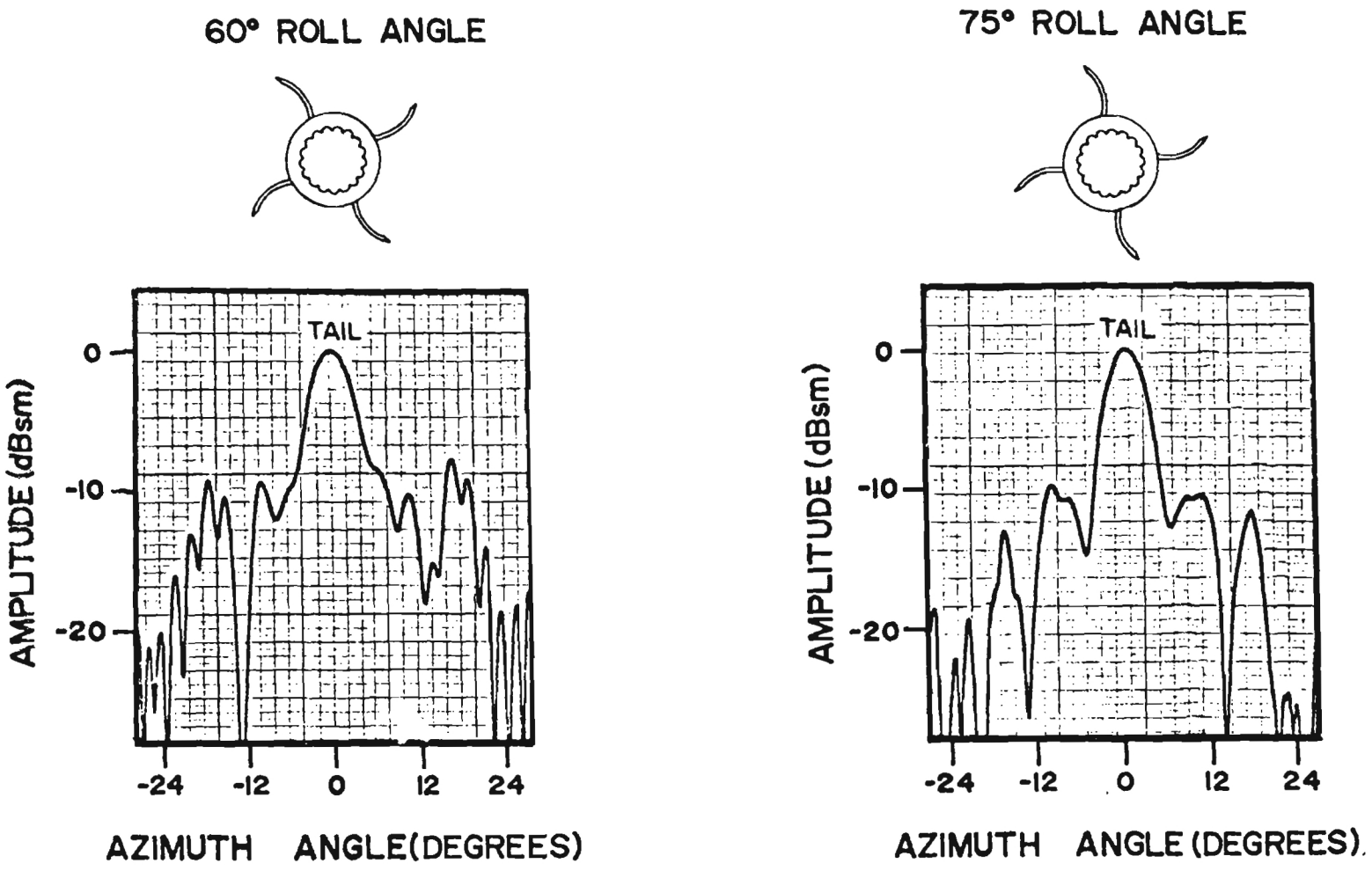

Figure B-11. Compact Range RCS Measurements of The Zuni Rocket Tail Section (Rear View) at 60° Roll Angle (Left) and 75° Roll Angle (Right), 10.0 GHz, and Vertical Polarization.

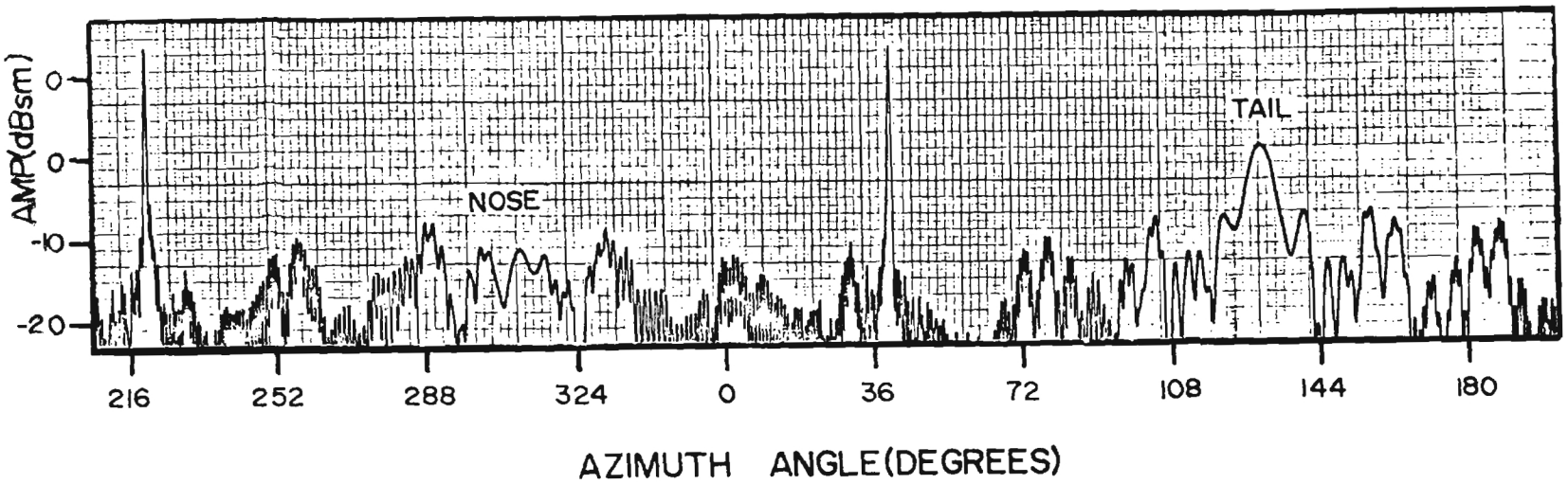

Figure B-12. Compact Range RCS Measurements of The Zuni Rocket (360° Azimuth Rotation) at 0° Roll Angle, 10.0 GHz, and Vertical Polarization.

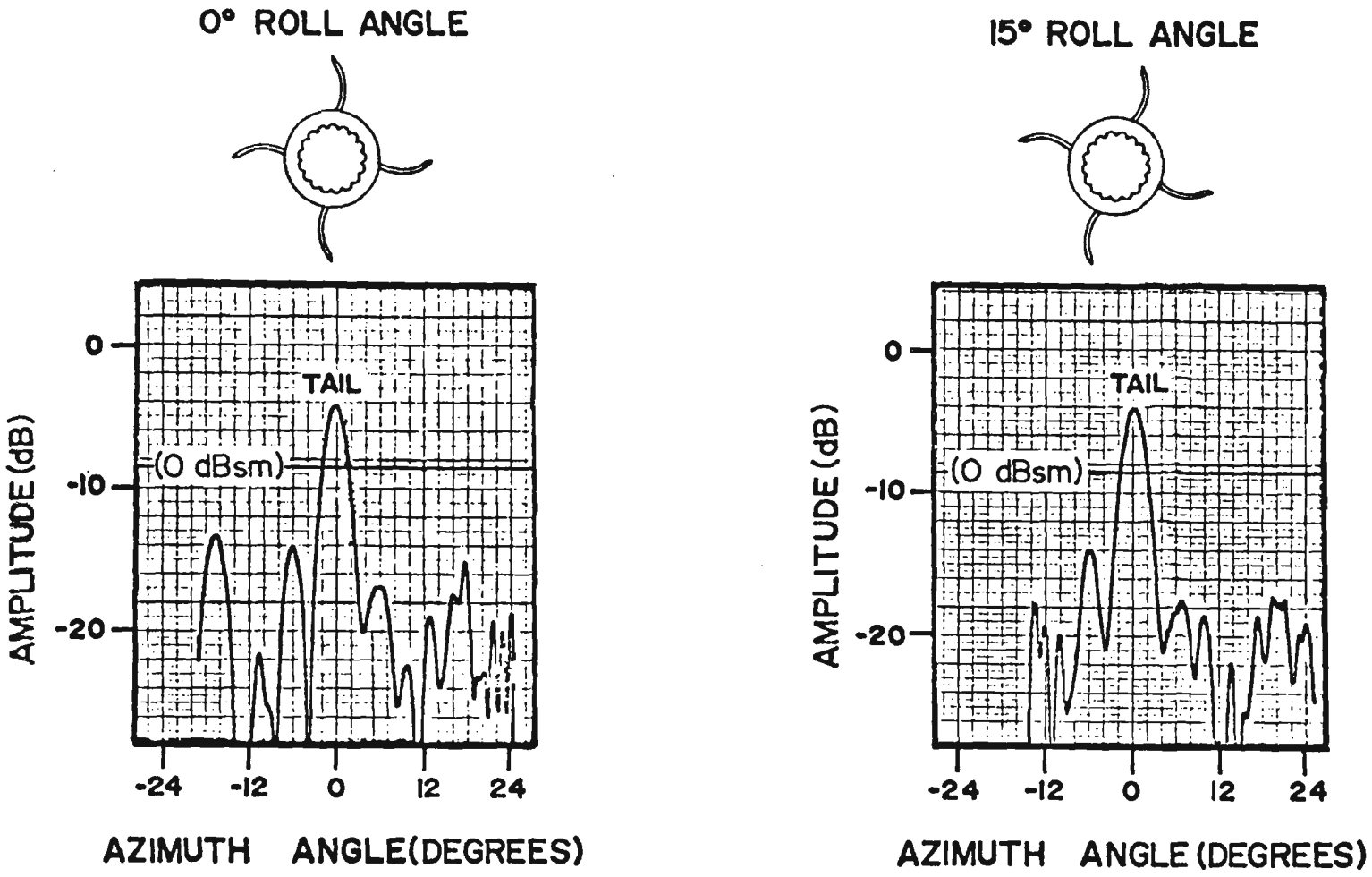

Figure B-13. Compact Range RCS Measurements of The Zuni Rocket Tail Section (Rear View) at 0° Roll Angle (Left)and 15° Roll Angle (Right), 16.0 GHz, and Vertical Polarization.

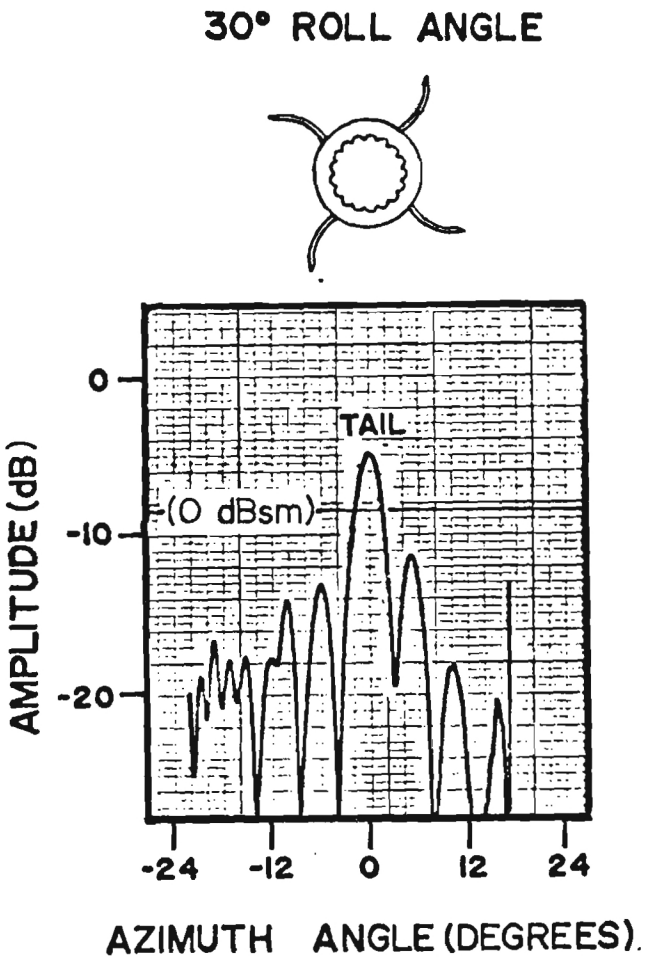

Figure B-14. Compact Range RCS Measurements of The Zuni Rocket Tail Section (Rear View) at 30° Roll Angle, 16.0 GHz, and Vertical Polarization.

Appendix C. Overview of Texas Instruments IR Experiment

Texas Instruments' primary objective in this effort was to determine detectability and to subsequently characterize the shape of the thermal signature produced by a Zuni rocket with an IR Sensor. If it was determined that an IR image of acceptable characteristics was available, a secondary objective was to attempt processing this data to determine rocket position along its trajectory. Data for the effort was obtained by monitoring two Zuni rockets at Redstone Arsenal (RSA), Huntsville, Alabama.

After analyzing the data collected at RSA, it was determined that the Zuni rocket possessed ample IR intensity level with a satisfactory IR image shape for processing with digital algorithm techniques to determine rocket position. The intensity and IR imagery shape allows the rocket to be detected out to 2 km and possibly more, which is a range perceived as a DAFFR system requirement.

Tracking information was obtained utilizing a Digital Tracker System which is designed to process IR imagery with general purpose software algorithms. Position information was produced for both flights that were monitored. An error of 0.3 mrad, considered excellent compared to other sensors, was computed for a flight segment representative of IR tracker performance. With improved tracking algorithms specifically designed for the Zuni, improvements in position accuracy are readily possible which will set the error contribution of an IR tracker to an insignificant level in the overall system error budget.

The use of an IR sensor in conjunction with a digital tracker to determine rocket trajectory for ballistic correction has been shown to be feasible. Texas Instruments is looking forward to participating in investigation studies which will yield an integrated system design to solve the problem of reducing ballistics dispersion of rocket systems.

Measured thermal imaging data for flights 1 and 2 are shown in Figures C-1 and C-2, respectively.

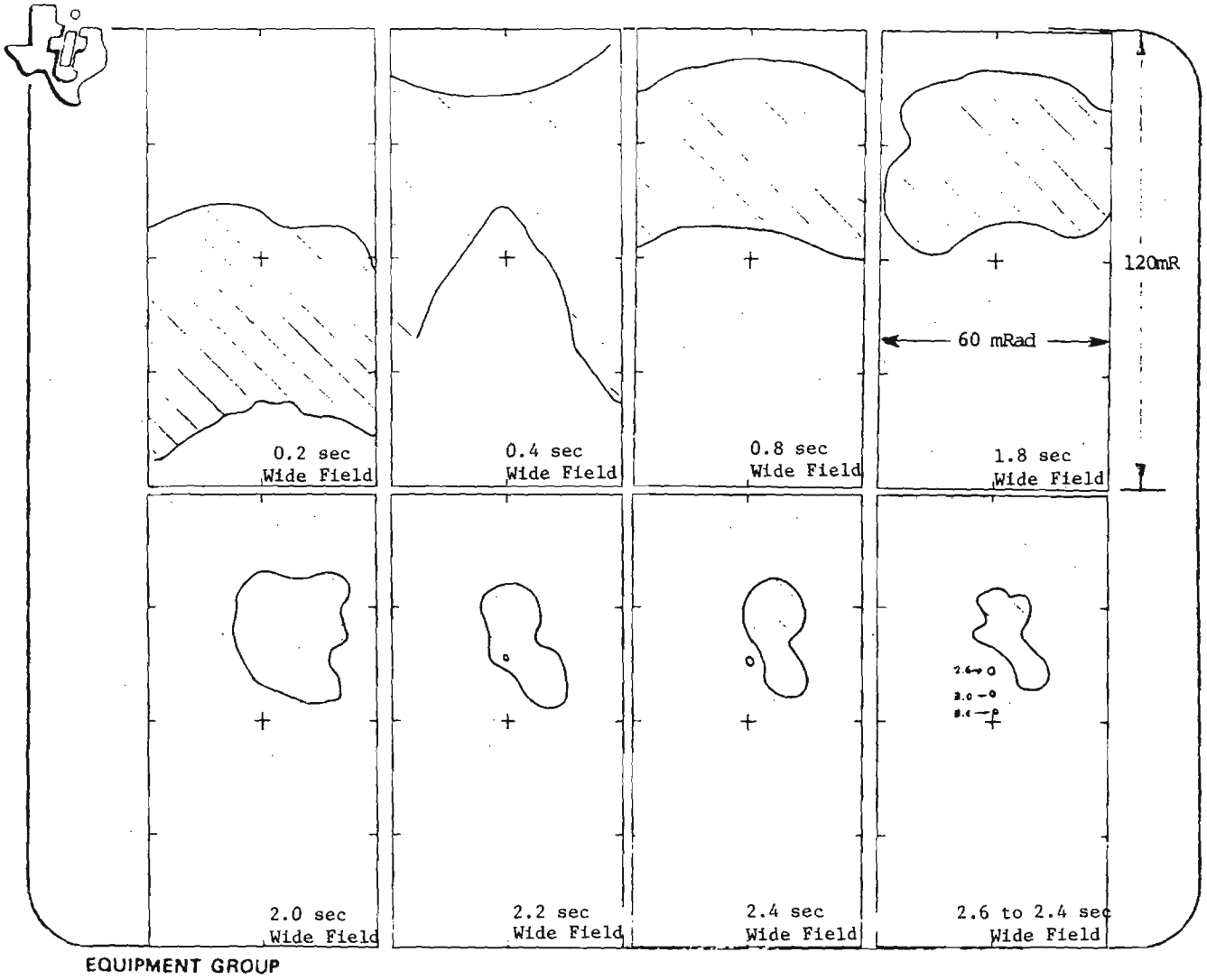

Figure C-1. Thermal Image Size for DAFFR Flight #1

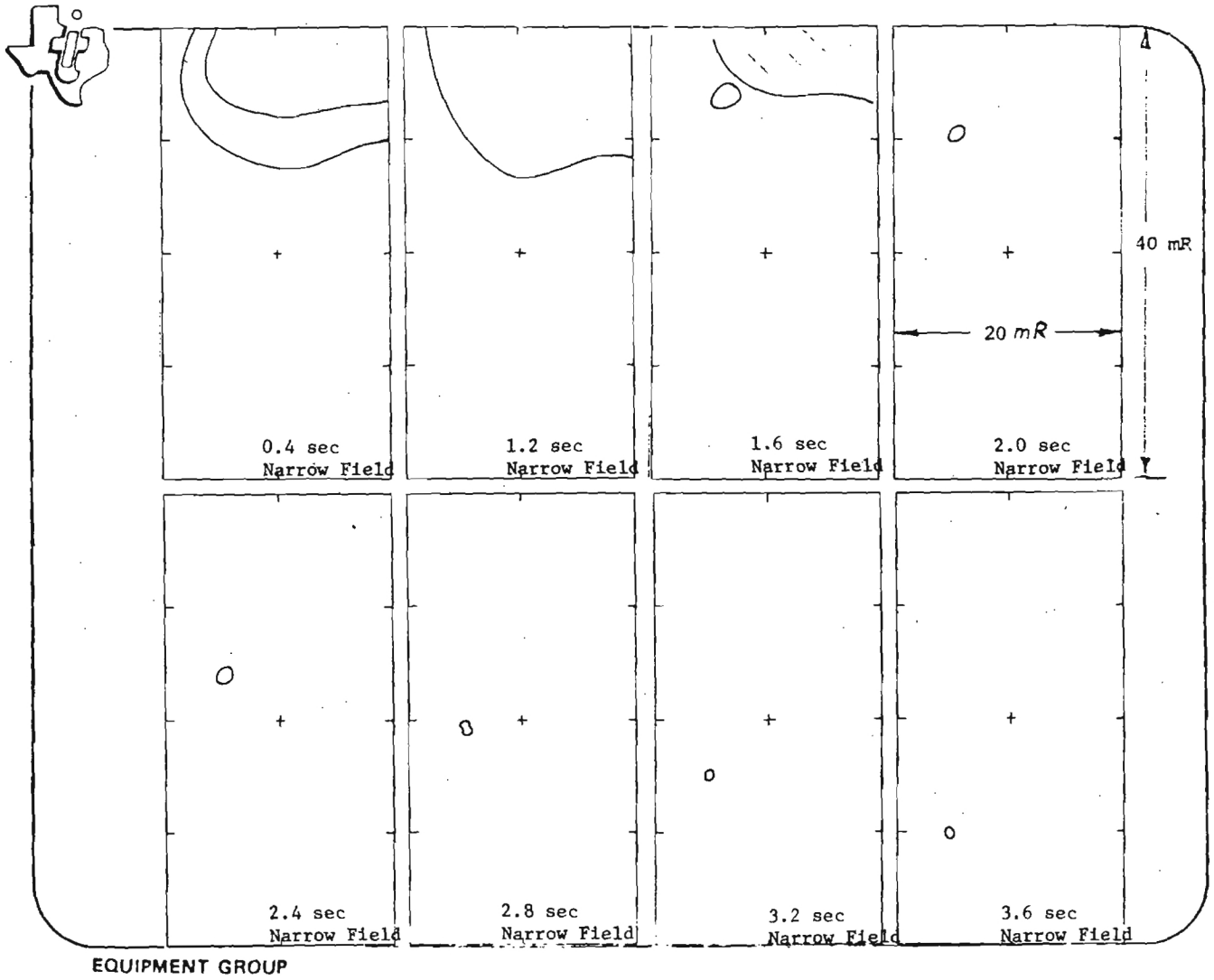

Figure C-2. Thermal Image Size for DAFFR Flight #2